“One-Pot” Synthesis of Organic Azides from Alcohols and Protected Sugars

by

Charles Alan Hartranft

Submitted in Partial Fulfillment of the Requirements

for the Degree of

Masters of Science

in the

Chemistry

Program

YOUNGSTOWN STATE UNIVERSITY

December 2008

"One-Pot" Synthesis of Organic Azides from Alcohols and Protected Sugars

Charles Alan Hartranft

I hereby release this thesis to the public. I understand this thesis will be made available from the OhioLINK ETD Center and the Maag Library Circulation Desk for public access. I also authorize the University or other individuals to make copies of this dissertation as needed for scholarly research.

Signature:

Charles Alan Hartranft, Student Date

Approvals:

Dr. Peter Norris, Thesis Advisor Date

Dr. John A. Jackson, Committee Member Date

Dr. Michael A. Serra, Committee Member Date

Dr. Peter J. Kasvinsky, Dean of Graduate Studies & Research Date

Thesis Abstract

This thesis deals with a novel “one-pot” synthesis of organic azides from simple alcohols as well as protected sugars. Experimentation led to the successful azidation of both classes of compounds while providing for the isolation and characterization of unexpected byproducts and side reactions. All findings were strongly supported by previous literature while yields of azide products isolated in this research were more than adequate.

Acknowledgements

First, I would like to sincerely thank Dr. Peter Norris for his advice and guidance over the last two years. Being able to transition from the biological science research of undergraduate studies to the field of synthetic organic chemistry was a difficult and arduous task made manageable only by the help of such an educator, advisor, and mentor. Additionally, I would like to thank the other chemistry department staff members who trained and aided me in the use of the various instruments. They include, but are not limited to, Dr. John Jackson, Dr. Roland Riesen, and Dr. Matthias Zeller.

I am most grateful to the YSU Chemistry Department and the YSU Graduate School for supporting me in pursuit of my degree. I would especially like to thank Dr. Timothy Wagner for his help in assisting me toward the completion of my degree while I pursue my future career in the field of medicine. I also want to sincerely thank all of the faculty and staff in the YSU Chemistry Department, in particular, my thesis committee members: Dr. John A. Jackson and Dr. Michael A. Serra.

I am extremely grateful to my entire family, especially my parents, who have worked so hard to afford me the privilege of not only an excellent education throughout my life but also a higher education by contributing to my school endeavors financially.

Lastly, I would like to thank my fellow graduate students who contributed in so many ways to my understanding and success in the laboratory. I would like to especially mention the following by name: Brian Dobosh, Jennie Patton, Steve Knapp, Lucas Beagle, Calvin Austin, Adam Cox, and Ryan Conway.

Table of Contents

List of Figures

List of Tables

Introduction

Organic Azides

Organic azides are carbon-containing compounds with an attached N_3 functional group (Figure 1).

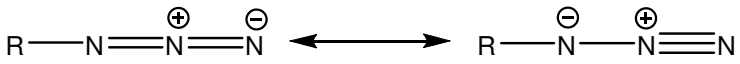

Figure 1: Resonance structures for a general organic azide.

These compounds were discovered in the mid-1860's and received significant attention nearly a century later when their application to aryl, alkyl, and acyl chemistry was studied. Organic azides have proven to be an extremely important bridge among the disciplines of chemistry, biology, medicine, and material science. Examples of such compounds from recent literature can be seen below in Figure 2.[1]

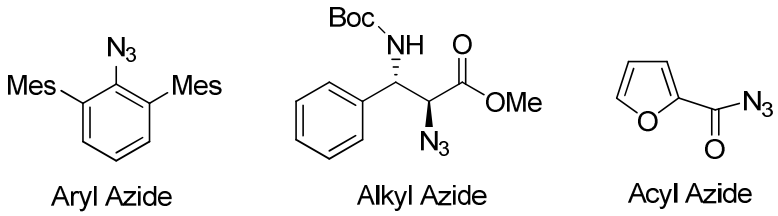

Figure 2: Different azide-containing molecules from recent literature.

Azide synthesis can be categorized into five main types as follows: (1) introduction of an N_3 group by substitution or addition, (2) introduction of an N_2 group (diazo transfer), (3) introduction of an N atom (diazotization), (4) cleavage of triazines,

and (5) rearrangements of azides.[1] Due to major differences in aliphatic and aromatic azides, properties and synthetic techniques for these two types of compounds are generally referred to separately.[1] For the purpose of this thesis, aliphatic azides will be the exclusive focus of the work presented.

Aliphatic azide synthesis is most commonly achieved through the use of nucleophilic substitution. More specifically, this is S_N2-type substitution where commonly an azide salt such as sodium azide is used as the nucleophilic source of nitrogen. At the electrophilic site of the corresponding substrate, functional groups such as halides, sulfonates, mesylates, triflates, as well as others may serve as sufficient leaving groups. For example, with bromide functioning as the leaving group and sodium azide as the nucleophile, an α-hydroxy-β-azido ester is formed. This compound serves as an intermediate to a final α-hydroxy-β-amino product used for amide synthesis (Equation 1).[2] This example also clearly demonstrates the versatility and usefulness of azide-containing compounds in the overall synthesis of nitrogen-containing species.

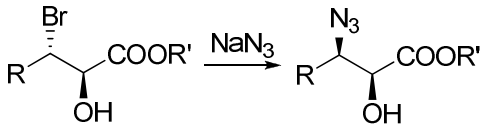

Equation 1.

Alcohols, the main topic of this research, may also be displaced by azides upon addition of reagents that increase the reactivity or leaving capability of the hydroxyl group. One way to achieve hydroxyl displacement by an azide is through the use of sulfonate ester intermediates. An example is the reaction of a diol with $SOCl_2$ in the

presence of base to produce a sulfonate ester-bridged diol. This compound is next reacted with an azide to produce the desired substitution product (Scheme 1).[3]

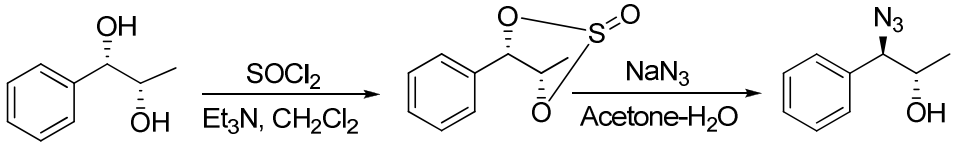

Scheme 1.

Furthermore, this alcohol-azide substitution is not simply limited to diols. Primary and secondary alcohols may be reacted with a wide range of sulfur-containing reagents including mesylates, tosylates, and triflates to name a few. The resulting sulfonate ester, a reasonably good leaving group, can be readily substituted by an azide in polar aprotic solvents to produce the desired product. Examples of such reactions from recent literature appear in natural product synthetic pathways. In Schemes 2 and 3 below, the intermediate mesylate and triflate esters are formed prior to S_N2 displacement by the azide nucleophile.[4,5]

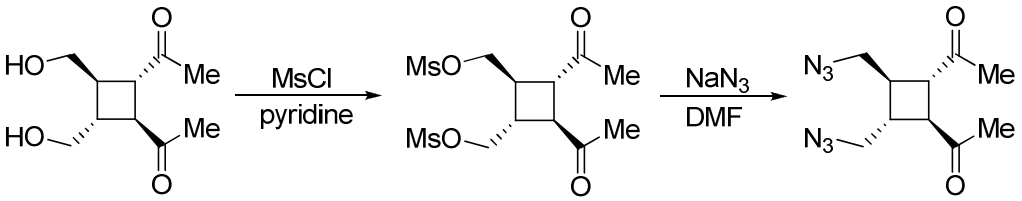

Scheme 2.

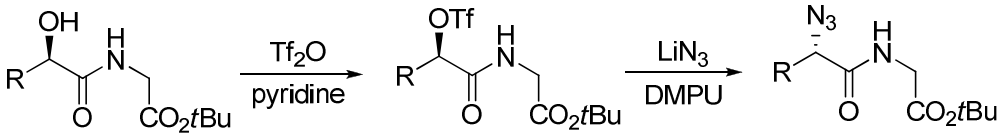

Scheme 3.

Replacing alcohols with azides using the methods described above is one of the more popular ways to introduce azides onto a molecule. However, this type of synthesis is fairly time-consuming being that it occurs in two separate steps. Once the sulfonate ester is produced, work-ups and separations are needed to isolate the intermediate. This ester must then be combined with the azide source in a second and separate reaction to achieve the final substitution and thus, the azide product.

In an attempt to avoid time-consuming intermediate work-ups and isolations, an application of the Mitsunobu reaction has been reported to synthesize azides from primary and secondary alcohols (Equation 2).[6] This "one-pot" reaction is quite useful due to the fact that it bypasses intermediate isolations and is thus considerably more time efficient. However, the phosphines used in this synthesis are normally troublesome to work with and create oxide byproducts that are often difficult to remove from reaction mixtures.

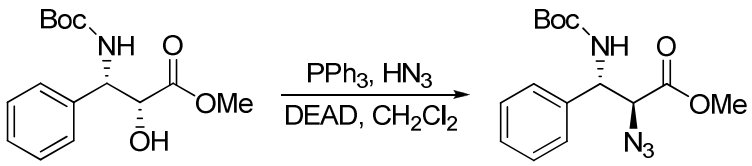

Equation 2.

Similarly, an additional "one-pot" synthesis has been reported in the literature involving a secondary alcohol reacted with diphenyl phosphorazidate (DPPA) and 1,8-diazobicyclo[5.4.0]undec-7-ene (DBU) to produce the desired azide (Equation 3).[7]

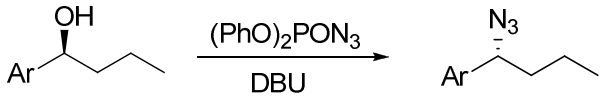

Equation 3.

Recently, thesis work from Youngstown State University reported an azidodeoxy sugar formed without the intermediate isolation and work-up of a sulfonate ester (Equation 4).[8]

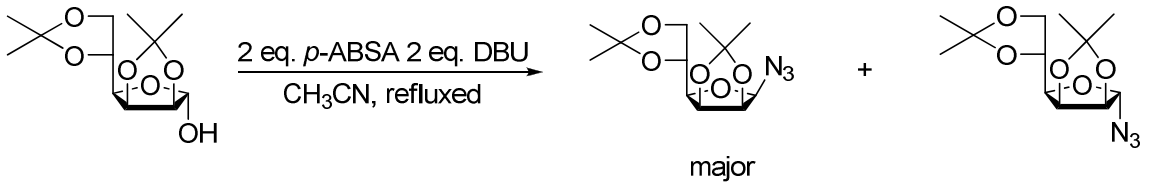

Equation 4.

The formed organic azides were the result of a side reaction occurring during a diazo ester synthesis shown below in Equation 5.[8]

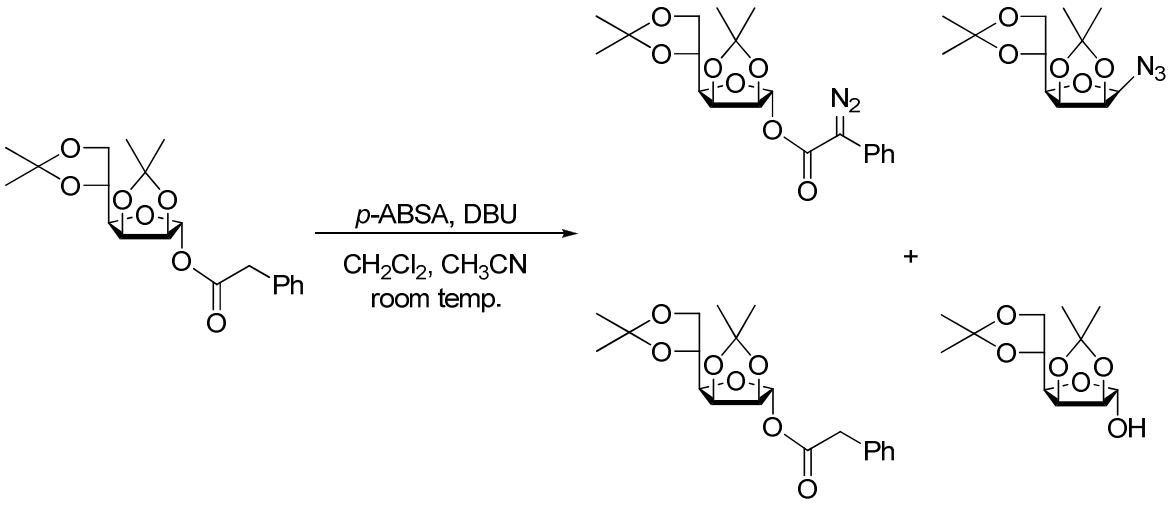

Equation 5.

The possibility that similar reagents could lead to a "one-pot" azide synthesis has sparked interest for further study of this reaction. Being able to synthesize azide compounds from alcohols in a "one-pot" manner would eliminate intermediate isolations and work-ups making the process much more efficient than the current "two-pot" standard. Additionally, the application of such a technique to a broad class of alcohol-containing molecules could help to determine its usefulness and scope of application.

Carbohydrates

One extremely diverse class of hydroxyl-containing compounds is carbohydrates, which are the most abundant organic molecules on earth and function centrally in the biological processes of chemical-energy storage, production, and metabolism in general.[9] Additionally, they provide structural contributions to several biologically essential macromolecules, for example deoxynucleosides and ribonucleosides, which are linked to one another *via* phosphodiester bonds, to form the nucleic acids DNA and RNA.

Structural representation of these compounds can be seen below in Figure 3.[9] It is through these carbohydrate-containing macromolecules that information essential for the biological structure and function of organisms is carried.

Figure 3: Deoxynucleoside and nucleoside structures found in DNA and RNA.

A carbohydrate is defined as a polyhydroxyaldehyde, polyhydroxyketone, or any substance that yields these compounds upon hydrolysis.[9] Furthermore, a carbohydrate that cannot be hydrolyzed to a simpler carbohydrate is referred to as a *monosaccharide*. Simple monosaccharides have the general formula $C_nH_{2n}O_n$ with one carbon in the form of either an aldehyde or ketone functional group. In addition to this functional group, the most common monosaccharides contain three to eight carbon atoms.[9] The nomenclature of these compounds reflects the two properties described above and examples may be seen below in Figure 4.

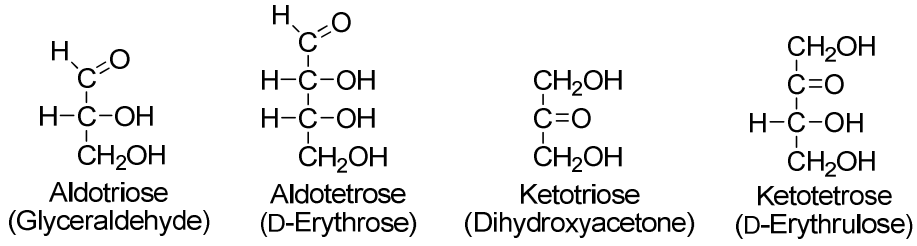

Figure 4: Examples of monosaccharide structures and nomenclature.

Furthermore, due to the chirality of these compounds, monosaccharides are assigned a D- or L- configuration depending. More conventionally, when drawn as a Fischer projection, the stereocenter farthest from the carbonyl carbon, the penultimate carbon, is chosen as the reference point. If the hydroxyl at this reference point is directed toward the right, then the stereoisomer is labeled D-. Similarly, if the hydroxyl group points to the left, the stereoisomer is labeled L- (Figure 5).[9]

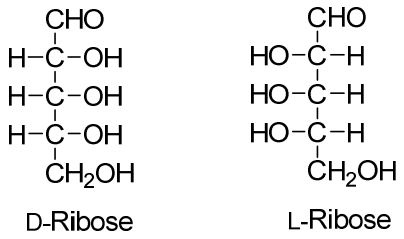

Figure 5: Fischer projections for D- and L- Ribose.

Within these monosaccharides, hydroxyl and carbonyl functional groups interact to form lactols, or cyclic hemiacetals. These ringed structures form readily when hydroxyl and carbonyl interactions produce a stable five- or six-membered ring. When this cycle formation occurs, a new stereocenter, called the anomeric carbon, is created at what was formerly the carbonyl carbon.[9] When discussing the terminology associated with carbohydrate chemistry, the designation β indicates the hydroxyl group of the anomeric carbon is on the same side of the ring when compared to the terminal carbon. Conversely, the designation α indicates the hydroxyl group of the anomeric carbon is on the opposite side of the ring when compared to the terminal carbon.[9] Lastly, 5-membered ring structures are termed furanose, while 6-membered ring structures are referred to as pyranose structures.[9] The information above is depicted below in Figure 6.

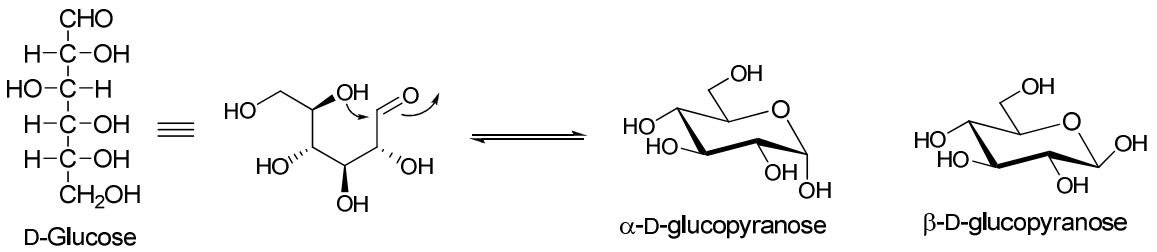

Figure 6: D-Glucose cyclization to α-D and β-D glucopyranose.

As illustrated above, the different structural forms of monosaccharides, either linear or cyclic, are in a constant state of equilibrium. One convenient method used to isolate sugars in their cyclic form is by the use of protecting groups. Figure 7 illustrates the use of isopropylidene protecting groups as a means to lock given sugars into their desired cyclic form(s).

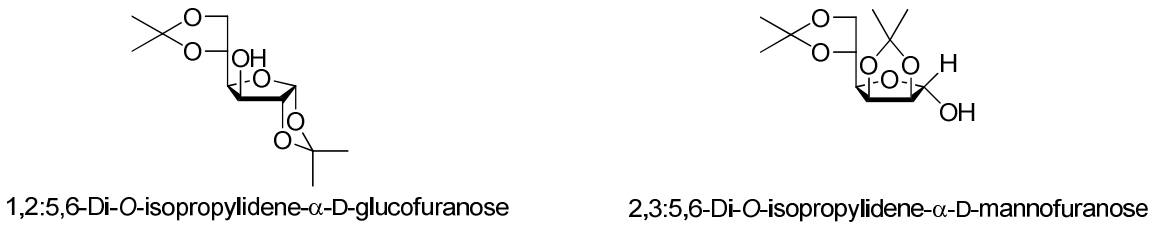

Figure 7: The use of isopropylidene as a protecting group.

Azide-derived Functionality

Attaching azides to various organic compounds allows for the introduction of an extremely wide range of functionality. Oftentimes, the resulting azide may simply be the end product, or goal, of the synthesis. One pharmaceutical example of an azide-containing compound is that of Zidovudine® (azidothymidine), a potent antiviral agent used in the treatment of HIV-infected individuals. In this example, azidothymidine, or

AZT (Figure 8), is a synthetic analogue of deoxythymidine where the 3' hydroxyl of the furanose ring has been synthetically replaced by an azide ($-N_3$) group.[10]

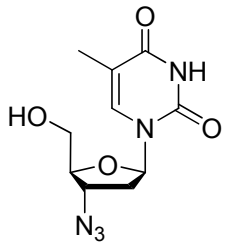

Figure 8: Structure of azidothymidine (AZT).

Extending beyond the azide functional group itself, numerous other compounds can be synthesized directly from azides by fairly straightforward reactions and functional group interconversions. Following the introduction of an azide group to a compound, functional group conversion to amides, heterocycles, and others is of great utility in the field of synthetic organic chemistry.

Amides

Amides are organic molecules in which an acyl group is bonded to an amine. They are classified as being either primary, secondary, or tertiary (Figure 9).[9]

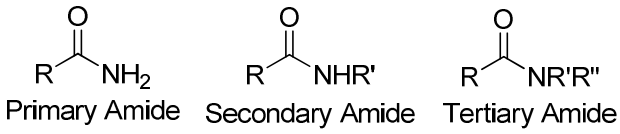

Figure 9: Structures of primary, secondary, and tertiary amides.

Amides are one of many biologically important nitrogen-containing functionalities. These structures are responsible for the principle linkages found in numerous naturally occurring products. Examples of these include polypeptides found in proteins and glycoproteins, which play extremely important roles in numerous cellular processes.[11]

Amide synthesis is a well-studied area of chemistry due its inherent application in natural product synthesis. An example is the resulting amide, or peptide bond, occurring between the amino acid asparagine and a protected sugar to yield the glycoprotein product seen below (Equation 6).[12]

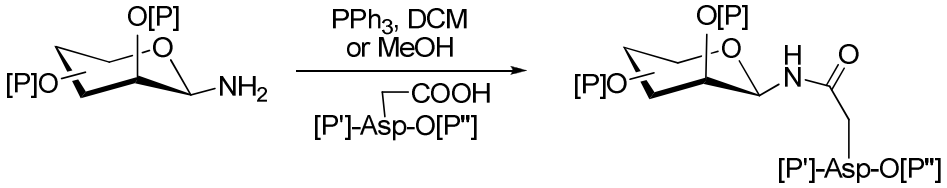

Equation 6.

Due to the wide range of products linked by amides, it is not surprising that their synthesis can occur through several different protocols. One of the most versatile methods of synthesizing amides is by the use of Staudinger-type reactions. These reactions involve attack on an azide by a phosphorus-containing compound acting as a Lewis base. This results in a loss of nitrogen (N_2) gas followed by the attack of an oxygen containing molecule on the phosphorus-bonded nitrogen. In the final step, a phosphine oxide byproduct is released and the resulting molecule, an amine or amide,

depends on the reagents used. In Scheme 4 below, a functionalized phosphine is used to produce the desired amide *via* the so-called Staudinger ligation.[13]

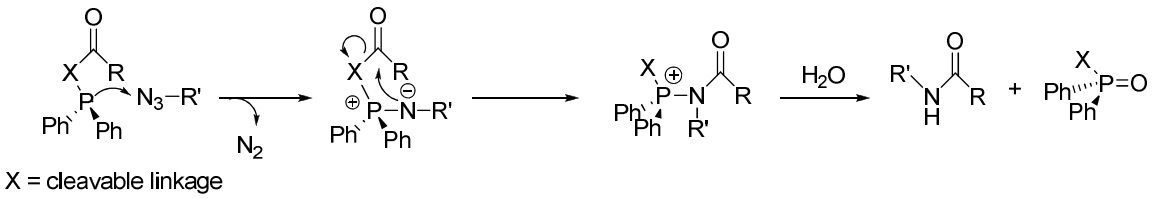

Scheme 4.

The Staudinger reaction is a very efficient as well as useful reaction for converting azides to amides.

Triazoles

Triazoles are a specific type of heterocycle; heterocycles being generally cyclic compounds in which the ring contains at least one non-carbon atom. In the case of triazoles, this non-carbon atom is nitrogen. Triazole compounds are aromatic heterocycles and include either one of a pair of isomeric chemical compounds. They are five-membered ring structures containing two carbon atoms and three nitrogen atoms. They follow the general molecular formula $C_2H_3N_3$ and are named based upon where the nitrogen atoms are located in the ring (Figure 10).[9]

Figure 10: 1,2,3- and 1,2,4-triazole isomers.

Traditionally, a 1,2,3-triazole can be synthesized through a dipolar cycloaddition reaction between an azide and an alkyne (Huisgen cycloaddition). More specifically, in attempts to control the regioselectivity of the process, copper (I) catalysts are employed in order to facilitate the regiospecificity leading exclusively to the 1,4-disubstituted 1,2,3-triazole product.[14] Equation 7 below illustrates the above in a reaction between a terminal alkyne and glycosyl azide to yield the glycosyl-1,2,3-triazole product.[15]

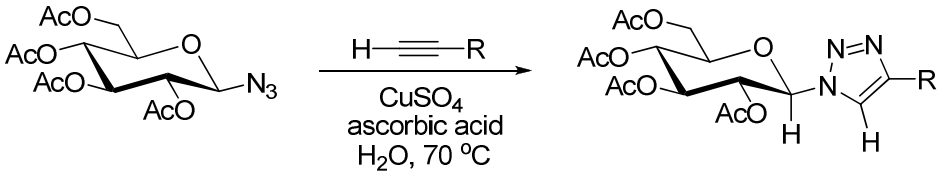

Equation 7.

Lastly, triazoles are of great clinical importance in the field of medicinal chemistry. These compounds serve as potent antifungal agents, for example, by inhibiting the biosynthesis of ergosterol, an essential component needed to maintain proper fungal cell membrane structure and integrity. An example of such a drug is Itraconazole® and is pictured below in Figure 11.[9]

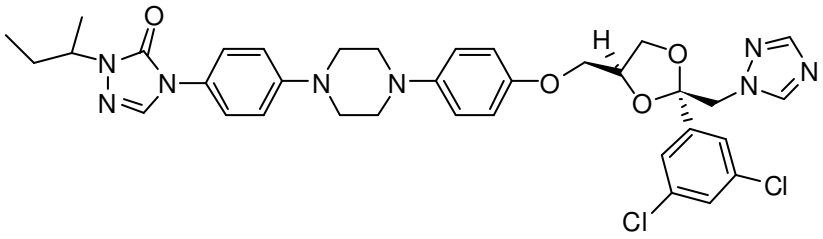

Figure 11: Structure of the antifungal drug Itraconazole.

As mentioned previously, amides as well as triazoles are merely two of many nitrogen functional groups that can be synthesized once an azide has been introduced into a compound. With nitrogen-containing compounds ubiquitous in the fields of medicinal and natural product chemistry, chemists will always need rapid, inexpensive, and material-efficient ways of introducing nitrogen into compounds.

Statement of Problem

In the fields of medicinal and biological chemistry, nitrogen-containing compounds occur frequently in numerous natural and essential processes. One class of these compounds in particular is organic azides. Traditional synthesis of azide-containing molecules can be a time-consuming process involving intermediate work-up and isolation steps. This research will explore a novel method for azide synthesis, from alcohol containing compounds, that consists of only a "one-pot" process, which is rapid as well as material-efficient.

Results and Discussion

Previous azidation with *p*-ABSA

Based on previous research conducted at Youngstown State University, it was shown that during an attempted diazo ester synthesis using phenacyl ester sugar **1** as starting material, a mixture was formed containing the following four compounds: diazo ester **2**, phenacyl ester **1**, azide **3**, and lactol **4** (Equation 8).[8]

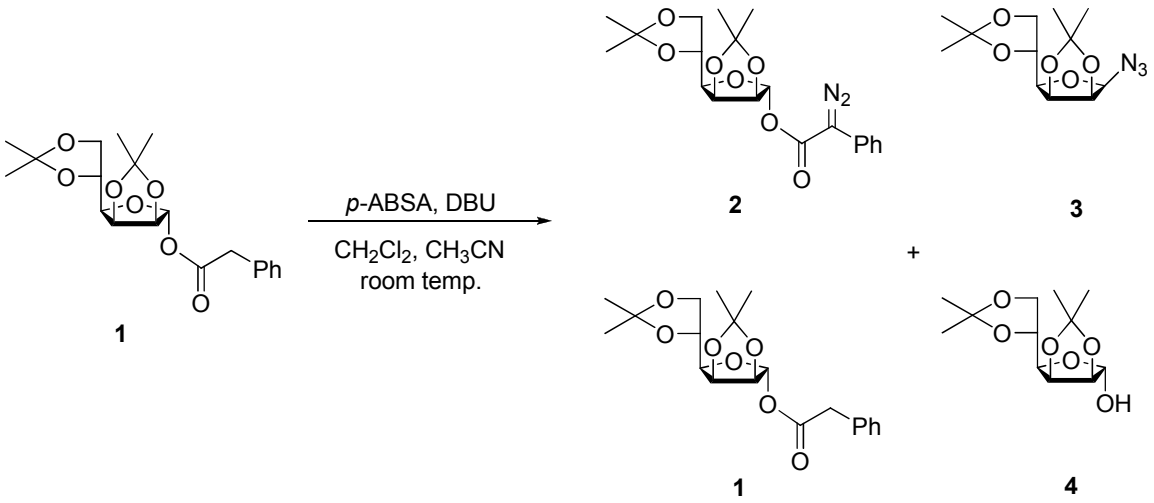

Equation 8.

Of the four compounds formed by the reaction, it was the azide **3** that was not anticipated. Lactol formation (**4**) in the reaction mixture was shown to be the result of 1,8-diazobicyclo[5.4.0]undec-7-ene (DBU) induced cleavage of the ester bond in **1**. It was this fact which lead to the following hypothesis: once the ester group of **1** was cleaved to an alcohol by the base DBU, the alcohol **4** was able to react with *p*-ABSA (Figure 12) to produce **3**.[8]

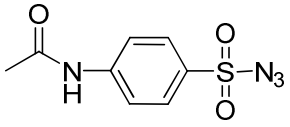

Figure 12: Structure of 4-Acetamidobenzene sulfonyl azide (*p*-ABSA).

Knowing the fact that sulfonate esters are commonly used in traditional azide synthesis, the following reaction mechanism was hypothesized based on *in situ* generation of the azide nucleophile (Figure 13).

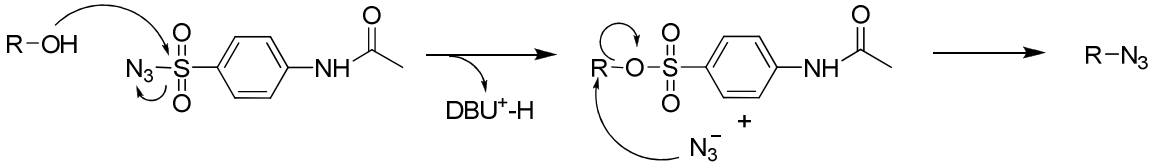

Figure 13: Mechanism for azide formation using *p*-ABSA, DBU, and R-OH.

Following the appearance of the azide by-product **3** in the diazo ester (**2**) synthesis above, other alcohol containing compounds were used in order to further elucidate the mechanism of azide formation. Equation 9 depicts the reaction between 1,2:3,4-di-*O*-isopropylidene-α-D-galactopyranose **5** and *p*-ABSA to form the sulfonate ester intermediate **6** but not the azide.[8]

Equation 9.

After numerous trials that involved varying solvent systems, amounts of azide transfer reagent *p*-ABSA, and starting materials used, standard reaction parameters were established for the "one-pot" azide synthesis (Equation 10).[8]

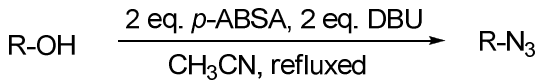

Equation 10.

Based on these standard reaction conditions, primary and secondary azidodeoxy sugar compounds were isolated with percent yields of around 50% maximum. Additionally, the primary and secondary sulfonate ester intermediates were sometimes isolated with typical percent yields of 50% - 80%.[8]

Experimentation with bases

In attempts to increase yields of azide formation via "one-pot" synthetic techniques, experimentation with several nitrogen-containing basic compounds was undertaken. In the initial reactions, 4-biphenylmethanol **7**, a primary alcohol, was used in conjunction with *p*-ABSA, the azide transfer reagent. The reactions were carried out in the solvent dimethyl formamide (DMF) for a duration of 3 hrs. The list of basic compounds tested in Equation 11 can be seen below in Table 1.

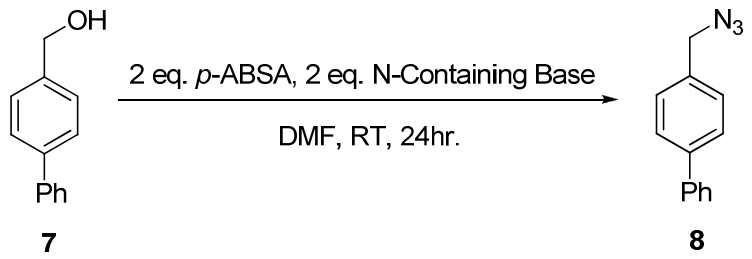

7 **8**

Equation 11.

Table 1. List of nitrogen-containing bases tested for "one-pot" azide synthesis.

Structure	Name	% Yield **8**
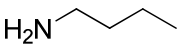	Butylamine	0
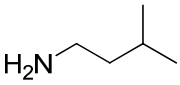	Isoamylamine	0
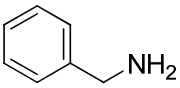	Benzylamine	0
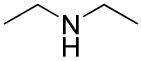	Diethylamine	0
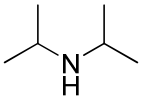	Diisopropylamine	0
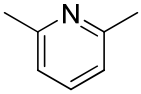	2,6-dimethylpyridine	0
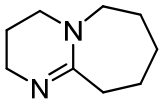	1,8-diazobicyclo[5.4.0]undec-7-ene	0

As indicated in Table 1, no azide product (**8**) was produced during the course of these azidation reactions. Additionally, it became apparent that increasing the equivalents of both *p*-ABSA and the base being tested resulted in no significant azide product formation. It was this observation which led to the indication that possibly a side reaction between the bases in use and *p*-ABSA was occurring and thus hindering desired product formation. In attempts to support this conclusion, DBU and *p*-ABSA were left to react in a vessel in the absence of a hydroxyl group as indicated in Equation 12.

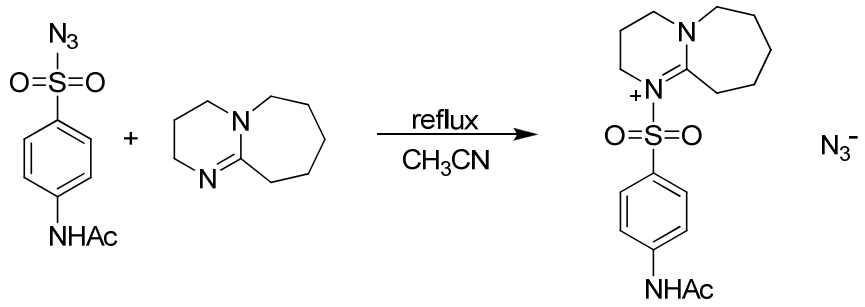

Equation 12.

While the reaction refluxed, IR spectroscopy was employed to monitor the progress of the reaction after one hour. Spectroscopy data indicated azide absorption at 2020 cm^{-1} which is significantly lower than that of *p*-ABSA alone at 2128 cm^{-1}. This shift toward the suspected anionic form of the azide also is supported by the fact that NaN_3 in solution alone exhibits absorption at 2000 cm^{-1}. While this *in situ* generation of anionic azide is troublesome to the goal of azidation in terms of simple organic alcohols, it may be useful for azidation reactions involving alkyl halides in order to avoid certain problems such as solubility issues associated with NaN_3 use (Equation 13).

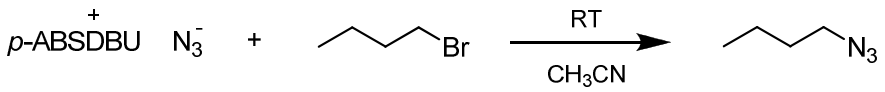

Equation 13.

Due to the lack of success in azidation reactions involving the conversion of **7** to **8**, research efforts shifted to the use of non-nitrogen-containing bases in an attempt to azidate alcohol-containing compounds in a novel, "one-pot" manner.

NaH-based azidation of simple primary alcohols

Following the failure of the various nitrogen-containing bases in the "one-pot" synthetic technique, it became clear that nitrogen sources are most likely out-competing alcohol functional groups as nucleophiles directed toward displacement of the azide group from *p*-ABSA. With the failure of the sulfonate ester intermediate to form, this amine-azide transfer reagent interaction severely limits desired azide product formation and subsequently product yields. With this known, research began to focus on sodium hydride as the next base of choice. As was the case with the nitrogen-containing base experiments, all reaction conditions were held constant at first, while only the use of sodium hydride was explored (Equation 14).

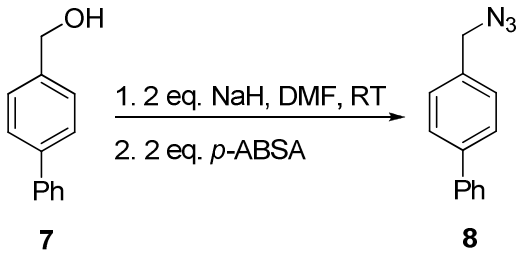

7 **8**

Equation 14.

Following the success of early reactions, equivalent amounts of both *p*-ABSA and NaH were varied in addition to the duration of time the reaction was left to stir at room temperature. After several trials, the conditions set forth in Equation 15 became the standard reaction conditions for all alcohol-containing compounds subjected to the novel "one-pot" synthetic technique.

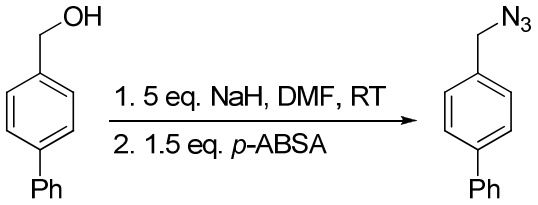

7 **8**

Equation 15.

Though 5 equivalents of NaH is a large excess, the reagent is extremely inexpensive as well as readily available. Once the NaH and **7** have been left to react at room temperature for 45 minutes, the azide transfer reagent *p*-ABSA is introduced into the reaction mixture to generate **8**. Following the addition of *p*-ABSA after this 45 minute period, TLC (1:1 hexanes: ethyl acetate) of the reaction mixture showed complete consumption of **7** after a period of three hours. Appearance of **8** (R_f = 0.69) (1:1

hexanes: ethyl acetate) was monitored by the staining of TLC plates in *p*-anisaldehyde which yields a bright yellow spot upon burning corresponding to formation of **8**. ^{1}H NMR analysis of the colorless oil (product **8**, 90% yield) indicates a two proton singlet at 4.47 ppm as well as a nine proton multiplet from 7.32-7.78 ppm which corresponds to data previously reported in the literature.[16] The appearance of IR absorption at 2099 cm^{-1} for the azide functional group of **8**, along with the disappearance of absorption at 3600 cm^{-1} for the alcohol functional group of **7**, was observed to confirm that azidation was successful. Finally, mass spectrometry data confirmed the formation of the azide product **8**, with a peak at 233.10 *m/z*, which is the calculated mass plus a sodium and hydrogen ion.

Next, additional simple primary alcohol systems were explored using the established reaction conditions. Benzene rings were included in the starting materials whenever possible due to the ease in monitoring the reaction progress via TLC due to the UV visibility of these compounds. In Equation 16, 1,4-benzenedimethanol **9**, a diol compound, was subjected to the same reaction conditions as set forth with Equation 15 with the exception of doubling the amounts of *p*-ABSA and NaH used with respect to the amount of alcohol.

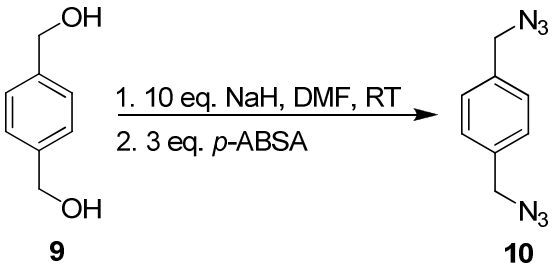

9 **10**

Equation 16.

In the case of Equation 16, and as mentioned for **7** to **8** conversion, TLC (1:1 hexanes: ethyl acetate) indicated complete consumption of **9** after a period of three hours following the addition of *p*-ABSA. Appearance of **10** (R_f = 0.68) (1:1 hexanes: ethyl acetate) was monitored by staining the plate with *p*-anisaldehyde which yielded a bright yellow spot upon burning corresponding to the azide. Isolation of product **10** as a clear, colorless oil by flash column chromatography was achieved in 84% yield. ^{1}H NMR indicated a four proton singlet at 4.45 ppm and a four proton singlet for aryl protons at 7.39 ppm. These values also correspond to those in the literature for the previously reported compound.[17] The appearance of IR absorption at 2099 cm^{-1} for the azide functional group of **10**, along with the disappearance of absorption at 3600 cm^{-1} for the alcohol functional group of **9**, was observed to confirm that azidation was successful. Mass spectrometry data also confirmed the formation of the azide product **10**, with a peak at 212.20 *m/z*, which is the calculated mass plus a sodium and hydrogen ion.

For completeness, 1,3-benzenedimethanol **11**, was tested in the "one-pot" synthetic technique in order to evaluate an additional diol system in which the alcohol functional groups are brought closer together as compared to **9** (Equation 17).

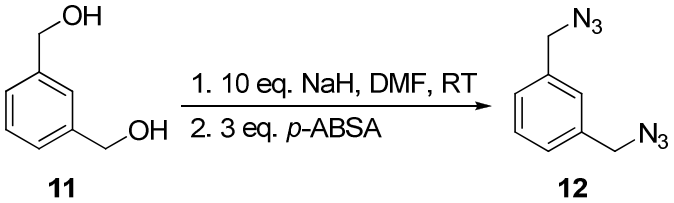

11 **12**

Equation 17.

As in Equations 15 and 16, TLC (1:3 hexanes: ethyl acetate) showed complete consumption of **11** after a period of three hours following the addition of *p*-ABSA to the reaction mixture. Appearance of **12** (R_f = 0.71) (1:3 hexanes: ethyl acetate) was monitored by staining with *p*-anisaldehyde which yielded a bright yellow spot upon burning corresponding to the azide. Isolation of product **12** as a clear and colorless oil was achieved in 86% yield while ^{1}H NMR analysis indicated a four proton singlet at 4.47 ppm and a four proton multiplet for aryl protons from 7.33-7.45 ppm. These values correspond to those in the literature for the previously reported compound.[18] The appearance of IR absorption at 2100 cm^{-1} for the azide functional group of **12**, along with the disappearance of absorption at 3600 cm^{-1} for the alcohol functional group of **11**, was observed to confirm that azidation was successful. Mass spectrometry data confirmed the formation of the azide product **12**, with a peak at 212.20 *m/z*, which is the calculated mass plus a sodium and hydrogen ion.

With such success in the azidation of primary alcohol systems, further research focused on the effectiveness of the "one-pot" synthetic technique as applied to simple secondary alcohol systems.

NaH based azidation of simple secondary alcohols

Following the azidation of **7**, **9**, and **11** to produce the desired azides **8**, **10**, and **12** in acceptable yields**,** simple secondary alcohols became the focus of research in order to further study the usefulness of the "one-pot" synthetic method. In the initial experimentation with simple carbohydrate-derived secondary alcohols, *p*-ABSA was shown to be unsuccessful in its ability to convert starting material to the respective azide

product. Following this observation, various azide transfer reagents similar in both chemical structure and properties to *p*-ABSA were considered for use in all further secondary alcohol azidation reactions. In hopes of decreasing reaction times as well as increasing product yields, 4-nitrobenzene sulfonyl azide (Figure 14) was selected as the alternative azide transfer reagent to *p*-ABSA. With the *para* functional group of *p*-NBSA much more electron-withdrawing than the corresponding *para* group of *p*-ABSA, it was anticipated that the intermediate sulfonate ester, once formed, would be much more prone to displacement by the *in situ* generated azide nucleophile.

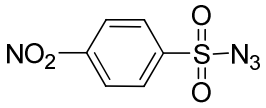

Figure 14: Structure of 4-nitrobenzene sulfonyl azide (*p*-NBSA).

p-NBSA was synthesized via a simple substitution reaction wherein the 4-nitrobenzene sulfonyl chloride was left to react with excess amounts of NaN_3 in anhydrous methanol for 24 hours (Equation 18).

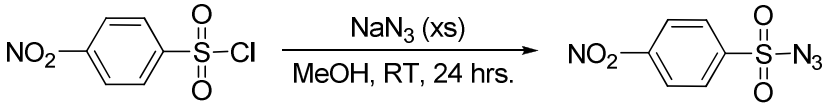

Equation 18.

In order to assure purity of the *p*-NBSA synthesized, the yellow crystalline solid was successfully re-crystallized from methanol before use in further "one-pot" azidation reactions. The crystal structure of *p*-NBSA is shown below in Figure 15.

4-nitrobenzene sulfonyl azide (*p*-NBSA)	X-Ray crystal structure of *p*-NBSA
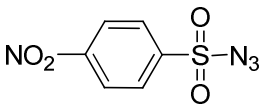	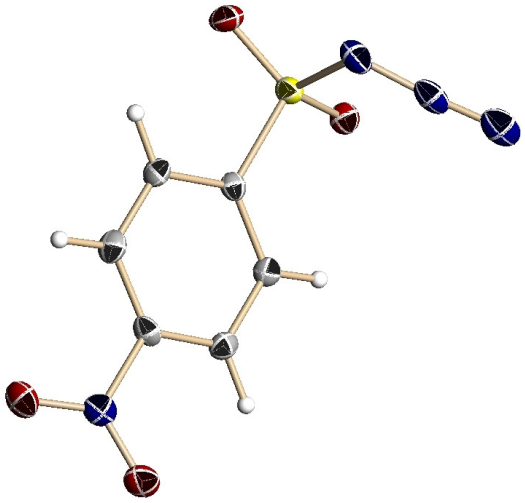

Figure 15: X-Ray crystal structure of 4-nitrobenzene sulfonyl azide (*p*-NBSA).

Once the purity of the azide transfer reagent had been verified, experimentation for "one-pot" azidations using secondary alcohols began with (±) 1-indanol (**13**). As indicated in Equation 19 below, a slightly larger amount of NaH was used as compared to similar azidation reactions involving simple primary alcohols.

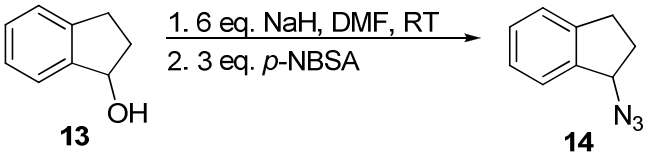

Equation 19.

After NaH and **13** had been left to react at room temperature for 45 minutes, the azide transfer reagent *p*-NBSA was introduced into the reaction mixture to generate **14**.

Following the addition of *p*-NBSA after this 45 minute period, TLC (20:1 hexanes: ethyl acetate) indicated complete consumption of starting material after three hours. Appearance of **14** (R_f = 0.45) (20:1 hexanes: ethyl acetate) was monitored by staining with *p*-anisaldehyde which yielded a bright yellow spot upon burning corresponding to formation of **14**. ^{1}H NMR spectra of the clear and colorless oil (product **14**, isolated in 80% yield), indicated a one proton doublet of doublets at 5.02 ppm as well as a four proton multiplet in the aryl range of 7.40-7.28 ppm. These values also correspond to those in the literature for the previously reported compound.[19] In the case of the single proton doublet of doublets, coupling constants for the signal were calculated to be 4.30 and 7.23 Hz. The appearance of IR absorption at 2094 cm^{-1} for the azide functional group of **14**, along with the disappearance of absorption at 3600 cm^{-1} for the alcohol functional group of **13**, was observed to confirm that azidation was successful. Finally, mass spectrometry data also confirmed the formation of the azide product **14**, with a peak at 183.00 *m/z*, which is the calculated mass plus a sodium and hydrogen ion.

Although the yield of **14** is acceptable, one unanticipated product was seen to be produced. With the nitro group of *p*-NBSA being so strongly electron-withdrawing, interaction between the oxygen atom of **13** and *p*-NBSA generated an aromatic nucleophilic substitution (S_NAr) product (**15**) (Figure 16) in addition to the anticipated sulfonate ester intermediate.

(**15**)	X-Ray crystal structure of (**15**)
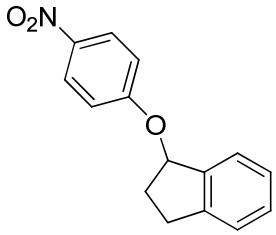	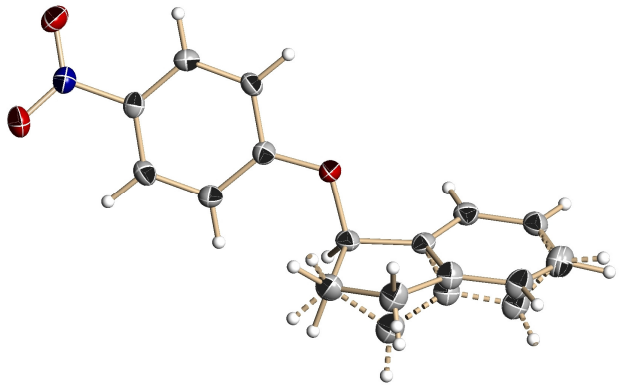

Figure 16: X-Ray crystal structure of S_NAr generated byproduct (**15**).

Based on literature regarding this type of nucleophilic substitution, it was proposed that the oxygen atom of **13**, acting as a nucleophile, attacked C-1 of the aryl ring rather than the sulfur atom which bears the azide leaving group. This direct attack on carbon, rather than sulfur, produces a resonance-stabilized carbanion intermediate prior to SO_3N_3 group displacement.[20] This process is depicted in Figure 17.

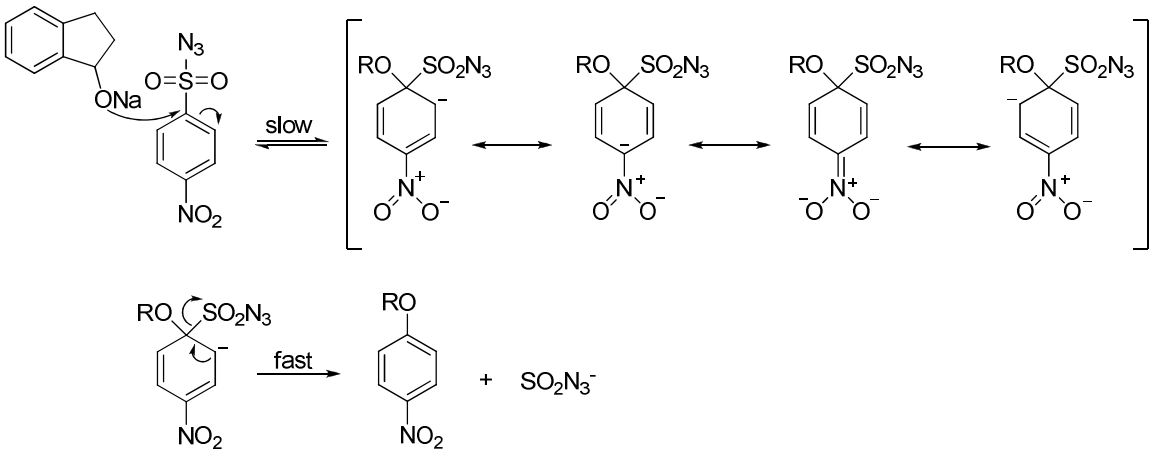

Figure 17: Proposed mechanism for formation of **15**.

In addition to the S_NAr reaction taking place, one additional reaction was observed in which DMF, the solvent used, reacted with *p*-NBSA to form the structure shown below in Figure 18.

(**16**)	X-Ray crystal structure of (**16**)
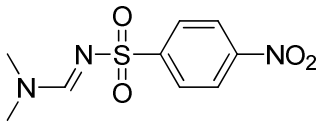	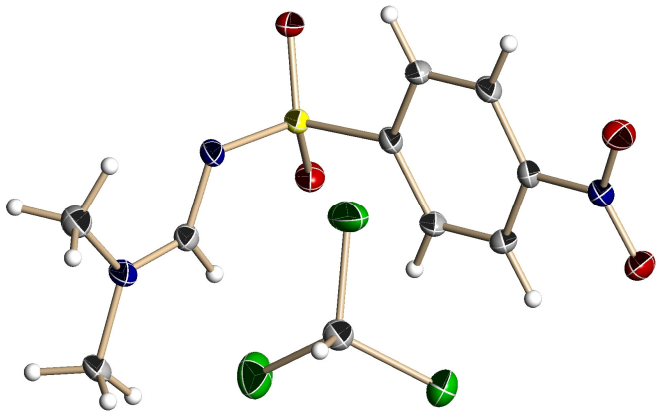

Figure 18: X-Ray crystal structure of DMF and *p*-NBSA reaction product (**16**).

Formation of **16** led to questioning of the mechanism by which it was produced. It appears as though an imine-forming-aza-Wittig type reaction had occured. However, while C=N bond formation along with N_2 loss support this statement, loss of the carbonyl oxygen atom from the original DMF molecule does not.

Though the overall yield of **14** produced by the azidation reaction was acceptable, the above two by-products lend insight as to where part of the product yield might be lost in terms of side reactions. It is also interesting to note that these reactions were not seen when dealing with *p*-ABSA. It remains clear that as the electron-withdrawing nature of

the *para* group on the azide transfer reagent increases, reactivity for not only azide formation but other product formation increases as well.

Finally, the secondary alcohol 2-indanol **17** was tested in order to see how azidations would be affected as the alcohol functional group placement moved away from the benzylic position (Equation 20).

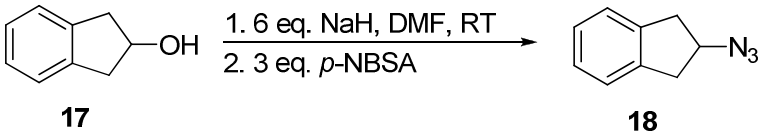

17 **18**

Equation 20.

After NaH and **17** had been left to react at room temperature for 45 minutes, the azide transfer reagent *p*-NBSA was introduced into the reaction mixture to generate **18**. Following the addition of *p*-NBSA after this 45 minute period, TLC (20:1 hexanes: ethyl acetate) showed complete consumption of **17** within three hours. Appearance of product (R_f = 0.42) (20:1 hexanes: ethyl acetate) was monitored by staining in *p*-anisaldehyde which yielded a bright yellow spot upon burning corresponding to the azide. The ^{1}H NMR data of the clear and colorless oil (product **18**, isolated in 86% yield), indicates a one proton multiplet at the range of 4.84-4.43 ppm as well as a four proton multiplet in the aryl region of 7.25-7.11 ppm. These values also correspond to those reported in the literature for the identical compound.[21] The appearance of IR absorption at 2097 cm^{-1} for the azide functional group of **18**, along with the disappearance of absorption at 3600 cm^{-1} for the alcohol functional group of **17**, was observed to confirm that azidation was successful. Finally, mass spectrometry data also confirmed the formation of the azide

product **18**, with a peak at 183.00 *m/z*, which is the calculated mass plus a sodium and hydrogen ion.

Following the successful characterization and isolation of azide products from the azidations discussed above, focus turned to protected cyclic sugar compounds to test the utility of the "one-pot" synthetic technique beyond the scope of only simple alcoholic compounds.

Azidation of protected carbohydrates

Due to the observed by-products formed during the azidation reactions of secondary alcohols using *p*-NBSA as the azide transfer reagent, parallel azidation reactions were performed using both *p*-ABSA and *p*-NBSA for selected protected sugars. First, 1,2:5,6-di-*O*-isopropylidene-α-D-glucofuranose (**19**) was studied as shown below in Equations 21 and 22.

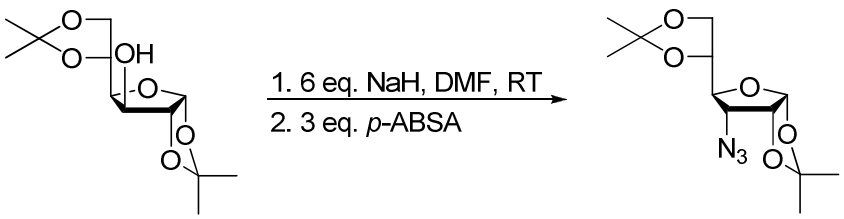

19 **20**

Equation 21.

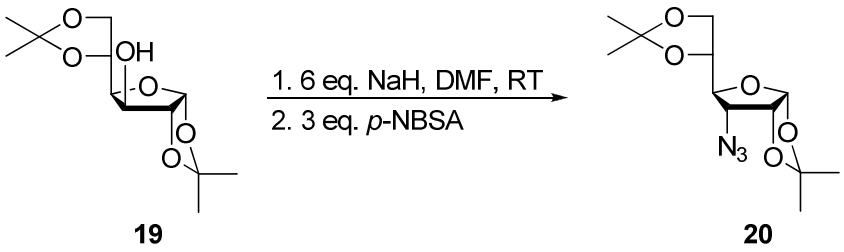

19 **20**

Equation 22.

For this protected sugar (**19**), the unprotected hydroxyl group is not only a secondary alcohol but is also extremely hindered due to the close proximity of the two isopropylidene protecting groups. For both Equations 21 and 22, no azide product formation was observed. Rather, formation of the sulfonate ester intermediates, **21** and **22**, were observed as the major products for the respected reactions (Figure 19).

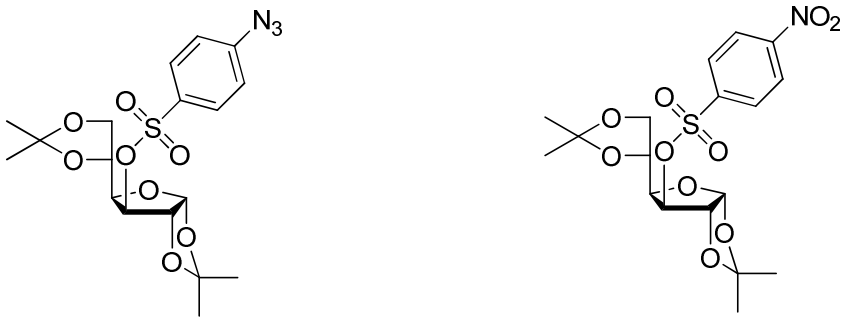

21 **22**

Figure 19: Major products for the azidation of **19** using *p*-ABSA and *p*-NBSA.

Prior to isolation of the *p*-ABSA-derived sulfonate ester intermediate, **21**, it was expected that the intermediate compound would exhibit the acetamido group at the *para* position as had been indicated in previous research.[8] However, ^{1}H NMR data lacked the presence of signals (s, 3H, -CH_3 α to C=O and s, 1H, N-H) which would support the

retention of the *para* acetamido group in the product. With these signals absent, but retention of the two 2H doublets at 7.94 and 7.16 ppm (similar to the initial *p*-ABSA reagent) indicated, it became clear that another functional group, capable of splitting the four aryl protons, just as the initial acetamido group had done, was now present. Further analysis by mass spectrometry and IR spectroscopy indicated the presence of the *in situ* generated azide group as the moiety that had replaced the original *para* acetamido group. IR data indicated absorption at 2118 cm^{-1} and mass spectrometry also confirmed the formation of the azide intermediate **21** with a peak at 464.10 *m/z*, which is the calculated mass of **21** plus a sodium ion.

As in the simple alcohol systems discussed above, after NaH and **19** had been left to react at room temperature for 45 minutes, *p*-ABSA or *p*-NBSA depending on the reaction studied, was introduced into the reaction mixture. Following the addition of *p*-ABSA after this 45 minute period, TLC (4:1 hexanes: ethyl acetate) showed complete consumption of **19** within 24 hours. Appearance of **21** (R_f = 0.20) (4:1 hexanes: ethyl acetate) was monitored by the staining of TLC plates with 5% H_2SO_4 in MeOH which yielded a dark brown spot upon burning corresponding to the sulfonate ester intermediate (**21**). The ^{1}H NMR data for the clear crystalline solid (product **21**, isolated in 76% yield), indicated two, aryl-2H doublets at 7.94 and 7.16 ppm. Finally, as mentioned previously, mass spectrometry data also confirmed the formation of the **21** with a peak at 464.10 *m/z*, which is the calculated mass plus a sodium ion.

Similarly, appearance of **22** (R_f = 0.25) (4:1 hexanes: ethyl acetate) was monitored by staining with 5% H_2SO_4 in MeOH which yielded a dark brown spot upon burning corresponding to the sulfonate ester intermediate (**22**). The ^{1}H NMR data of the

yellow crystalline solid (product **22**, isolated in 71% yield), indicated the presence of two 2H doublets in the aryl region at 8.22 and 7.08 ppm. For both doublet signals, the coupling constants were calculated to be 9.28 Hz. Mass spectrometry data also confirmed the formation of **22** with a peak at 469.40 *m/z*, which is the calculated mass plus a sodium ion and proton. Finally, all signals included in ^{1}H and ^{13}C NMR data corresponded to those previously reported for the synthesis and isolation of **22**.[8]

Following the reactions using 1,2:5,6-di-*O*-isopropylidene-α-D-glucofuranose (**19**), 1,2:3,4-di-*O*-isopropylidene-α-D-galactopyranose (**5**) was studied in a similar manner. The "one-pot" azidation reactions conducted using **5** are shown below in Equations 23 and 24.

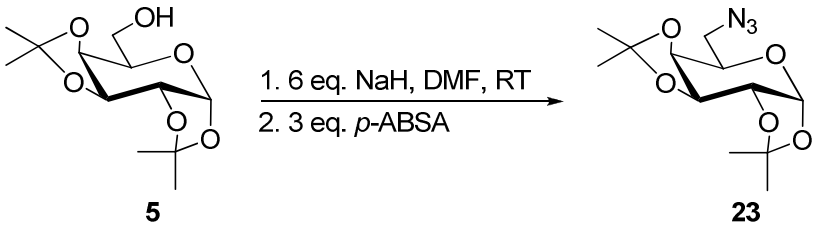

Equation 23.

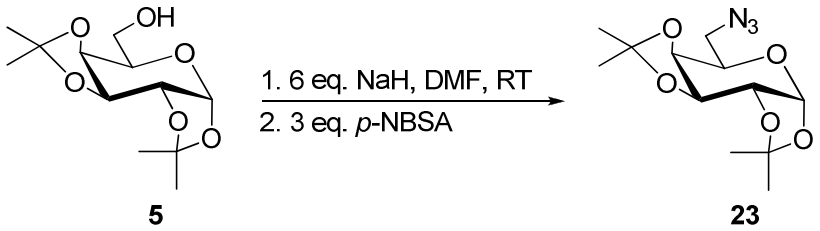

Equation 24.

Unlike **19**, the azidation of **5** involved an unprotected alcohol functional group that was primary rather than secondary in nature. However, similar to **19**, the alcohol functional group is extremely hindered due to the surrounding isopropylidene protecting groups. With that said, it was believed that the exposed primary hydroxyl group of the protected sugar would be more prone to undergoing azidation based on the proposed S_N2 mechanism of the "one-pot" azidation method. For both Equations 23 and 24 however, no azide product formation was observed. Rather, formation of the sulfonate ester intermediates, **24** and **25**, were observed as the major products for the respected reactions (Figure 20).

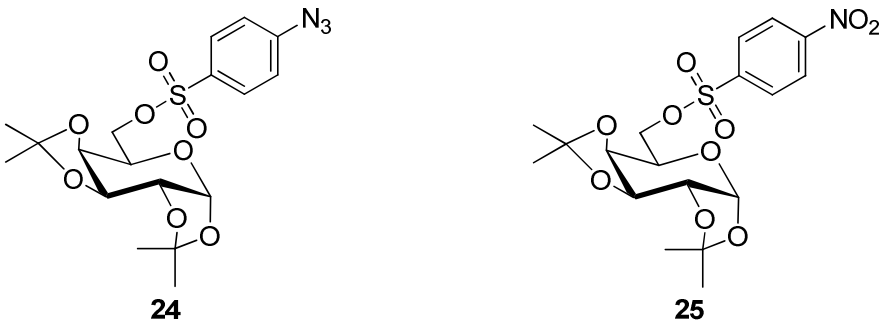

Figure 20: Major products for the azidation of **5** using *p*-ABSA and *p*-NBSA.

As above, after NaH and **5** had been left to react at room temperature for 45 minutes, *p*-ABSA or *p*-NBSA depending on the reaction being studied, was introduced into the reaction mixture. Following the addition of *p*-ABSA, TLC (4:1 hexanes: ethyl acetate) showed complete consumption of **5** within 24 hours. Appearance of **24** (R_f = 0.19) (4:1 hexanes: ethyl acetate) was monitored by staining with 5% H_2SO_4 in MeOH which yielded a dark brown spot upon burning corresponding to the sulfonate ester intermediate (**24**). The ^{1}H NMR data for the clear and colorless oil (product **24**, isolated

in 84% yield), indicated two 2H doublets in the aryl regions of 7.91 and 7.16 ppm. As was the case for the *p*-ABSA based azidations of **19**, the acetamido group of the original azide transfer reagents was seen to be replaced by the *in situ* generated azide nucleophile. Mass spectrometry data also confirmed the formation of the **24** with a peak at 464.20 *m/z*, which is the calculated mass plus a sodium ion. Finally, an IR absorption at 2129 cm^{-1} also supports the formation of **24**.

Similarly, appearance of **25** (R_f = 0.27) (4:1 hexanes: ethyl acetate) was monitored by staining with 5% H_2SO_4 in MeOH which yielded a dark brown spot upon burning corresponding to the sulfonate ester intermediate (**25**). The ^1H NMR data for the yellow solid (product **25**, isolated in 83% yield), indicated the presence two 2H doublets in the aryl region at 8.19 and 7.02 ppm. For doublet signals, the coupling constant were calculated to be 9.28 and 9.32 Hz. Mass spectrometry data also confirmed the formation of **25** with a peak at 469.30 *m/z*, which is the calculated mass plus a sodium ion and proton. Finally, all signals included in ^1H and ^{13}C NMR data corresponded to those previously reported for the synthesis and isolation of and **25**.[8]

Finally, 2,3:5,6-di-*O*-isopropylidene-α-D-mannofuranose (**26**), was studied to assess the ability of the "one-pot" azidation method at an anomeric carbon position. The "one-pot" method conducted using **26** is shown below in Equation 25.

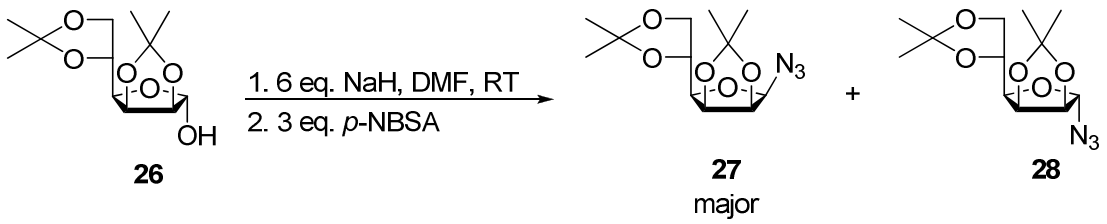

26 **27** major **28**

Equation 25.

As in the carbohydrate systems discussed above, after NaH and **26** had been left to react at room temperature for 45 minutes, *p*-NBSA was introduced into the reaction mixture. Following the addition of the azide transfer reagents after this 45 minute period, TLC (4:1 hexanes: ethyl acetate) showed complete consumption of **26** within 24 hours. Appearance of **27** (R_f = 0.19) and **28** (R_f = 0.38) (4:1 hexanes: ethyl acetate) was monitored by the staining of TLC plates with 5% H_2SO_4 in MeOH which yielded a dark brown spot upon burning corresponding to the azide products (**27** and **28**). Both ^{1}H and ^{13}C NMR data corresponded to that previously reported for the synthesis and isolation of both anomers.[8] Additionally, mass spectrometry data also confirmed the formation of both anomers with peaks at 308.10 *m/z*, which is the calculated mass plus a sodium ion. Finally, IR absorptions at 2126 and 2116 cm^{-1} support the formation of both **27** and **28** in 79% yield total.

In conclusion, it was shown the novel "one-pot" azidation method was able to successfully convert both primary and secondary simple alcohols to their corresponding azides. Additionally, it was shown to be somewhat successful in the azidations of protected carbohydrate compounds in which a free hydroxyl group was left exposed. In the case of these sugar compounds, the success of azidation was shown to be directly dependent on the steric crowding and thus accessibility of the *in situ* generated azide nucleophile to access the sulfonate ester intermediate. For both simple alcohols and protected carbohydrate compounds, unexpected intermediates and byproducts were isolated despite the fact azide product yields were acceptable. In terms of further research, additional simple alcohol compounds, both primary and secondary, could be explored. Additionally, variations of functional groups at the *para* position of the azide

transfer reagent would be a useful way to elucidate and study more byproducts and side reactions while attempting to find the reagent which minimizes these occurrences and affords the highest azide product yield. Finally, the effect of introducing further reactants beyond the azide transfer reagents could be explored in order to expand the scope of the "one-pot" synthetic method to additional compounds. Functional groups such as amides and triazoles, which are easily derived from azides through well studied synthetic techniques, could be likely candidates for this type of research.

Experimental

General Procedures

Reactions were analyzed by TLC on Whatman aluminum-backed plates. Purifications *via* flash column chromatography used 70-270 mesh 60-Å silica gel. Nuclear Magnetic Resonance spectra were recorded on samples dissolved in $CDCl_3$ or DMSO using Bruker Avance II and Avance III systems, at a frequency of 400 MHz for ^1H spectra and 100 MHz for ^{13}C spectra. All chemical shifts were recorded in parts per million (ppm). Signals are labeled as follows: s (singlet), d (doublet), dd (doublet of doublets), ddd (doublet of doublet of doublets), m (multiplet) and coupling constants (*J*) are measured in Hertz. All mass spectra were obtained through the use of a Bruker Esquire LC-MS instrument. Infrared spectra were recorded on a Thermo Electron Corporation IR 200 spectrophotometer.

Experimentation with bases

Synthesis of 4-(azidomethyl)biphenyl (8) from 4-biphenylmethanol (7).

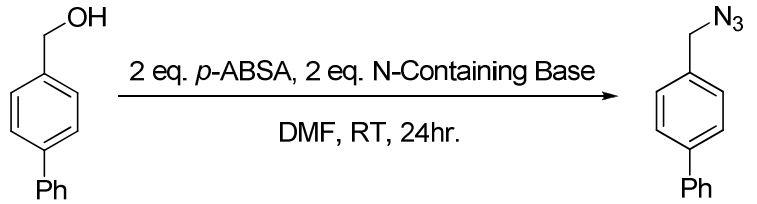

7 **8**

In a 100 mL round-bottom flask equipped with septum and magnetic stir bar, 4-biphenylmethanol (0.92 g, 5.0 mmol) (**7**) was dissolved in anhydrous DMF (30 mL). The

flask was flushed with N_2 gas and immediately *p*-ABSA (2.40 g, 10.0 mmol) and the appropriate nitrogen-containing base (Table 1) were added. The reaction was left to stir at room temperature for three hours and was monitored by TLC (hexanes: ethyl acetate) to indicate the amount of starting material **7** consumed. None of the listed bases were effective in producing the desired azide product (**8**).

***In situ* generation of anionic azide from *p*-ABSA and DBU**

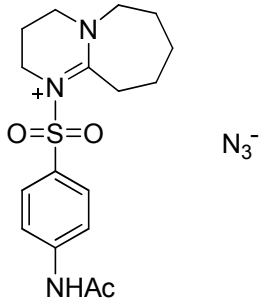

In a 100 mL round-bottom flask equipped with septum and magnetic stir bar, *p*-ABSA (1.20 g, 5.0 mmol) was dissolved in CH_3CN (30 mL). The flask was flushed with N_2 gas and immediately DBU (0.75 mL, 5.0 mmol) was syringed into the reaction vessel. IR spectroscopy was used to monitor the progress of the reaction after one hour and samples used for analysis were not worked up prior to testing. Data indicated azide absorption at 2020 cm^{-1} which suggests *in situ* generation of anionic azide.

NaH-based azidation of simple primary alcohols

Synthesis of 4-(azidomethyl)biphenyl (8) from 4-biphenylmethanol (7).

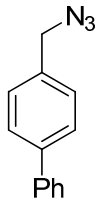

8

In a 100 mL round-bottom flask equipped with septum and magnetic stir bar, 4-biphenylmethanol (0.95 g, 5.1 mmol) (**7**) was dissolved in anhydrous DMF (30 mL). The flask was flushed with N_2 gas and sodium hydride (1.02 g, 25.5 mmol) was added. The reaction was left to stir at room temperature for one hour under a N_2 atmosphere. At one hour, 4-acetamidobenzene sulfonyl azide (*p*-ABSA) (1.80 g, 7.7 mmol) was added and the reaction was left to stir at room temperature under N_2 atmosphere for three hours until TLC (1:1 hexanes: ethyl acetate) showed consumption of starting material. Appearance of **8** (R_f = 0.69) (1:1 hexanes: ethyl acetate) was monitored by staining in *p*-anisaldehyde which yielded a bright yellow spot upon burning corresponding to formation of **8**. Upon completion, the reaction mixture was added to a 250 mL separatory funnel containing 150 mL of cyclohexane and 25 mL of distilled water. Following separation, the cyclohexane layer was collected, dried over $MgSO_4$, filtered, and solvent removed by rotary evaporation at 40 ^{o}C. The crude product was purified by flash column chromatography using a 5:1 hexanes:ethyl acetate solvent system. Pure 4-(azidomethyl)biphenyl (0.98 g, 4.6 mmol) (**8**) was collected as a clear and colorless oil.

^{1}H NMR (400 MHz, DMSO-d_6) δ 7.78-7.32 (m, 9H), 4.47 (s, 2H).

^{13}C NMR (100 MHz, DMSO-d_6) δ 140.41, 140.06, 135.24, 129.52 (double intensity), 129.41 (double intensity), 128.04, 127.43 (double intensity), 127.14 (double intensity), 53.72.

IR absorption: 2099 cm^{-1} for azide functional group.

MS: Calculated: 209.10 *m/z*, Found: (ESI pos) 233.10 *m/z* (M+Na^{+}+H^{+}).

Synthesis of 1,4-bis(azidomethyl)benzene (9) from 1,4-benzenedimethanol (10).

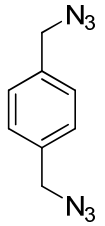

10

In a 100 mL round-bottom flask equipped with septum and magnetic stir bar, 1,4-benzenedimethanol (0.87 g, 6.3 mmol) (**9**) was dissolved in anhydrous DMF (30 mL). The flask was flushed with N_2 gas and sodium hydride (2.52 g, 63.0 mmol) was added. The reaction was left to stir at room temperature for one hour under N_2 atmosphere. At one hour, 4-acetamidobenzene sulfonyl azide (*p*-ABSA) (4.68 g, 18.9 mmol) was added and the reaction was left to stir at room temperature under N_2 atmosphere for three hours

until TLC (1:1 hexanes: ethyl acetate) showed consumption of starting material. Appearance of **10** (R_f = 0.68) (1:1 hexanes: ethyl acetate) was monitored by staining in *p*-anisaldehyde which yielded a bright yellow spot upon burning corresponding to formation of **10**. Upon completion, the reaction mixture was added to a 250 mL separatory funnel containing 150 mL of cyclohexane and 25 mL of distilled water. Following separation, the cyclohexane layer was collected, dried over $MgSO_4$, filtered, and solvent removed by rotary evaporation at 40 ^oC. The crude product was purified by flash column chromatography using a 3:1 hexanes:ethyl acetate solvent system. Pure 1,4-bis(azidomethyl)benzene (1.01 g, 5.3 mmol) (**10**) was collected as a clear and colorless oil.

^1H NMR (400 MHz, DMSO-d_6) δ 7.39 (s, 4H), 4.45 (s, 4H).

^{13}C NMR (100 MHz, DMSO-d_6) δ 135.75, 129.00 (double intensity), 53.42.

IR absorption: 2099 cm^{-1} for azide functional group.

MS: Calculated: 188.08 *m/z*, Found: (ESI pos) 212.20 *m/z* ($M+Na^+ + H^+$).

Synthesis of 1,3-bis(azidomethyl)benzene (12) from 1,3-benzenedimethanol (11).

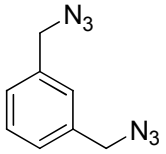

12

In a 100 mL round-bottom flask equipped with septum and magnetic stir bar, 1,3-benzenedimethanol (1.05 g, 7.6 mmol) (**11**) was dissolved in anhydrous DMF (30 mL). The flask was flushed with N_2 gas and sodium hydride (3.04 g, 76.0 mmol) was added. The reaction was left to stir at room temperature for one hour under N_2 atmosphere. At one hour, 4-acetamidobenzene sulfonyl azide (*p*-ABSA) (5.65 g, 22.8 mmol) was added and the reaction was left to stir at room temperature under N_2 atmosphere for three hours until TLC (1:3 hexanes: ethyl acetate) showed consumption of starting material. Appearance of **12** (R_f = 0.71) (1:3 hexanes: ethyl acetate) was monitored by staining in *p*-anisaldehyde which yielded a bright yellow spot upon burning corresponding to formation of **12**. Upon completion, the reaction was added to a 250 mL separatory funnel containing 150 mL of cyclohexane and 25 mL of distilled water. Following separation, the cyclohexane layer was collected, dried over $MgSO_4$, filtered, and solvent removed by rotary evaporation at 40 ^{o}C. The crude product was purified by flash column chromatography using a 4:1 hexanes:ethyl acetate solvent system. Pure 1,3-bis(azidomethyl)benzene (1.22 g, 6.5 mmol) (**12**) was collected as a clear and colorless oil.

^{1}H NMR (400 MHz, DMSO-d_6) δ 7.45-7.33 (m, 4H), 4.47 (s, 4H).

^{13}C NMR (100 MHz, DMSO-d_6) δ 136.66, 129.53, 128.69 (double intensity), 128.55 (double intensity), 53.84 (double intensity).

IR absorption: 2100 cm^{-1} for azide functional group.

MS: Calculated: 188.08 *m/z*, Found: (ESI pos) 212.20 *m/z* ($M+Na^+ + H^+$).

NaH-based azidation of simple secondary alcohols

Synthesis of (±) 1-azido-2,3-dihydro-1*H*-indene (14) from (±) 1-indanol (13).

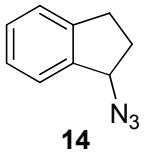

14

In a 100 mL round-bottom flask equipped with septum and magnetic stir bar, (±) 1-indanol (0.40 g, 3.0 mmol) (**13**) was dissolved in anhydrous DMF (30 mL). The flask was flushed with N_2 gas and sodium hydride (0.72 g, 18.0 mmol) was added. The reaction was left to stir at room temperature for one hour under N_2 atmosphere. At one hour, 4-nitrobenzene sulfonyl azide (*p*-NBSA) (2.05 g, 9.0 mmol) was added and the reaction was left to stir at room temperature under N_2 atmosphere for three hours until TLC (20:1 hexanes: ethyl acetate) showed consumption of starting material. Appearance of **14** (R_f = 0.45) (20:1 hexanes: ethyl acetate) was monitored by staining in *p*-anisaldehyde which yielded a bright yellow spot upon burning corresponding to formation of **14**. Upon completion, the reaction was added to a 250 mL separatory funnel containing 150 mL of cyclohexane and 25 mL of distilled water. Following separation, the cyclohexane layer was collected, dried over $MgSO_4$, filtered, and solvent removed by rotary evaporation at 40 ^oC. The crude product was purified by flash column chromatography using a 20:1 hexanes:ethyl acetate solvent system. Pure (±) 1-azido-2,3-dihydro-1*H*-indene (0.38 g, 2.4 mmol) (**14**) was collected as a clear and colorless oil.

^{1}H NMR (400 MHz, DMSO-d_6) δ 7.40-7.28 (m, 4H), 5.02 (dd, 1H, J = 4.30, 7.23 Hz), 3.09-2.98 (m, 1H), 2.86-2.78 (m, 1H), 2.43-2.33 (m, 1H) 2.02-1.93 (m, 1H).

^{13}C NMR (100 MHz, DMSO-d_6) δ 144.14, 140.92, 129.40, 127.24, 125.60, 125.00, 65.78, 32.50, 30.44.

IR absorption: 2094 cm^{-1} for azide functional group.

MS: Calculated: 159.19 *m/z*, Found: (ESI pos) 183.00 *m/z* (M+Na^{+}+H^{+}).

Synthesis of 2-azido-2,3-dihydro-1*H*-indene (18) from 2-indanol (17).

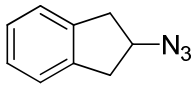

18

In a 100 mL round-bottom flask equipped with septum and magnetic stir bar, 2-indanol (0.40 g, 3.0 mmol) (**17**) was dissolved in anhydrous DMF (30 mL). The flask was flushed with N_2 gas and sodium hydride (0.72 g, 18.0 mmol) was added. The reaction was left to stir at room temperature for one hour under N_2 atmosphere. At one hour, 4-nitrobenzene sulfonyl azide (*p*-NBSA) (2.05 g, 9.0 mmol) was added and the reaction was left to stir at room temperature under N_2 atmosphere for three hours until TLC (20:1 hexanes: ethyl acetate) showed consumption of starting material. Appearance of **18** (R_f = 0.42) (20:1 hexanes: ethyl acetate) was monitored by staining in *p*-anisaldehyde which yielded a bright yellow spot upon burning corresponding to

formation of **18**. Upon completion, the reaction was added to a 250 mL separatory funnel containing 150 mL of cyclohexane and 25 mL of distilled water. Following separation, the cyclohexane layer was collected, dried over $MgSO_4$, filtered, and solvent removed by rotary evaporation at 40 ^{o}C. The crude product was purified by flash column chromatography using a 20:1 hexanes:ethyl acetate solvent system. Pure 2-azido-2,3-dihydro-1*H*-indene (0.42 g, 2.6 mmol) (**18**) was collected as a clear and colorless oil.

^{1}H NMR (400 MHz, DMSO-d_6) δ 7.25-7.11 (m, 4H), 4.84-4.43 (m, 1H), 3.19 (dd, 2H, J = 6.5, 16.4 Hz), 2.88 (dd, 2H, J = 3.39, 16.38 Hz).

^{13}C NMR (100 MHz, DMSO-d_6) δ 140.42 (double intensity), 126.90 (double intensity), 124.69 (double intensity), 61.64, 38.65 (double intensity).

IR absorption: 2097 cm^{-1} for azide functional group.

MS: Calculated: 159.19 *m/z*, Found: (ESI pos) 183.00 *m/z* ($M+Na^{+}+H^{+}$).

Azidation of protected carbohydrates

Synthesis of the 6-*O*-(*p*-azido)benzenesulfonate ester of 1,2:5,6-di-*O*-isopropylidene-α-D-glucofuranose (21) from 1,2:5,6-di-*O*-isopropylidene-α-D-glucofuranose (19).

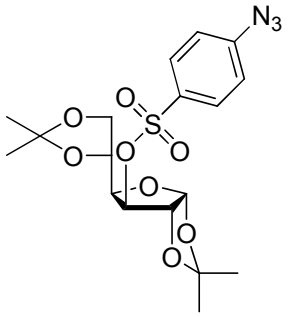

21

In a 100 mL round-bottom flask equipped with septum and magnetic stir bar, 1,2:5,6-di-*O*-isopropylidene-α-D-glucofuranose (1.0 g, 3.8 mmol) (**19**) was dissolved in anhydrous DMF (50 mL). The flask was flushed with N_2 gas and sodium hydride (0.55 g, 23.0 mmol) was added. The reaction was left to stir at room temperature for 45 minutes under N_2 atmosphere. At 45 minutes, 4-acetamidobenzene sulfonyl azide (*p*-ABSA) (2.74 g, 11.4 mmol) was added and the reaction was left to stir overnight at room temperature until TLC (4:1 hexanes: ethyl acetate) showed consumption of starting material. Appearance of **21** (R_f = 0.20) (4:1 hexanes: ethyl acetate) was monitored by staining with 5% H_2SO_4 in MeOH which yielded a dark brown spot upon burning corresponding to formation of **21**. Upon completion, the reaction was added to a 250 mL separatory funnel containing 150 mL of cyclohexane and 25 mL of distilled water. Following separation, the cyclohexane layer was collected, dried over $MgSO_4$, filtered, and solvent removed by rotary evaporation at 40 ^oC. The crude product was purified by flash column chromatography using a 4:1 hexanes:ethyl acetate solvent system. The pure

6-*O*-(*p*-azido)benzenesulfonate ester of 1,2:5,6-di-*O*-isopropylidene-α-D-glucofuranose (1.28 g, 2.9 mmol) (**21**) was collected as a colorless crystaline solid.

^{1}H NMR (400 MHz, $CDCl_3$) δ 7.94 (d, 2H, Ar-H, J = 8.96 Hz), 7.16 (d, 2H, Ar-H, J = 8.97 Hz), 5.94 (d, 1H, H-1, J = 3.68 Hz), 4.85 (d, 1H, H-2, J = 3.72 Hz), 4.79 (d, 1H, H-3, J = 2.4 Hz), 4.04-3.90 (m, 4H, H-4, H-5, H-6, H-6'), 1.49 (s, 3H, $-CH_3$), 1.32 (s, 3H, $-CH_3$), 1.21 (s, 3H, $-CH_3$), 1.16 (s, 3H, $-CH_3$).

^{13}C NMR (100 MHz, $CDCl_3$) δ 146.27, 131.55, 130.44 (double intensity), 119.34 (double intensity), 112.60, 109.17, 105.11, 83.33, 82.32, 79.78, 71.73, 67.17, 26.71, 26.61, 26.21, 24.99.

IR absorption: 2118 cm^{-1} for azide functional group.

MS: Calculated: 441.12 *m/z*, Found: (ESI pos) 464.10 *m/z* ($M+Na^+$).

Synthesis of the 6-*O*-(*p*-nitro)benzenesulfonate ester of 1,2:5,6-di-*O*-isopropylidene-α-D-glucofuranose (22) from 1,2:5,6-di-*O*-isopropylidene-α-D-glucofuranose (19).

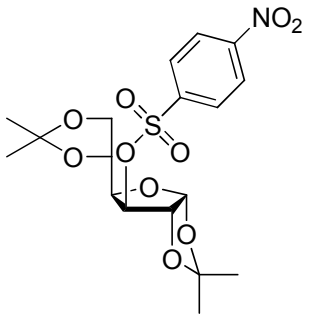

22

In a 100 mL round-bottom flask equipped with septum and magnetic stir bar, 1,2:5,6-di-*O*-isopropylidene-α-D-glucofuranose (0.72 g, 2.8 mmol) (**19**) was dissolved in anhydrous DMF (50 mL). The flask was flushed with N_2 gas and sodium hydride (0.40 g, 16.8 mmol) was added. The reaction was left to stir at room temperature for 45 minutes under N_2 atmosphere. At 45 minutes, 4-nitrobenzene sulfonyl azide (*p*-NBSA) (1.90 g, 8.3 mmol) was added and the reaction was left to stir overnight at room temperature until TLC (4:1 hexanes: ethyl acetate) showed consumption of starting material. Appearance of **22** (R_f = 0.25) (4:1 hexanes: ethyl acetate) was monitored by staining with 5% H_2SO_4 in MeOH which yielded a dark brown spot upon burning corresponding to formation of **22**. Upon completion, the reaction was added to a 250 mL separatory funnel containing 150 mL of cyclohexane and 25 mL of distilled water. Following separation, the cyclohexane layer was collected, dried over $MgSO_4$, filtered, and solvent removed by rotary evaporation at 40 ^{o}C. The crude product was purified by flash column chromatography using a 4:1 hexanes:ethyl acetate solvent system. Pure 6-*O*-(*p*-

nitro)benzenesulfonate ester of 1,2:5,6-di-*O*-isopropylidene-α-D-glucofuranose (0.89 g, 2.0 mmol) (**22**) was collected as a yellow crystaline solid.

^{1}H NMR (400 MHz, $CDCl_3$) δ 8.22 (d, 2H, Ar-H, J = 9.28 Hz), 7.08 (d, 2H, Ar-H, J = 9.28 Hz), 5.96 (d, 1H, H-1, J = 3.84 Hz), 4.84 (d, 1H, H-2, J = 3.09 Hz), 4.59 (d, 1H, H-3, J = 3.84 Hz), 4.43-4.07 (m, 4H, H-4, H-5, H-6, H-6'), 1.56 (s, 3H, -CH_3), 1.43 (s, 3H, -CH_3), 1.33 (s, 3H, -CH_3), 1.30 (s, 3H, -CH_3).

^{13}C NMR (100 MHz, $CDCl_3$) δ 162.00, 142.31, 125.98 (double intensity), 115.51 (double intensity), 112.46, 109.47, 105.29, 82.31, 80.76, 80.39, 71.97, 67.28, 26.90, 26.68, 26.24, 25.22.

MS: Calculated: 445.10 *m/z*, Found: (ESI pos) 469.40 *m/z* ($M+Na^+$+H^+).

Synthesis of the 6-*O*-(*p*-azido)benzenesulfonate ester of 1,2:3,4-di-*O*-isopropylidene-α-D-galactopyranose (24) from 1,2:3,4-di-*O*-isopropylidene-α-D-galactopyranose (5).

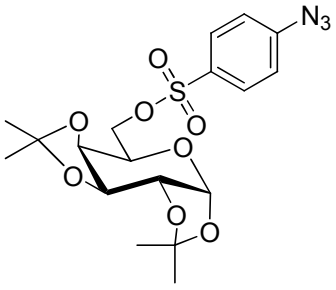

24

In a 100 mL round-bottom flask equipped with septum and magnetic stir bar, 1,2:3,4-di-*O*-isopropylidene-α-D-galactopyranose (1.00 g, 3.8 mmol) (**5**) was dissolved in anhydrous DMF (50 mL). The flask was flushed with N_2 gas and sodium hydride (0.55 g, 23.0 mmol) was added. The reaction was left to stir at room temperature for 45 minutes under N_2 atmosphere. At 45 minutes, 4-acetamidobenzene sulfonyl azide (*p*-ABSA) (2.73 g, 11.4 mmol) was added and the reaction was left to stir overnight at room temperature until TLC (4:1 hexanes: ethyl acetate) showed consumption of starting material. Appearance of **24** (R_f = 0.19) (4:1 hexanes: ethyl acetate) was monitored by staining with 5% H_2SO_4 in MeOH which yielded a dark brown spot upon burning corresponding to formation of **24**. Upon completion, the reaction was added to a 250 mL separatory funnel containing 150 mL of cyclohexane and 25 mL of distilled water. Following separation, the cyclohexane layer was collected, dried over $MgSO_4$, filtered, and solvent removed by rotary evaporation at 40 ^oC. The crude product was purified by flash column chromatography using a 4:1 hexanes:ethyl acetate solvent system. The pure 6-*O*-(*p*-azido)benzenesulfonate ester of 1,2:3,4-di-*O*-isopropylidene-α-D-galactopyranose (1.41 g, 3.2 mmol) (**24**) was collected as a clear and colorless oil.

^{1}H NMR (400 MHz, $CDCl_3$) δ 7.91 (d, 2H, Ar-H, J = 8.84 Hz), 7.16 (d, 2H, Ar-H, J = 8.77 Hz), 5.45 (d, 1H, H-1, J = 4.96 Hz), 4.60 (dd, 1H, H-3, J = 2.56, 7.84 Hz), 4.30 (dd, 1H, H-2, J = 2.57, 4.97 Hz), 4.25-4.19 (m, 2H, H-4, H-5), 4.14-4.04 (m, 2H, H-6, H-6'), 1.51 (s, 3H, -CH_3), 1.35 (s, 3H, -CH_3), 1.32 (s, 3H, -CH_3), 1.29 (s, 3H, -CH_3).

^{13}C NMR (100 MHz, $CDCl_3$) δ 145.91, 131.79, 130.10 (double intensity), 119.44 (double intensity), 109.64, 108.97, 96.11, 70.53, 70.43, 70.29, 68.56, 65.90, 26.00, 25.83, 24.89, 24.36.

IR absorption: 2129 cm^{-1} for azide functional group.

MS: Calculated: 441.12 *m/z*, Found: (ESI pos) 464.20 *m/z* ($M+Na^+$).

Synthesis of the 6-*O*-(*p*-nitro)benzenesulfonate ester of 1,2:3,4-di-*O*-isopropylidene-α-D-galactopyranose (25) from 1,2:3,4-di-*O*-isopropylidene-α-D-galactopyranose (5).

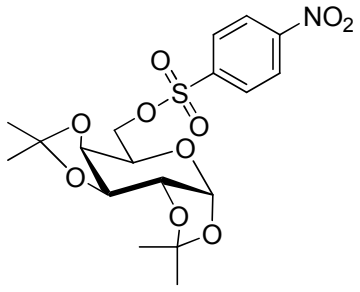

25

In a 100 mL round-bottom flask equipped with septum and magnetic stir bar, 1,2:3,4-di-*O*-isopropylidene-α-D-galactopyranose (0.91 g, 3.5 mmol) (**5**) was dissolved in anhydrous DMF (50 mL). The flask was flushed with N_2 gas and sodium hydride (0.50 g, 21.0 mmol) was added. The reaction was left to stir at room temperature for 45 minutes under N_2 atmosphere. At 45 minutes, 4-nitrobenzene sulfonyl azide (*p*-NBSA) (2.40 g, 10.5 mmol) was added and the reaction was left to stir overnight at room temperature

until TLC (4:1 hexanes: ethyl acetate) showed consumption of starting material. Appearance of **25** (R_f = 0.27) (4:1 hexanes: ethyl acetate) was monitored by staining with 5% H_2SO_4 in MeOH which yielded a dark brown spot upon burning corresponding to formation of **25**. Upon completion, the reaction was added to a 250 mL separatory funnel containing 150 mL of cyclohexane and 25 mL of distilled water. Following separation, the cyclohexane layer was collected, dried over $MgSO_4$, filtered, and solvent removed by rotary evaporation at 40 ^oC. The crude product was purified by flash column chromatography using a 4:1 hexanes:ethyl acetate solvent system. The pure 6-*O*-(*p*-nitro)benzenesulfonate ester of 1,2:3,4-di-*O*-isopropylidene-α-D-galactopyranose (1.29 g, 2.9 mmol) (**25**) was collected as a yellow solid.

^1H NMR (400 MHz, $CDCl_3$) δ 8.19 (d, 2H, Ar-H, J = 9.32 Hz), 7.02 (d, 2H, Ar-H, J = 9.28 Hz), 5.59 (d, 1H, H-1, J = 5.00 Hz), (dd, 1H, H-2, J = 2.50, 7.90 Hz), 4.39-4.20 (m, 5H, H-3, H-4, H-5, H-6, H-6'), 1.54 (s, 3H, -CH_3), 1.47 (s, 3H, -CH_3), 1.36 (s, 6H, 2 x -CH_3).

^{13}C NMR (100 MHz, $CDCl_3$) δ 163.68, 141.64, 125.81 (double intensity), 114.72 (double intensity), 109.59, 108.85, 96.32, 70.87, 70.61, 70.45, 67.60, 66.23, 26.06, 25.98, 24.89, 24.42.

MS: Calculated: 445.10 *m/z*, Found: (ESI pos) 469.30 ($M+Na^+ + H^+$).

Synthesis of 1-azido-1-deoxy-2,3:5,6-di-*O*-isopropylidene-β- (27) and -α-D-mannofuranose (28) from 2,3:5,6-di-*O*-isopropylidene-α-D-mannofuranose (26).

27
major

+

28

In a 100 mL round-bottom flask equipped with septum and magnetic stir bar, 2,3:5,6-di-*O*-isopropylidene-α-D-mannofuranose (1.00 g, 3.8 mmol) (**26**) was dissolved in anhydrous DMF (50 mL). The flask was flushed with N_2 gas and sodium hydride (0.55 g, 23.0 mmol) was added. The reaction was left to stir at room temperature for 45 minutes under N_2 atmosphere. At 45 minutes, 4-nitrobenzene sulfonyl azide (*p*-NBSA) (2.60 g, 11.4 mmol) was added and the reaction was left to stir overnight at room temperature until TLC (4:1 hexanes: ethyl acetate) showed consumption of starting material. Appearances of **27** (R_f = 0.19) and **28** (R_f = 0.38) (4:1 hexanes: ethyl acetate) were monitored by staining with 5% H_2SO_4 in MeOH which yielded dark brown spots upon burning corresponding to formation of **27** and **28**. Upon completion, the reaction was added to a 250 mL separatory funnel containing 150 mL of cyclohexane and 25 mL of distilled water. Following separation, the cyclohexane layer was collected, dried over $MgSO_4$, filtered, and solvent removed by rotary evaporation at 40 ^oC. The crude product was purified by flash column chromatography using a 4:1 hexanes:ethyl acetate solvent system. Pure 1-azido-1-deoxy-2,3:5,6-di-*O*-isopropylidene-β-D-mannofuranose (0.52 g, 1.8 mmol) (**27**) and 1-azido-1-deoxy-2,3:5,6-di-*O*-isopropylidene-α-D-mannofuranose

(0.35 g, 1.2 mmol) (**28**) were collected as a clear syrups. In total, 0.87 g (2.0 mmol) of azide product (**27** and **28**) was produced in 79% total yield.

1-Azido-1-deoxy-2,3:5,6-di-*O*-isopropylidene-β-D-mannofuranose (27)

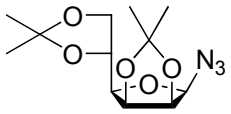

27
major

^{1}H NMR (400 MHz, $CDCl_3$) δ 4.78 (dd, 1H, H-3, J = 3.60, 6.04 Hz), 4.69 (dd, 1H, H-2, J = 3.61, 6.05), 4.47 (ddd, 1H, H-5, J = 4.56, 6.00, 7.52 Hz), 4.42 (d, 1H, H-1, J = 3.60 Hz), 4.16-4.08 (m, 2H, H-6, H-6'), 3.61 (dd, 1H, H-4, J = 3.60, 7.52 Hz), 1.56 (s, 3H, -CH_3), 1.45 (s, 3H, -CH_3), 1.39 (s, 3H, -CH_3), 1.37 (s, 3H, -CH_3).

^{13}C NMR (100 MHz, $CDCl_3$) δ 113.59, 109.29, 89.08, 81.11, 79.51, 78.54, 72.88, 66.75, 26.93, 25.21, 25.15, 24.35.

IR absorption: 2126 cm^{-1} for azide functional group.

MS: Calculated: 285.13 *m/z*, Found: (ESI pos) 308.10 *m/z* ($M+Na^+$).

1-Azido-1-deoxy-2,3:5,6-di-*O*-isopropylidene-α-D-mannofuranose (28)

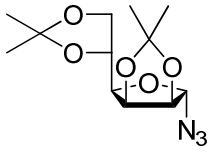

28

^{1}H NMR (400 MHz, $CDCl_3$) δ 5.45 (s, 1H, H-1), 4.79 (dd, 1H, H-3, J = 3.56, 5.88 Hz), 4.48 (d, 1H, H-2, J = 5.92), 4.42 (ddd, 1H, H-5, J = 4.34, 6.16, 7.66 Hz), 4.14-4.02 (m, 3H, H-4, H-6, H-6'), 1.47 (s, 6H, 2 x -CH_3), 1.38 (s, 3H, -CH_3), 1.32 (s, 3H, -CH_3).

^{13}C NMR (100 MHz, $CDCl_3$) δ 113.16, 109.40, 95.49, 85.05, 81.92, 79.57, 72.81, 66.83, 26.89, 25.86, 25.11, 24.55.

IR absorption: 2116 cm^{-1} for azide functional group.

MS: Calculated: 285.13 *m/z*, Found: (ESI pos) 308.10 *m/z* ($M+Na^+$).

References

1. Brase, S.; Gil, C.; Knepper, K.; Zimmerman, V., "Organic azides: An exploding diversity of a unique class of compounds," *Angew. Chem. Int. Ed.* **2005**, *44,* 5188-5240.
2. Righi, G.; D'Achille, C.; Pescatore, G.; Bonini, C., "New stereoseletive synthesis of the peptidic aminopeptidase inhibitors Bestatin, Phesbestin, and Probestin," *Tetrahedron Lett.* **2003**, *44*, 6999-7002.
3. Sayyed, I. A.; Sudalai, A., "Asymmetric synthesis of L-DOPA and (*R*)-Selegiline via OsO_4 – catalyzed asymmetric dihydroxylation," *Tetrahedron: Asymmetry* **2004**, *15*, 3111-3116.
4. Baran, P. S.; Zografos, A. L.; O'Malley, D. P., "Short total synthesis of (±)-Sceptrin," *J. Am. Chem. Soc.* **2004**, *126,* 3726-3727.
5. Tanaka, H.; Sawayama, A. M.; Wandless, T. J., "Enantioselective total synthesis of Ustiloxin D," *J. Am. Chem. Soc.* **2003**, *125,* 6864-6865.
6. Lee, S. H.; Yoon, J.; Chung, S. H.; Lee, Y. S. *Tetrahedron Lett.* **1993**, *34,* 6475-6478.
7. Thompson, A. S.; Humphrey, G. R.; DeMarco, A. M.; Mathre, D. J.; Grabowski, E. J. J., "Direct conversion of activated alcohols to azides using diphenyl phosphorazidate. A practical alternative to Mitsunobu conditions," *J. Org. Chem.* **1993**, *58*, 5886-5888.
8. Sauci, Iulia, Alisa. (2006) *Synthesis and Decompostion of Novel Diazosugars*: *2004-2006*. Masters thesis. Youngstown State University.

9. Brown, W. H.; Foote, C. S., Fundamental derivatives of carboxylic acids. *Organic Chemistry*, 3rd Edition, Emily Barrosse: Orlando, Fl. 2002; 646.
10. Katzung, B. G., Antiviral Agents. *Basic & Clinical Pharmacology*, 10th Edition, McGraw-Hill Medical: 2007; 806
11. Temelkoff, D. P.; Smith, C.; Kibler, D.; Norris, P., "Application of bis(diphenylphosphino)ethane (DPPE) in Staudinger-type *N*-glycopyranosyl amide synthesis," *Carbohydr. Res.* **2006**, *341*, 1645-1656.
12. Davis, B. G., "Synthesis of glycoproteins," *Chem. Rev.* **2002**, *102*, 579-601.
13. Saxon, E.; Armstrong, J. I.; Bertozzi, C. R., "A "traceless" Staudinger ligation for the chemoselective synthesis of amide bonds," *Org. Lett.* **2000**, *2*, 2141-2143.
14. Rostovtsev, V. V.; Green, L. G.; Fokin, V. V.; Sharpless, K. B., "A stepwise Huisgen cycloaddition process: copper (I)-catalyzed regioselective "ligation" of azides and terminal alkynes," *Angew. Chem. Int. Ed.* **2002**, *41*, 2596-2599.
15. Akula, R. A.; Temelkoff, D. P.; Artis, N. D.; Norris, P., "Rapid access to glucopyranosyl-1,2,3-triazoles via Cu(I)-catalyzed reactions in water," *Heterocycles* **2004**, *63*, 2719-2725.
16. Amegadzie, A. K.; Gardinier, K. M.; Hembre, E. J, "Tachykinin receptor antagonists," WIPO **2005**, Pub. No.: WO/2005/000821 Accessed: 7/19/2008 at http://www.wipo.int/pctdb/en/wo.jsp?IA=US2004015579&DISPLAY=STATUS
17. Zhang, G.; Fang, L.; Zhu, L.; Sun, D.; Wang, P. G., "Syntheses and biological activity of bisdaunorubicins," *Bioorg. Med. Chem.* **2006**, *14*, 426-434.
18. Haridas, V.; Lal, K; Sharma, Y. K.; Upreti, S., "Design, synthesis and self-assembling properties of novel triazolophanes," *Org. Lett.* **2008**, *10*, 1645-1647.

19. Breton, G. W.; Daus, K. A.; Kropp, P. J., "Surface mediated reactions. Addition of hydrazoic acid to alkenes," *J. Org. Chem.* **1992**, *57*, 6646-6649.

20. March, J.; Smith, M. B., Aromatic nucleophilic substitution. *March's Advanced Organic Chemistry*, 5th Edition, John Wiley & Sons: New York, NY. 2001; 850-853.

21. Bowers, N. I.; Boyd, D. R.; Sharma, N. D.; Goodrich, P. A., "Stereoselective benzylic hydroxylation of 2-substituted indanes using toluene dioxygenase as biocatalyst," *J. Chem. Soc., Perkin Trans.* **1999**, *1*, 1453-1461.

Appendix A

NMR, IR and Mass Spectra

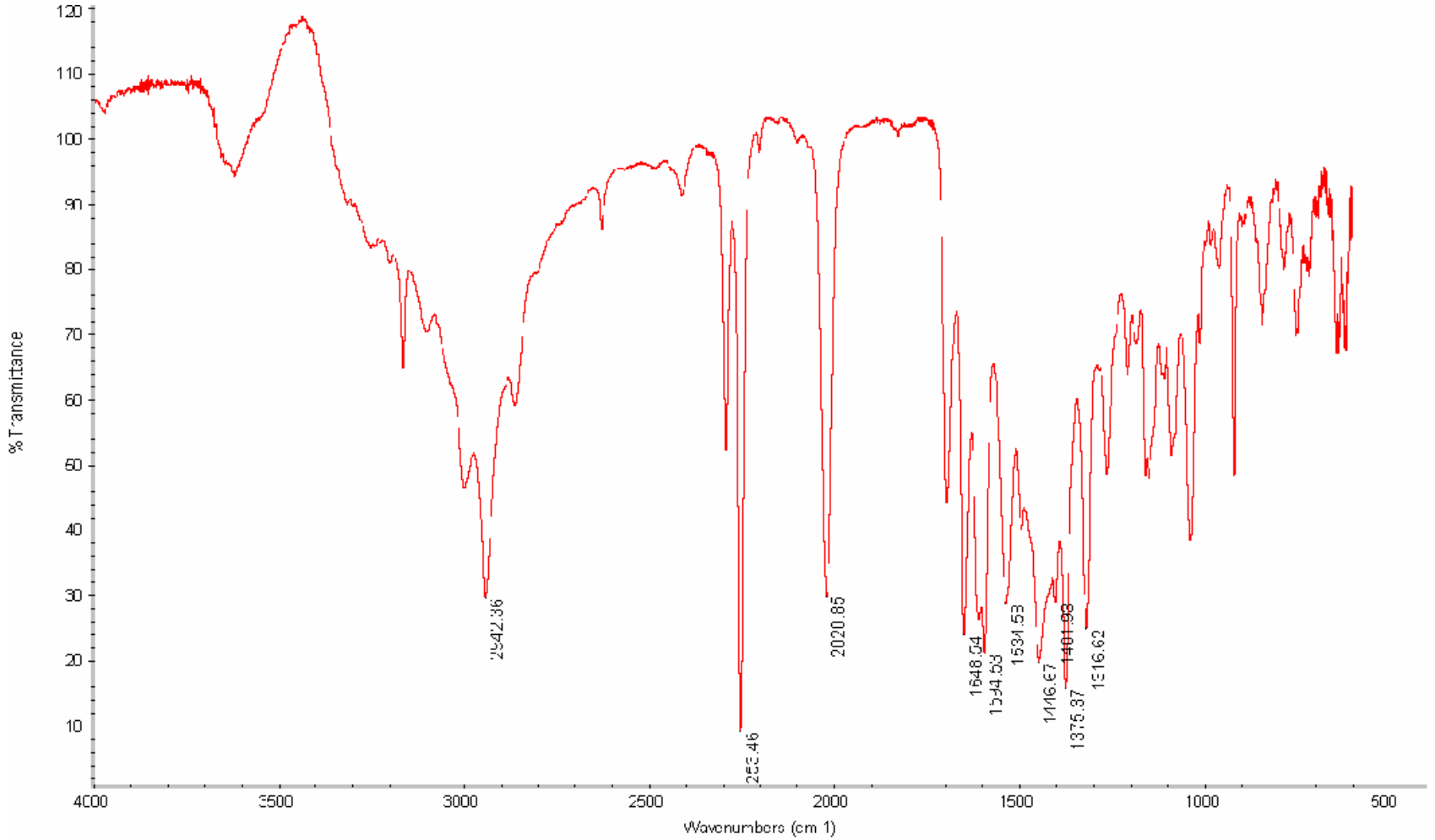

Figure 21: IR spectrum of *in situ* generation of N_3^- from *p*-ABSA and DBU.

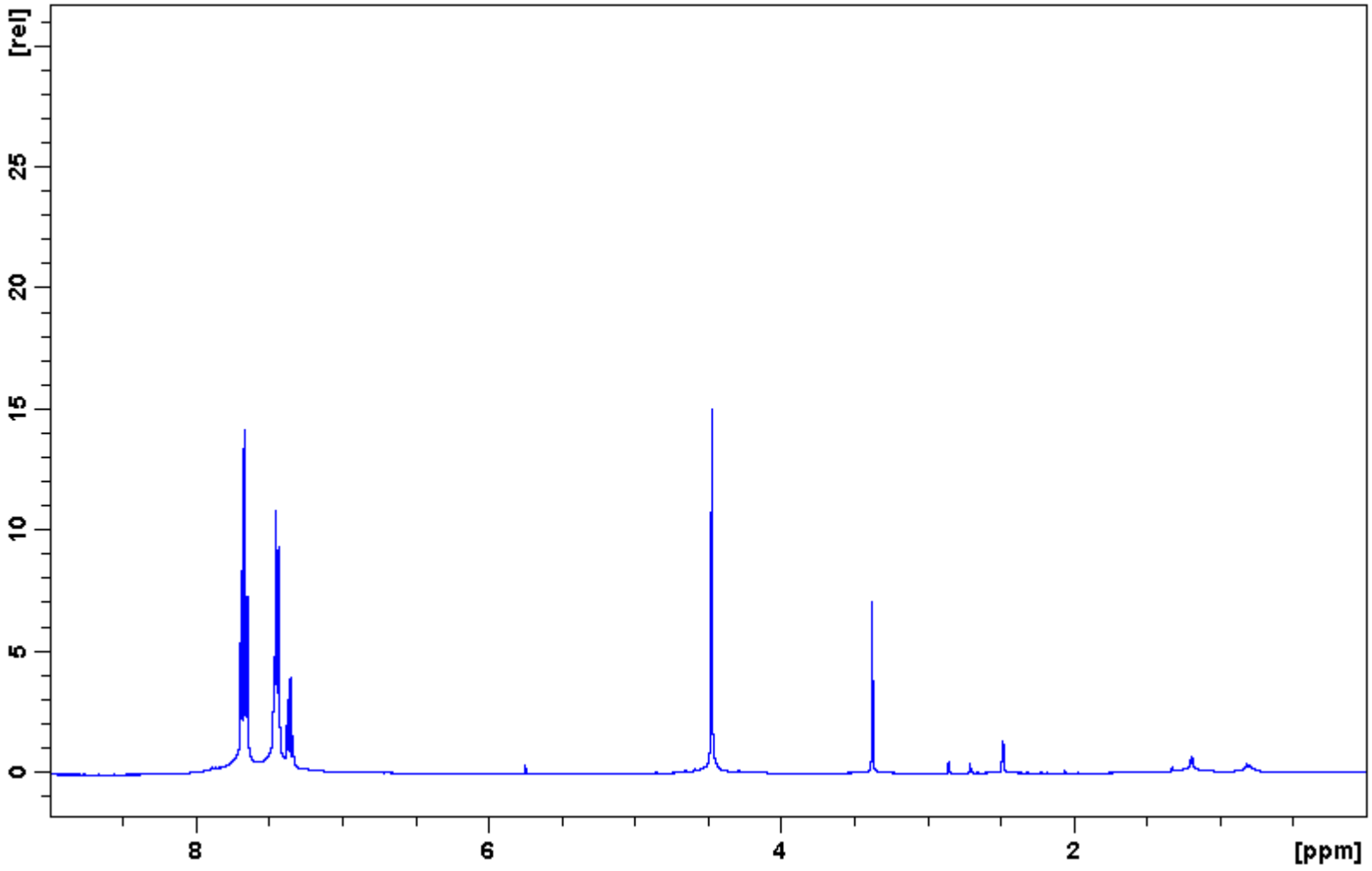

Figure 22: ^{1}H NMR spectrum of 4-(azidomethyl)biphenyl (**8**).

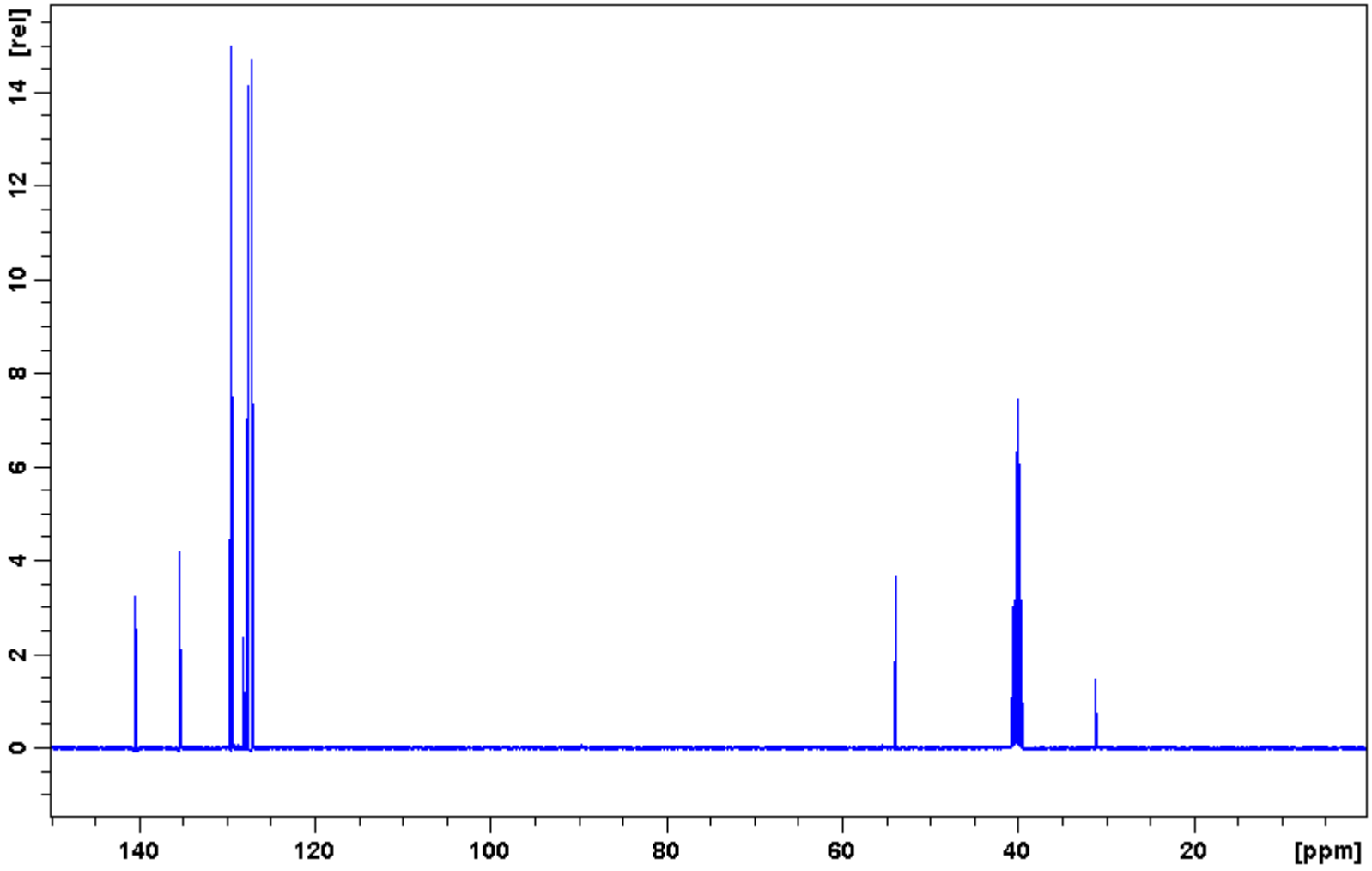

Figure 23: ^{13}C NMR spectrum of 4-(azidomethyl)biphenyl (**8**).

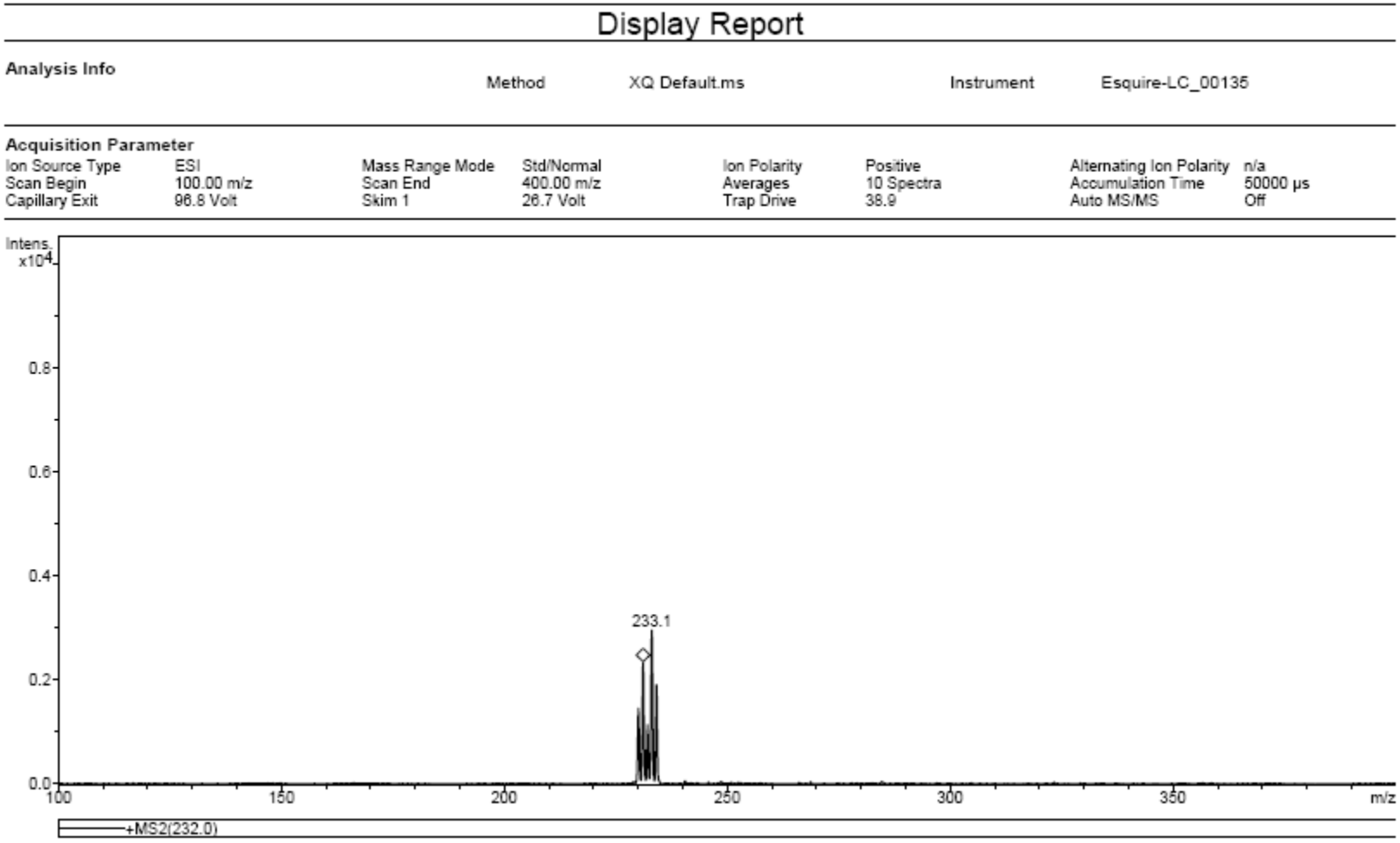

Figure 24: Mass spectrum of 4-(azidomethyl)biphenyl (**8**).

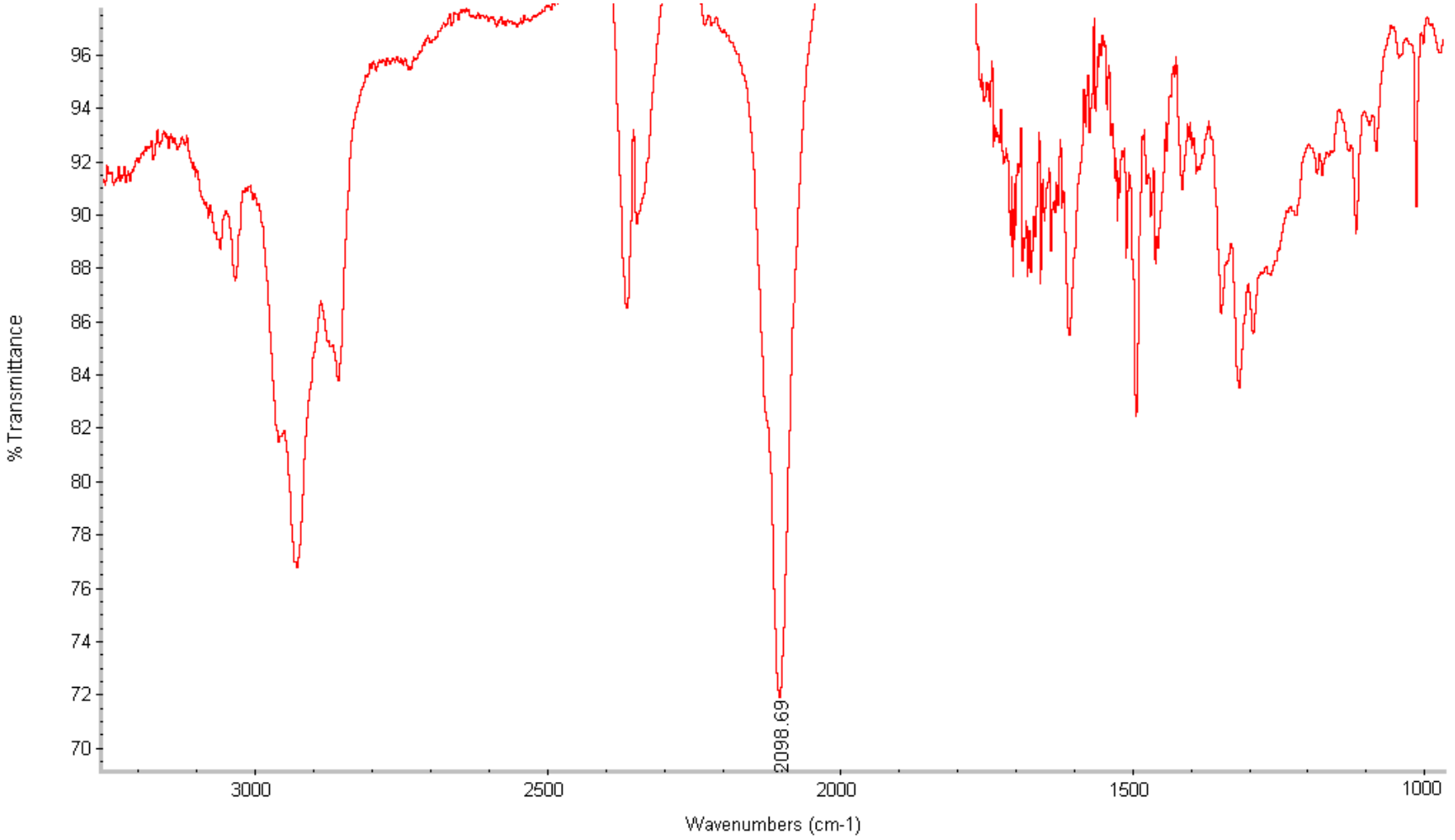

Figure 25: IR spectrum of 4-(azidomethyl)biphenyl (**8**).

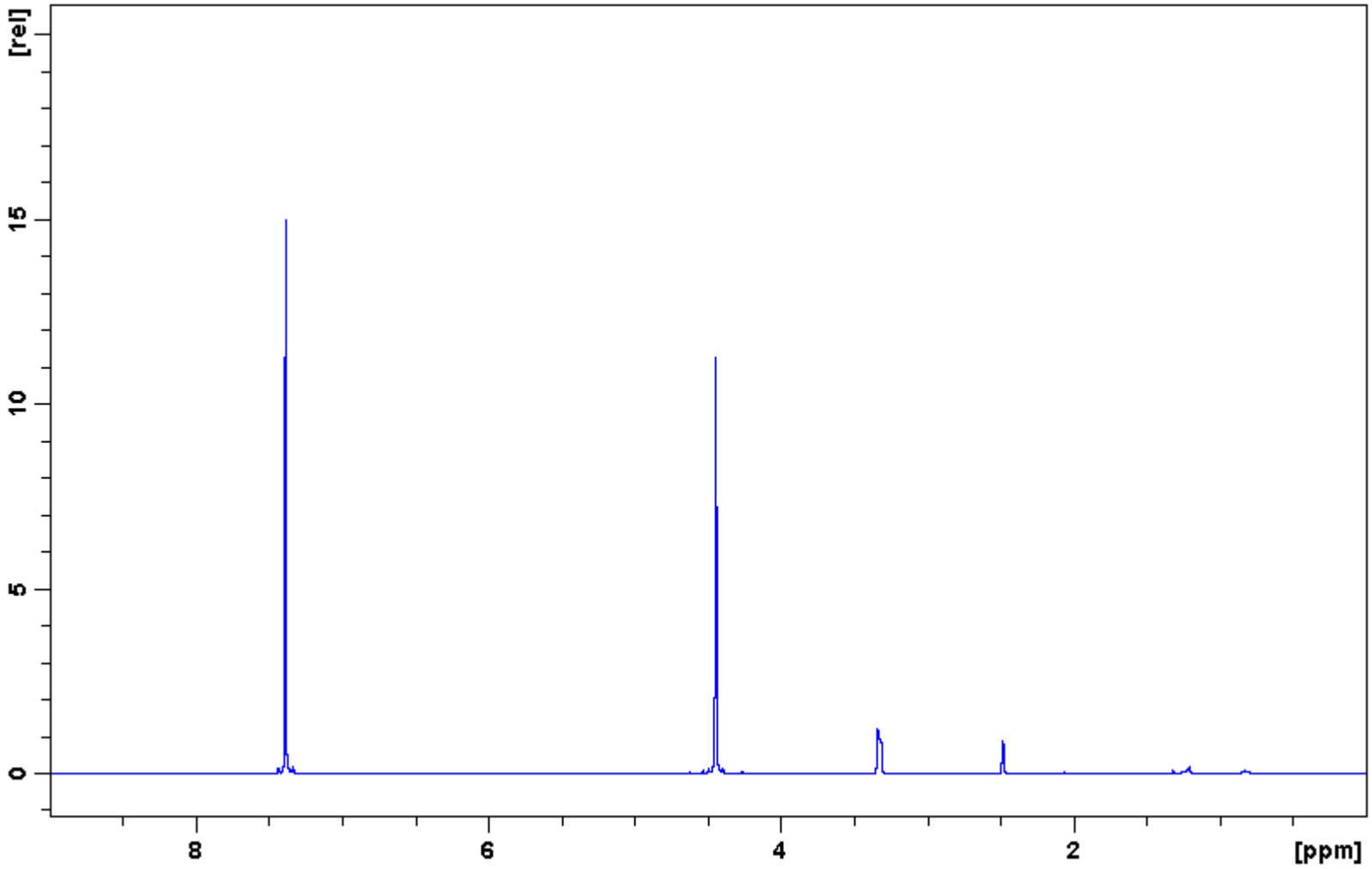

Figure 26: ^{1}H NMR spectrum of 1,4-bis(azidomethyl)benzene (**10**).

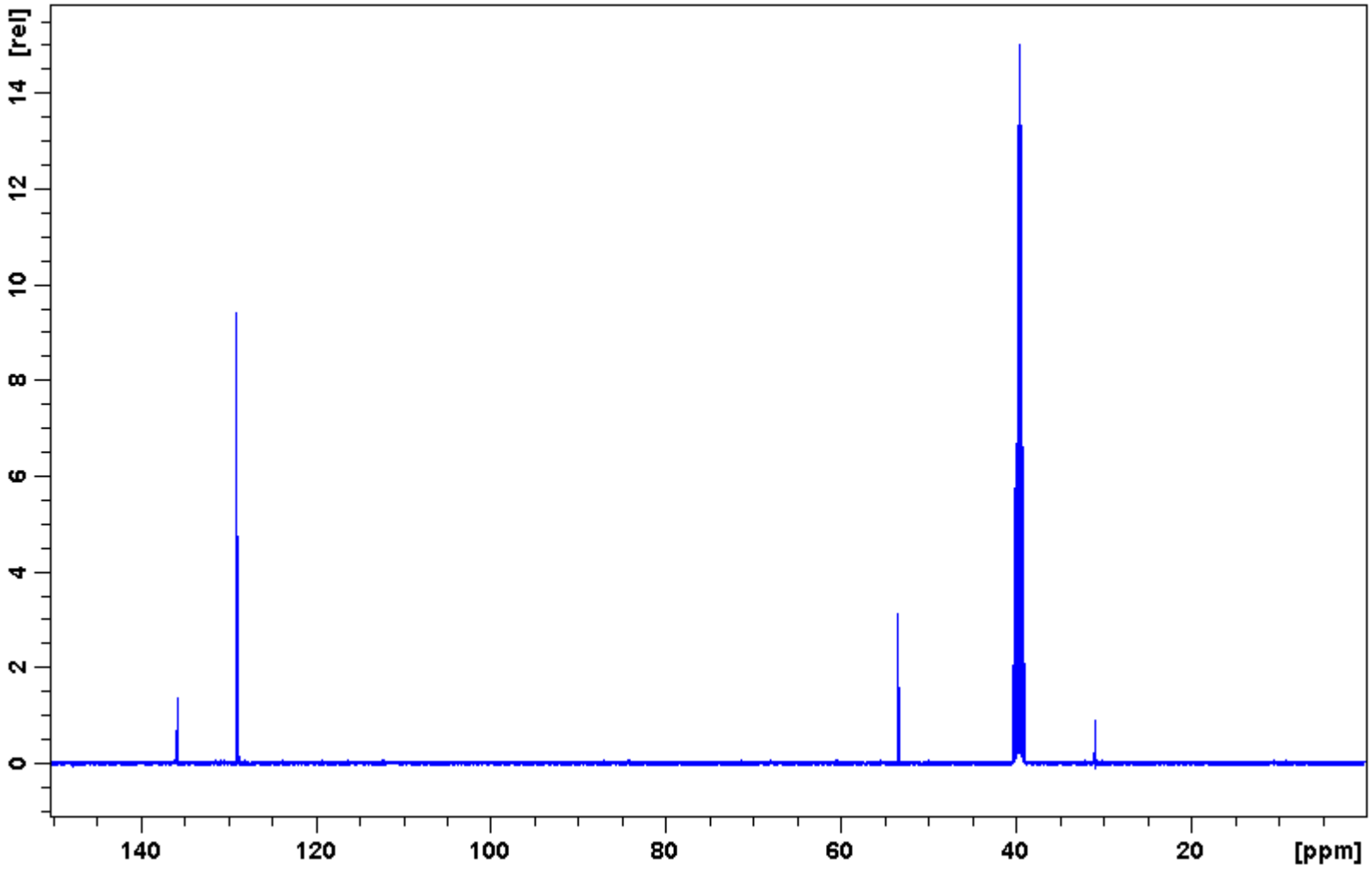

Figure 27: ^{13}C NMR spectrum of 1,4-bis(azidomethyl)benzene (**10**).

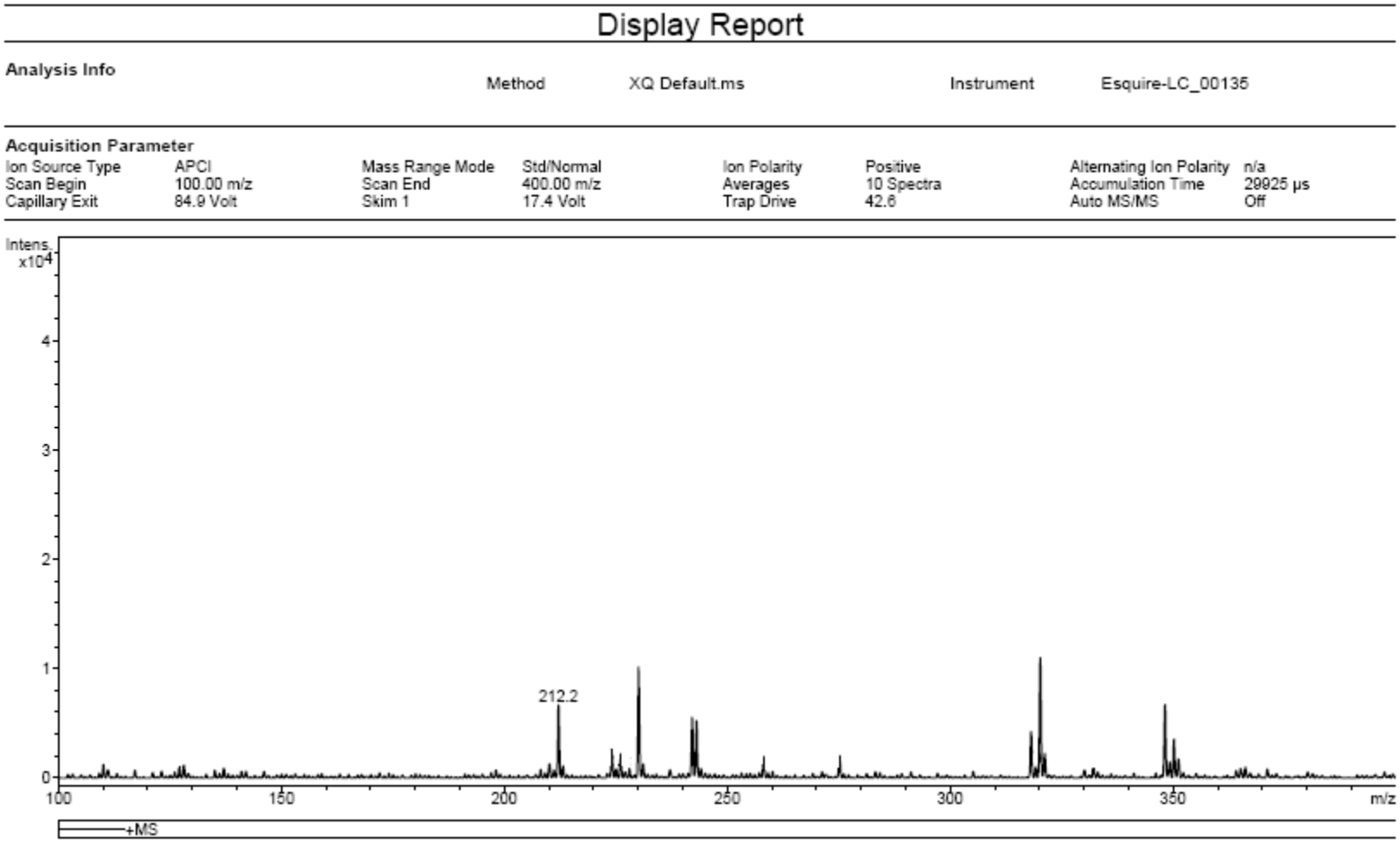

Figure 28: Mass spectrum of 1,4-bis(azidomethyl)benzene (**10**).

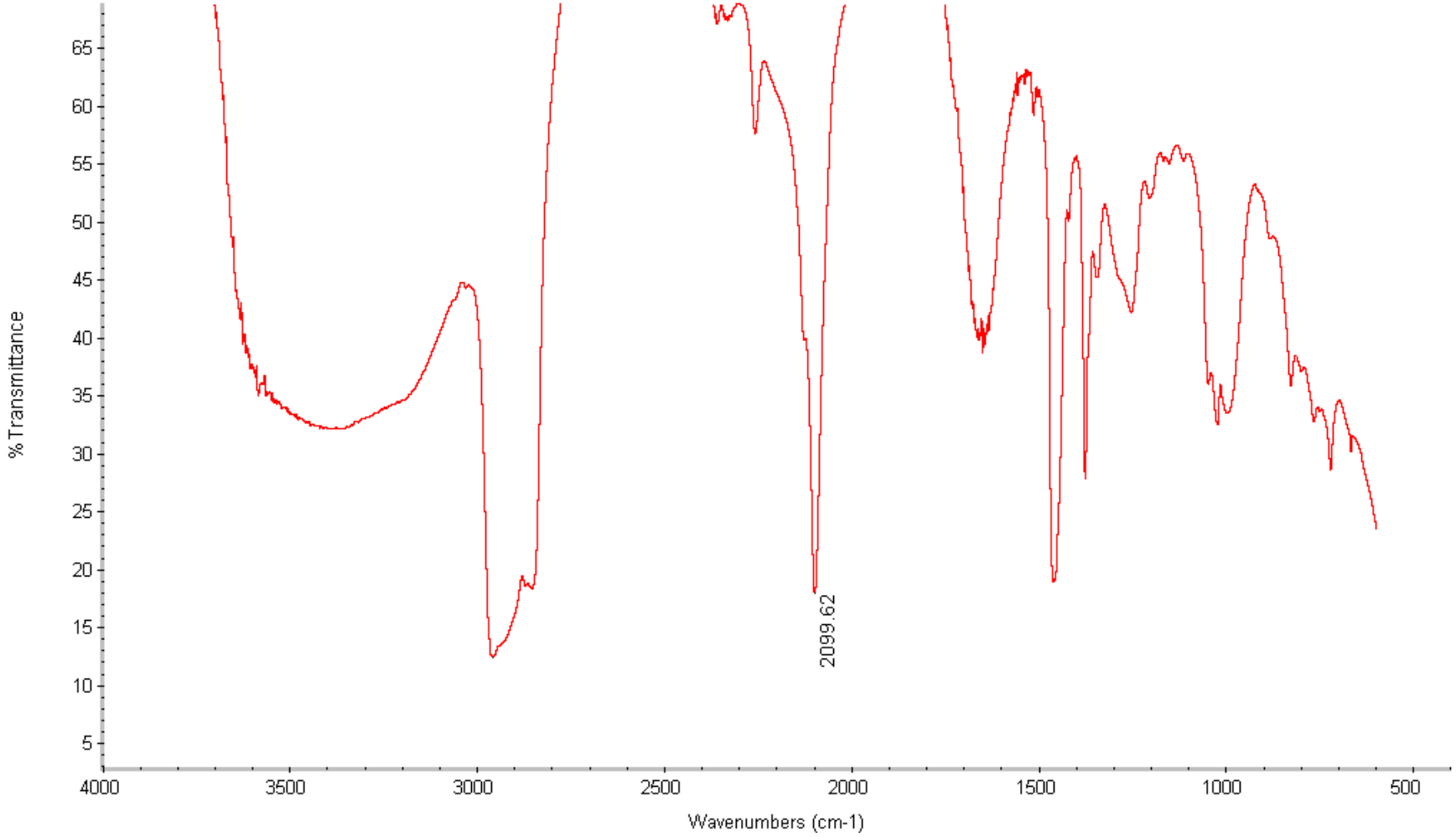

Figure 29: IR spectrum of 1,4-bis(azidomethyl)benzene (**10**).

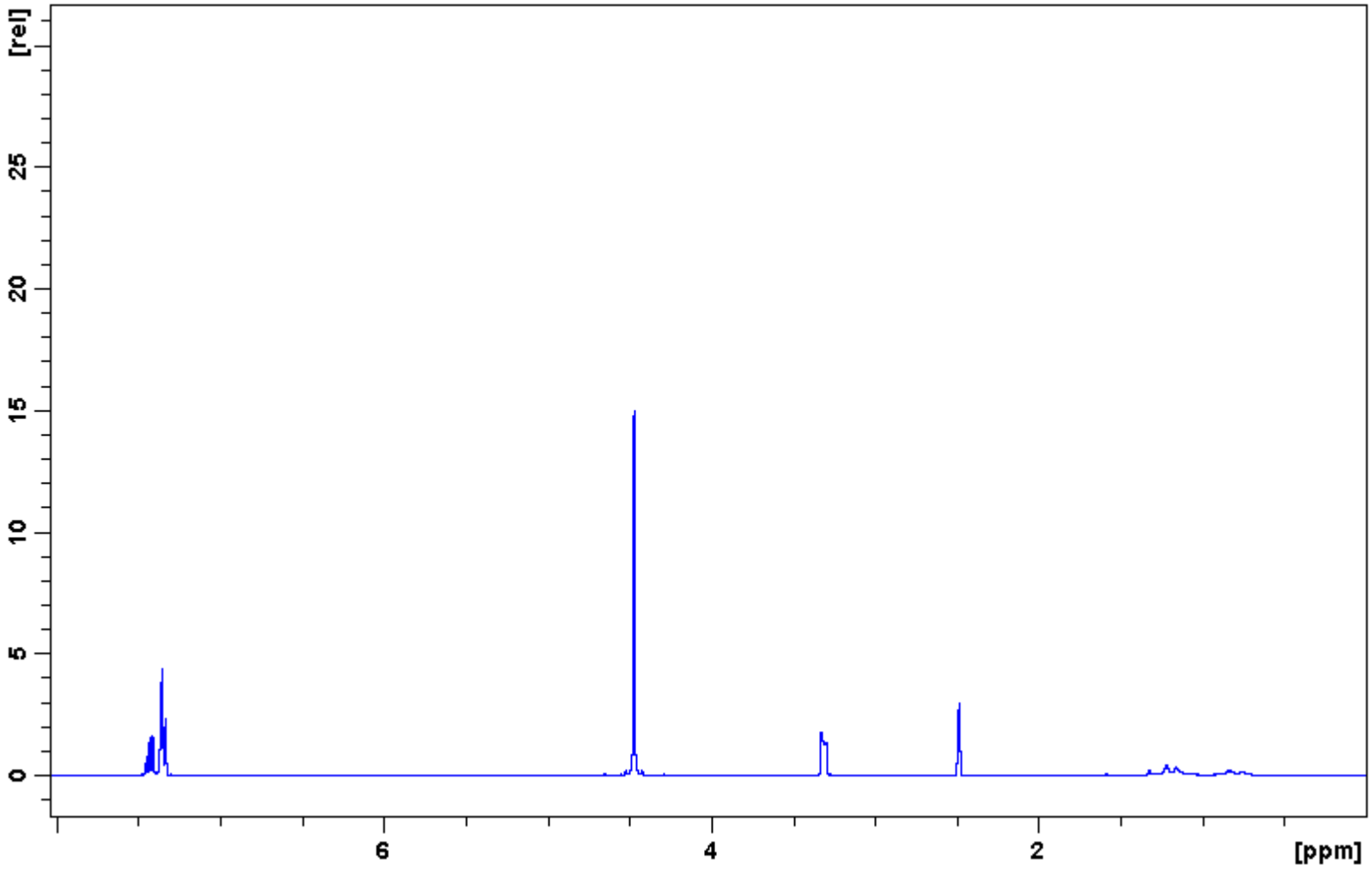

Figure 30: ^{1}H NMR spectrum of 1,3-bis(azidomethyl)benzene (**12**).

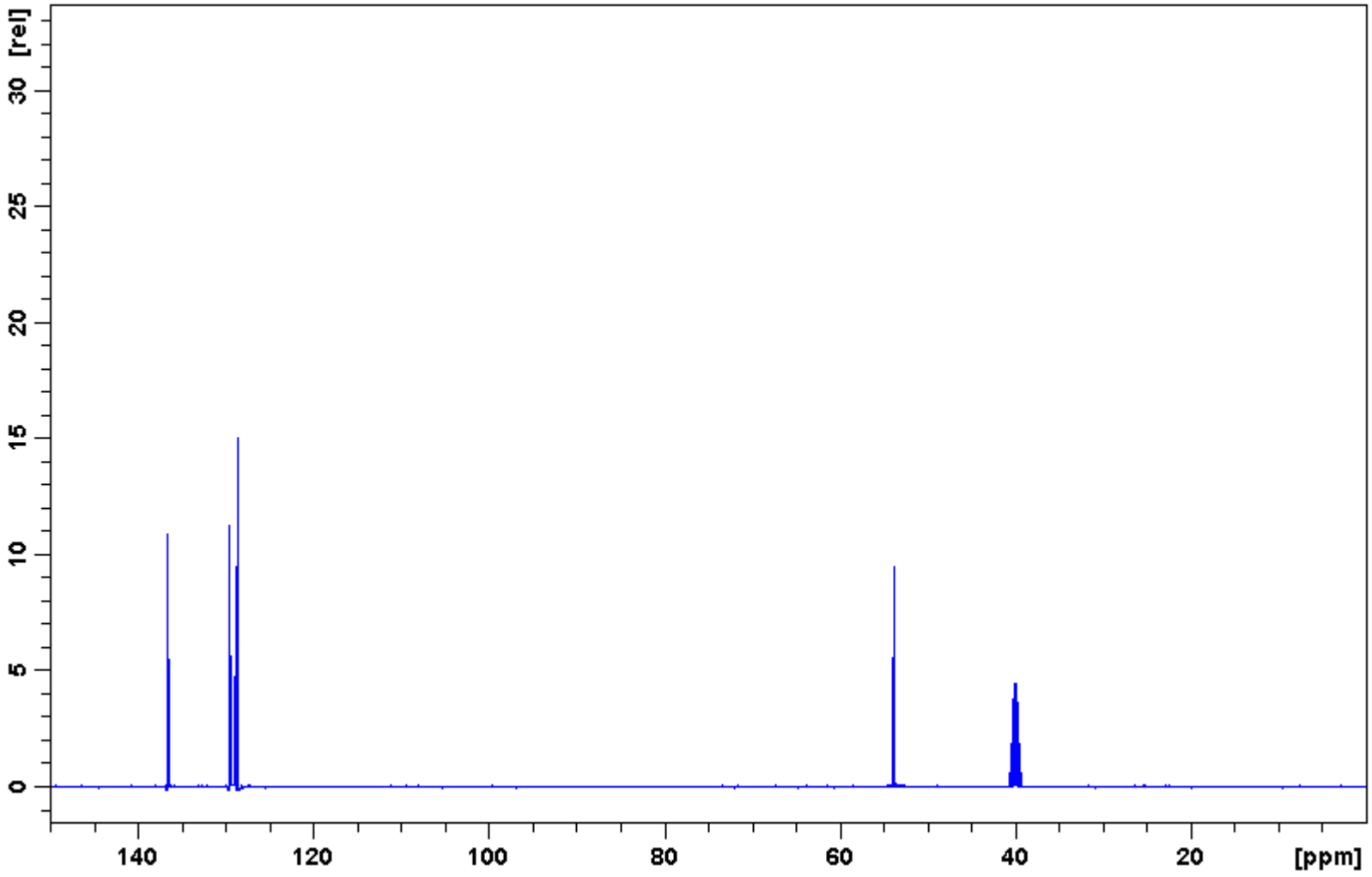

Figure 31: ^{13}C NMR spectrum of 1,3-bis(azidomethyl)benzene (**12**).

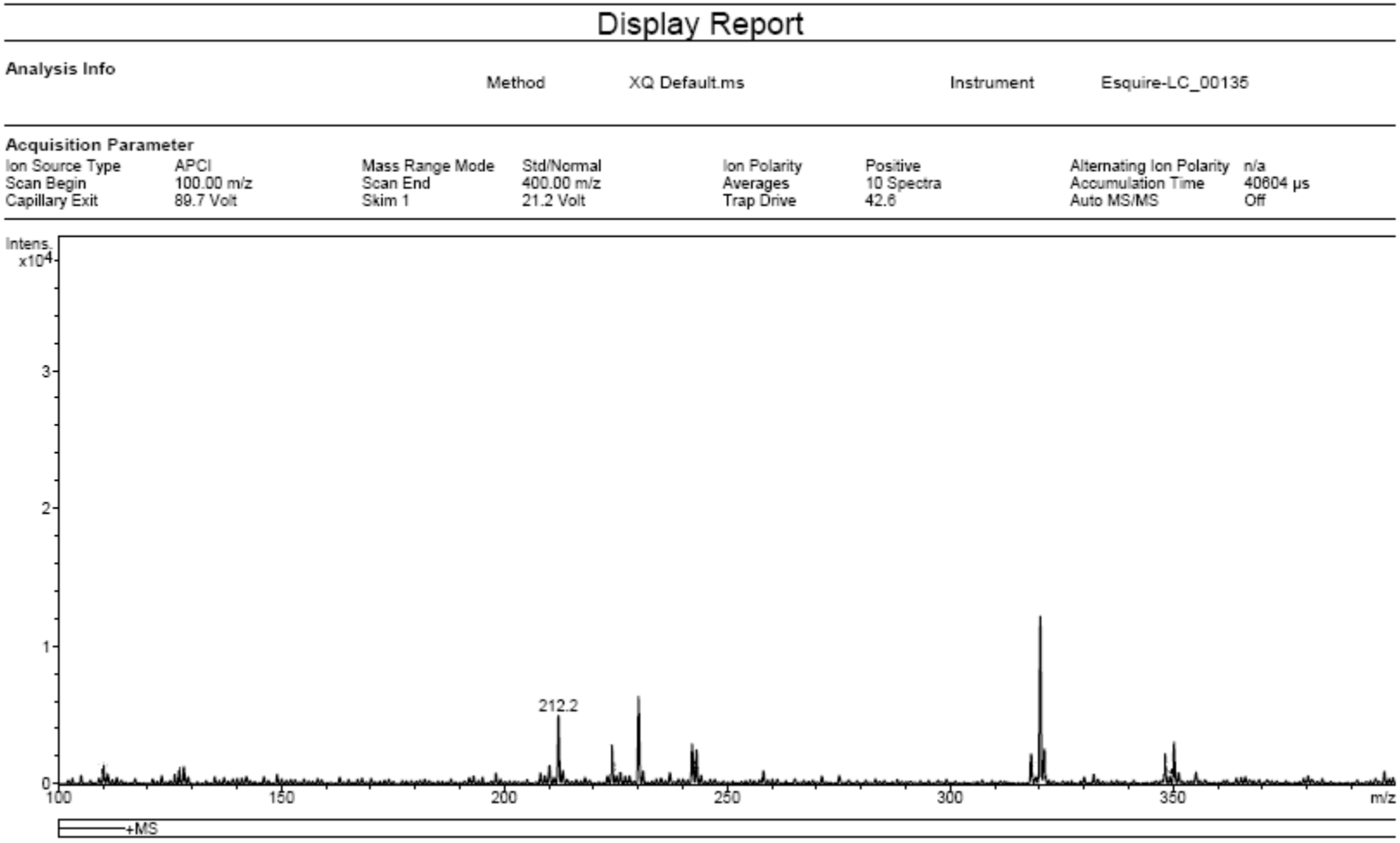

Figure 32: Mass spectrum of 1,3-bis(azidomethyl)benzene (**12**).

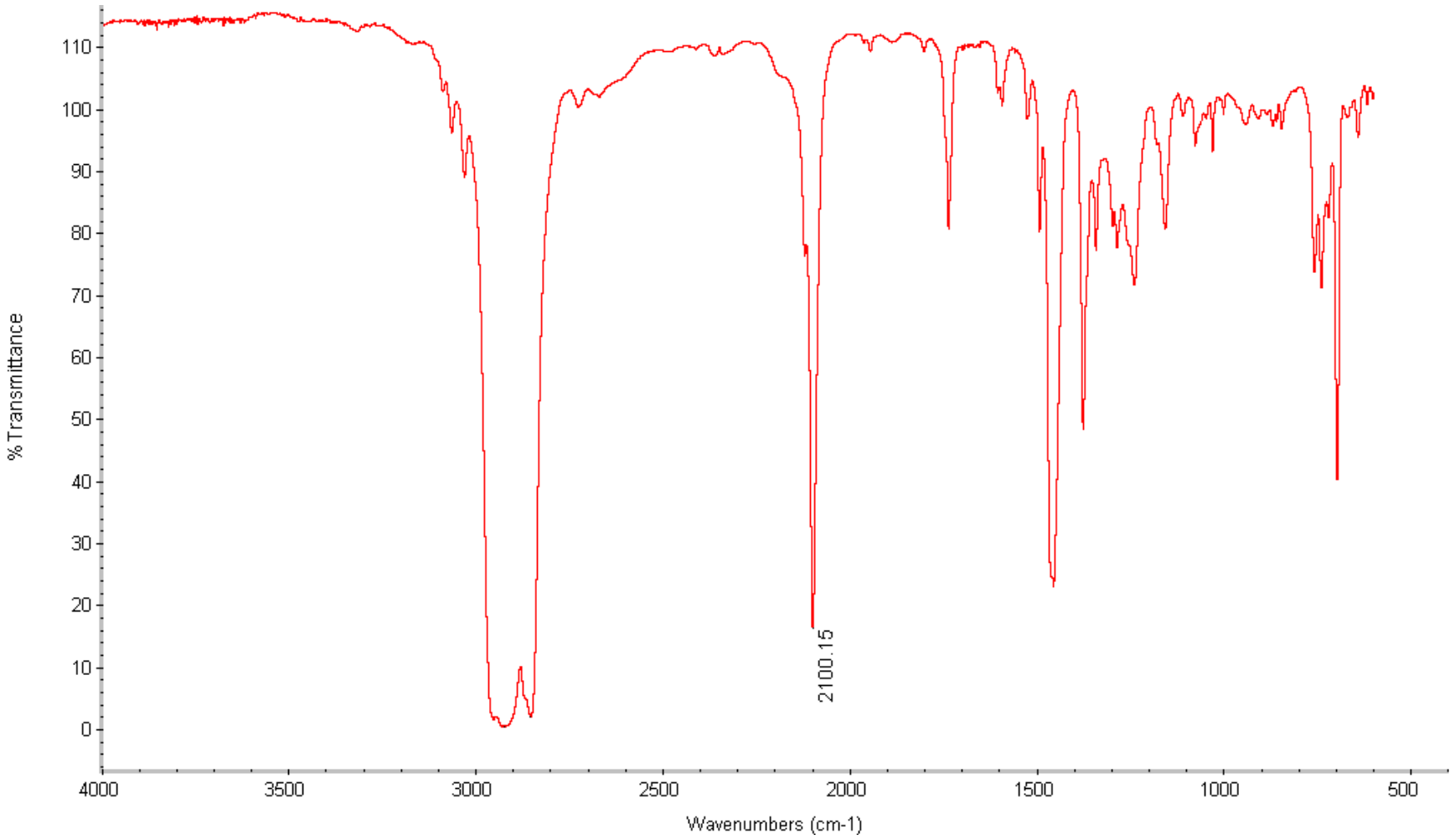

Figure 33: IR spectrum of 1,3-bis(azidomethyl)benzene (**12**).

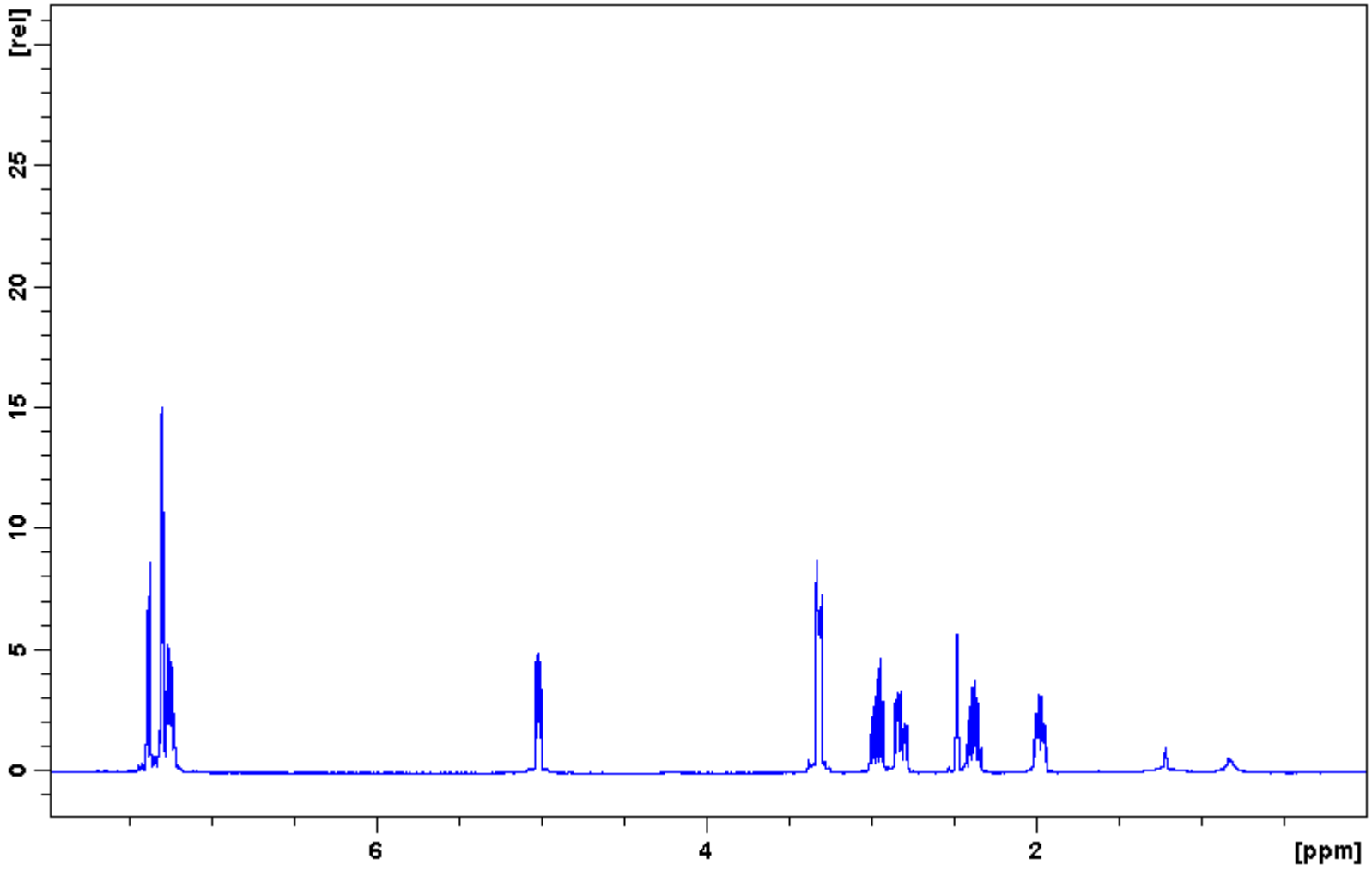

Figure 34: ^{1}H NMR spectrum of (±) 1-azido-2,3-dihydro-1*H*-indene (**14**).

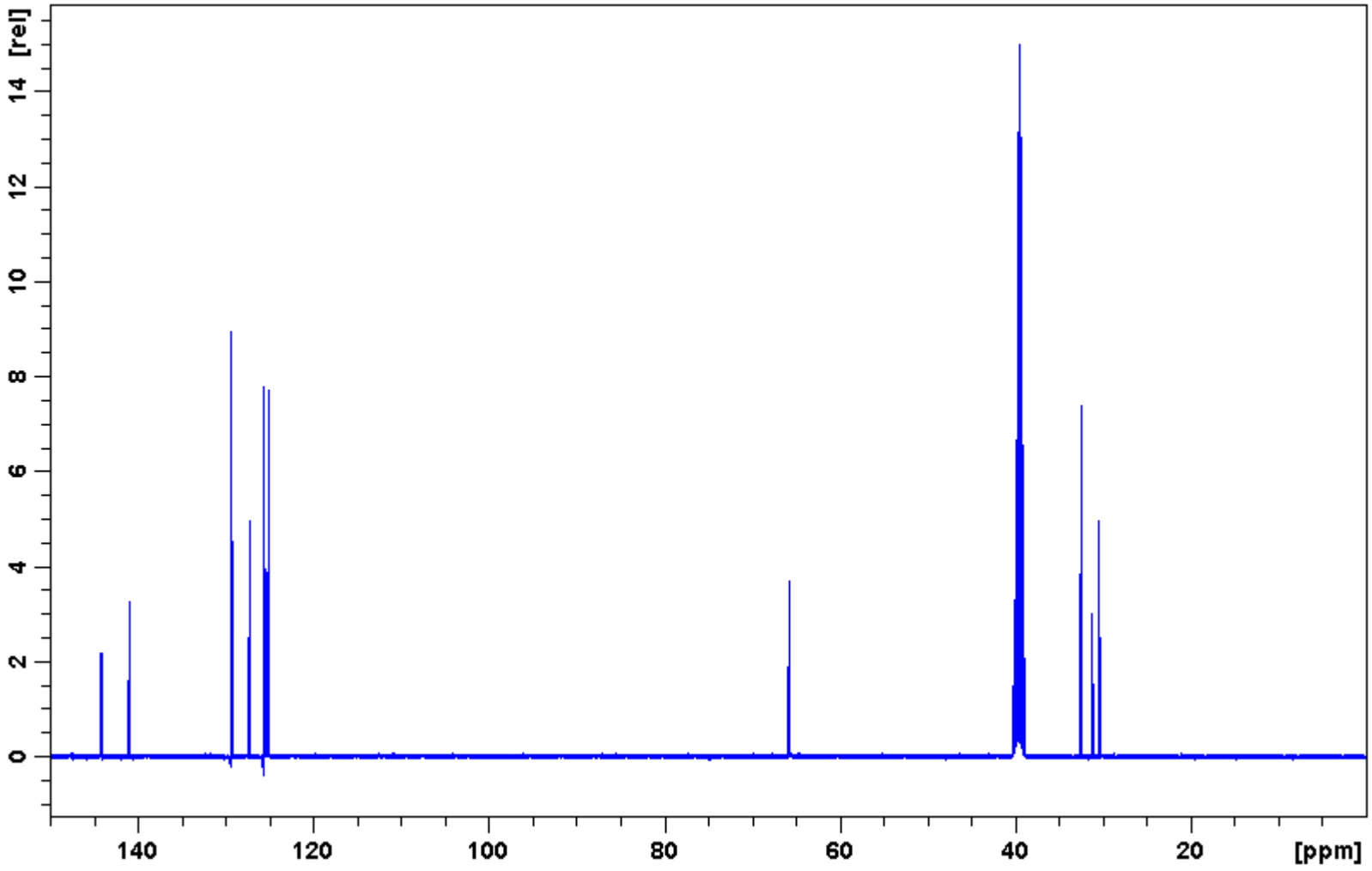

Figure 35: ^{13}C NMR spectrum of (±) 1-azido-2,3-dihydro-1*H*-indene (**14**).

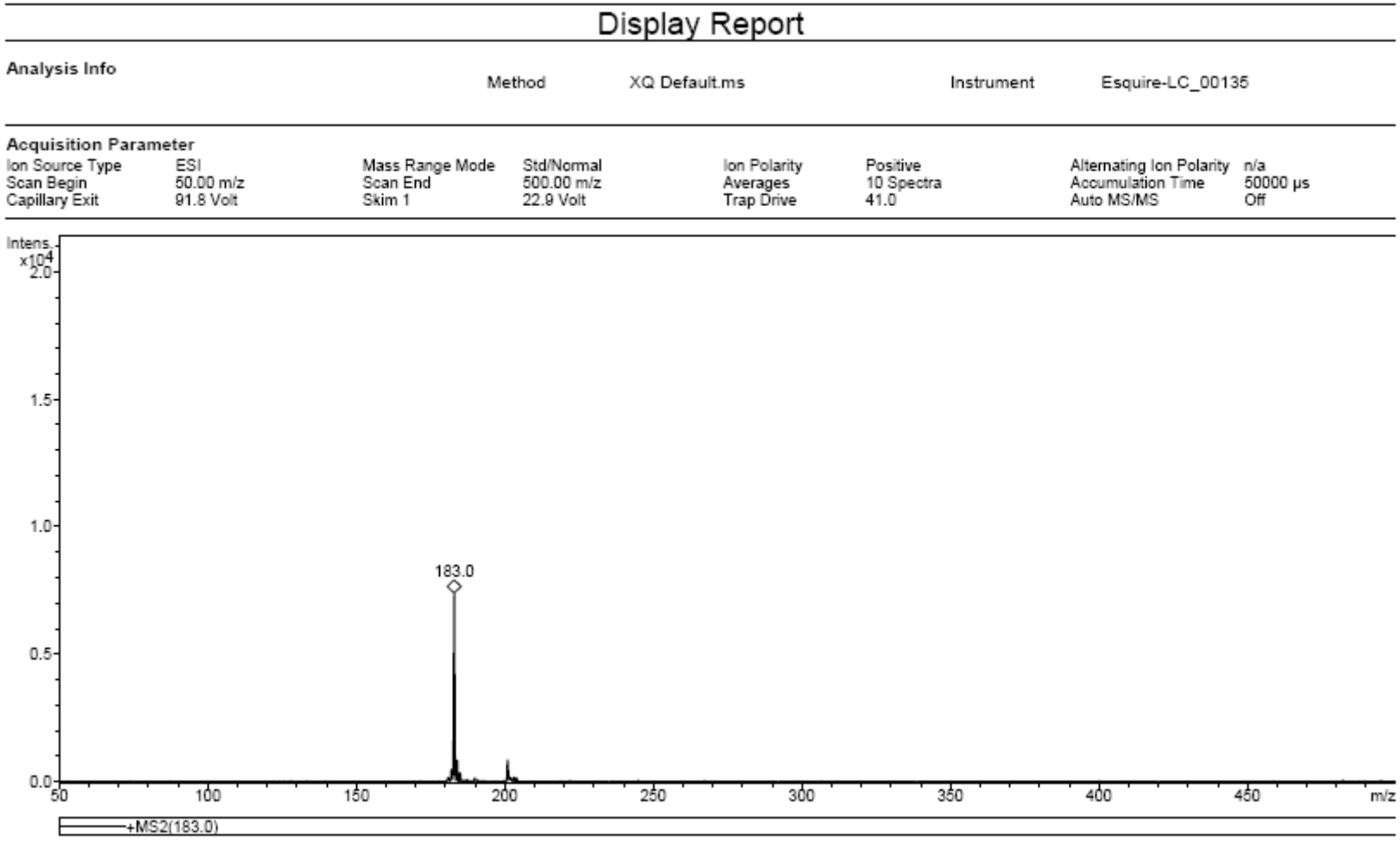

Figure 36: Mass spectrum of (±) 1-azido-2,3-dihydro-1*H*-indene (**14**).

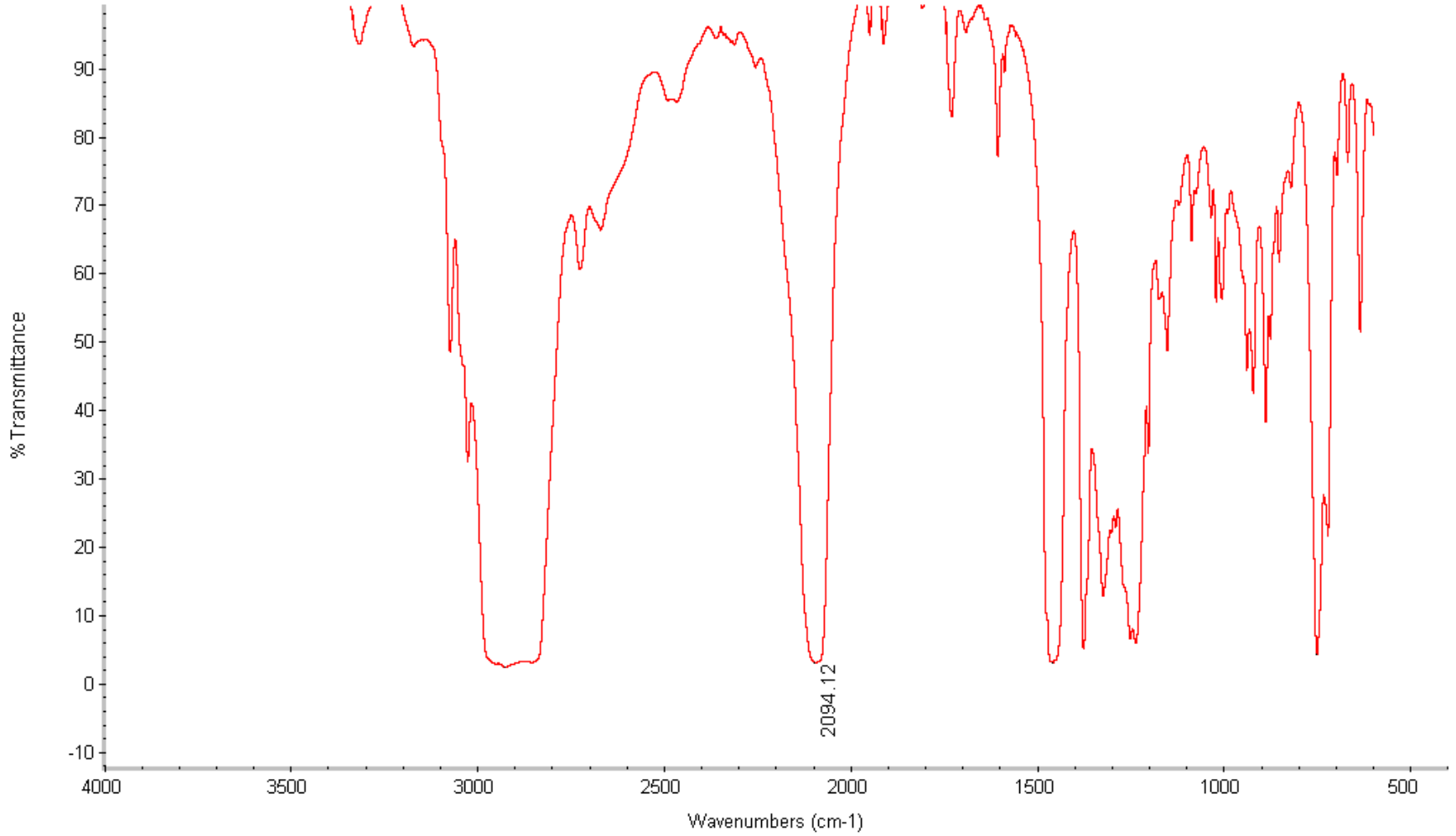

Figure 37: IR spectrum of (±) 1-azido-2,3-dihydro-1*H*-indene (**14**).

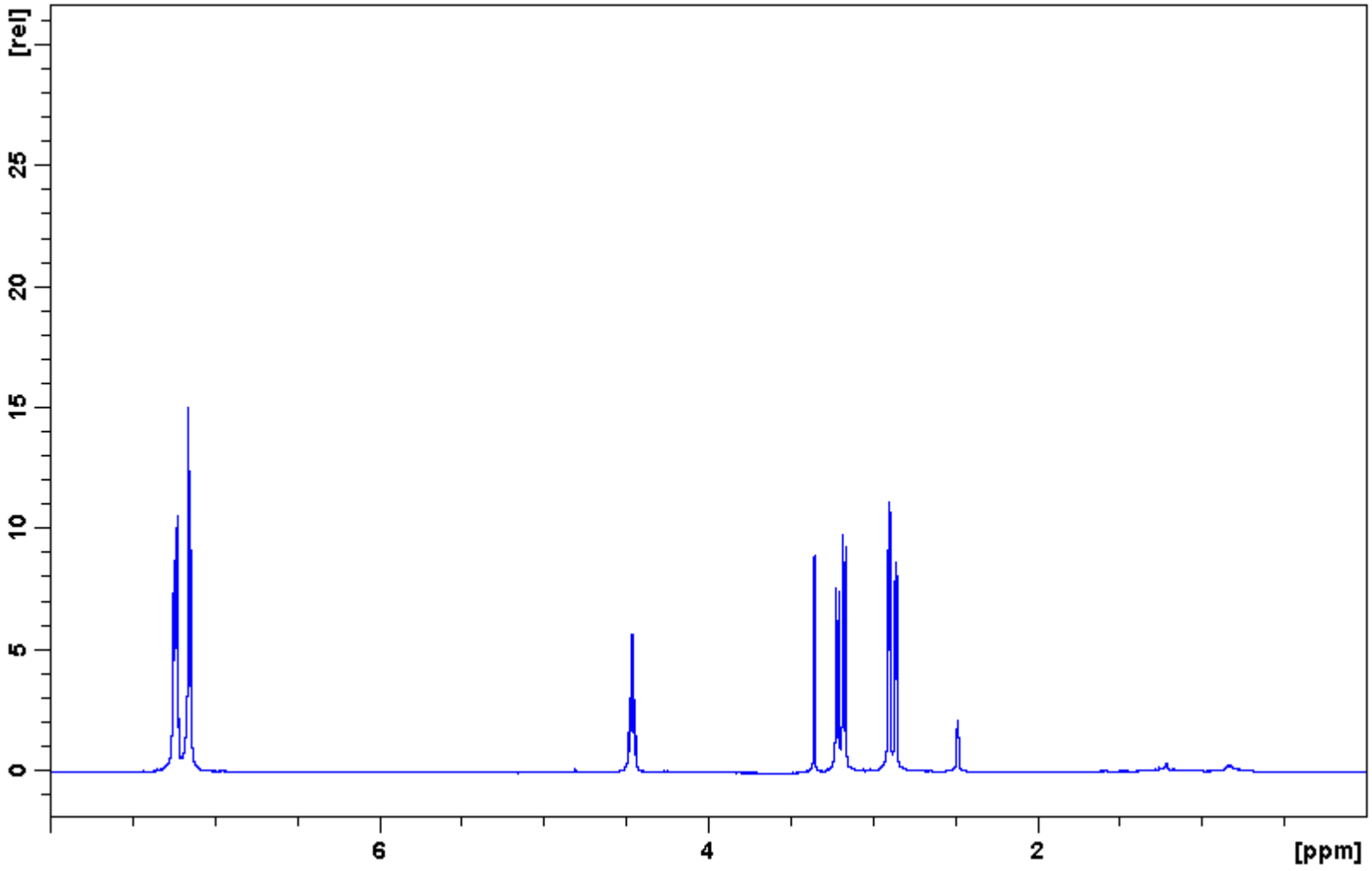

Figure 38: ^{1}H NMR spectrum of 2-azido-2,3-dihydro-1*H*-indene (**18**).

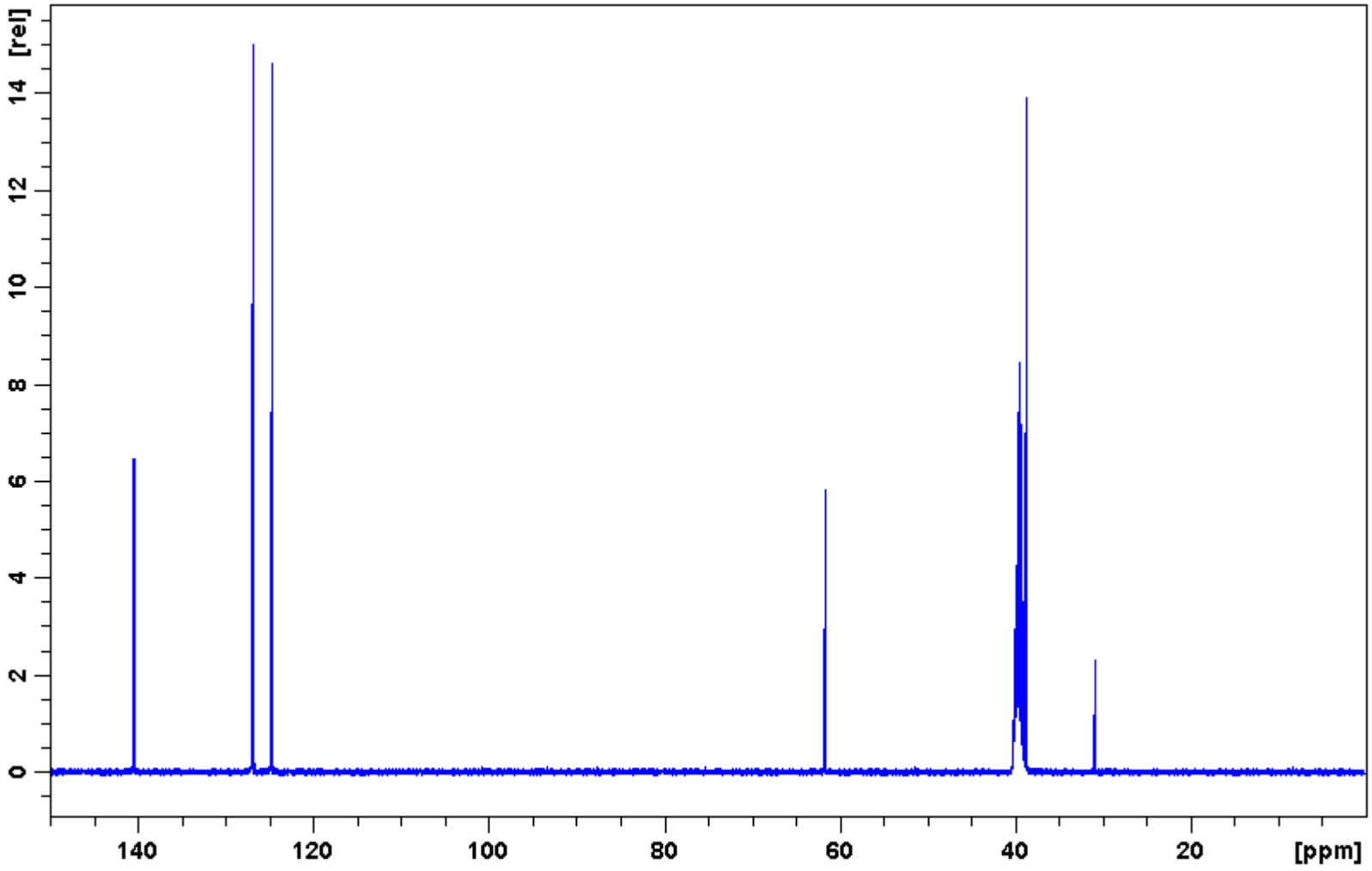

Figure 39: ^{13}C NMR spectrum of 2-azido-2,3-dihydro-1*H*-indene (**18**).

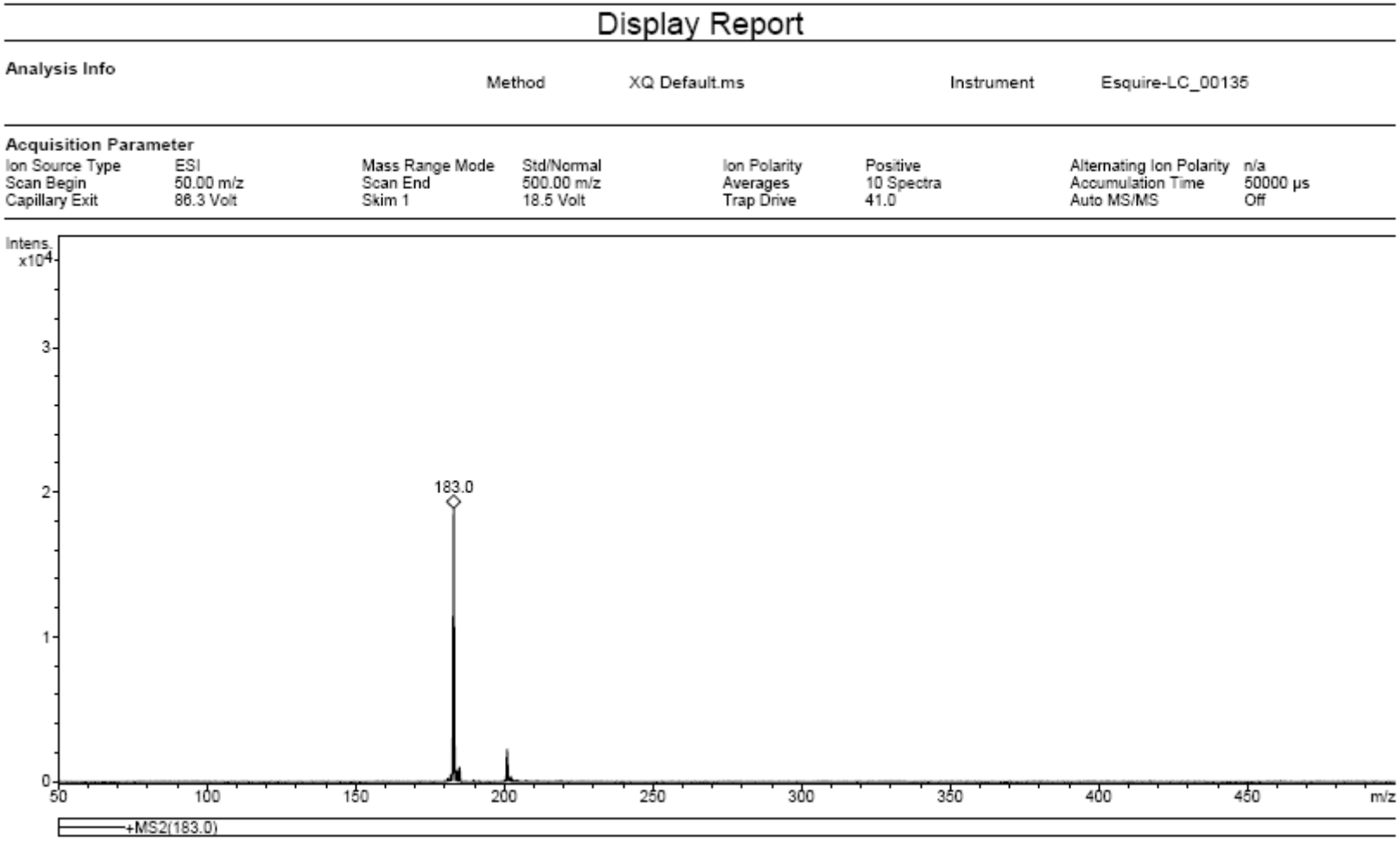

Figure 40: Mass spectrum of 2-azido-2,3-dihydro-1*H*-indene (**18**).

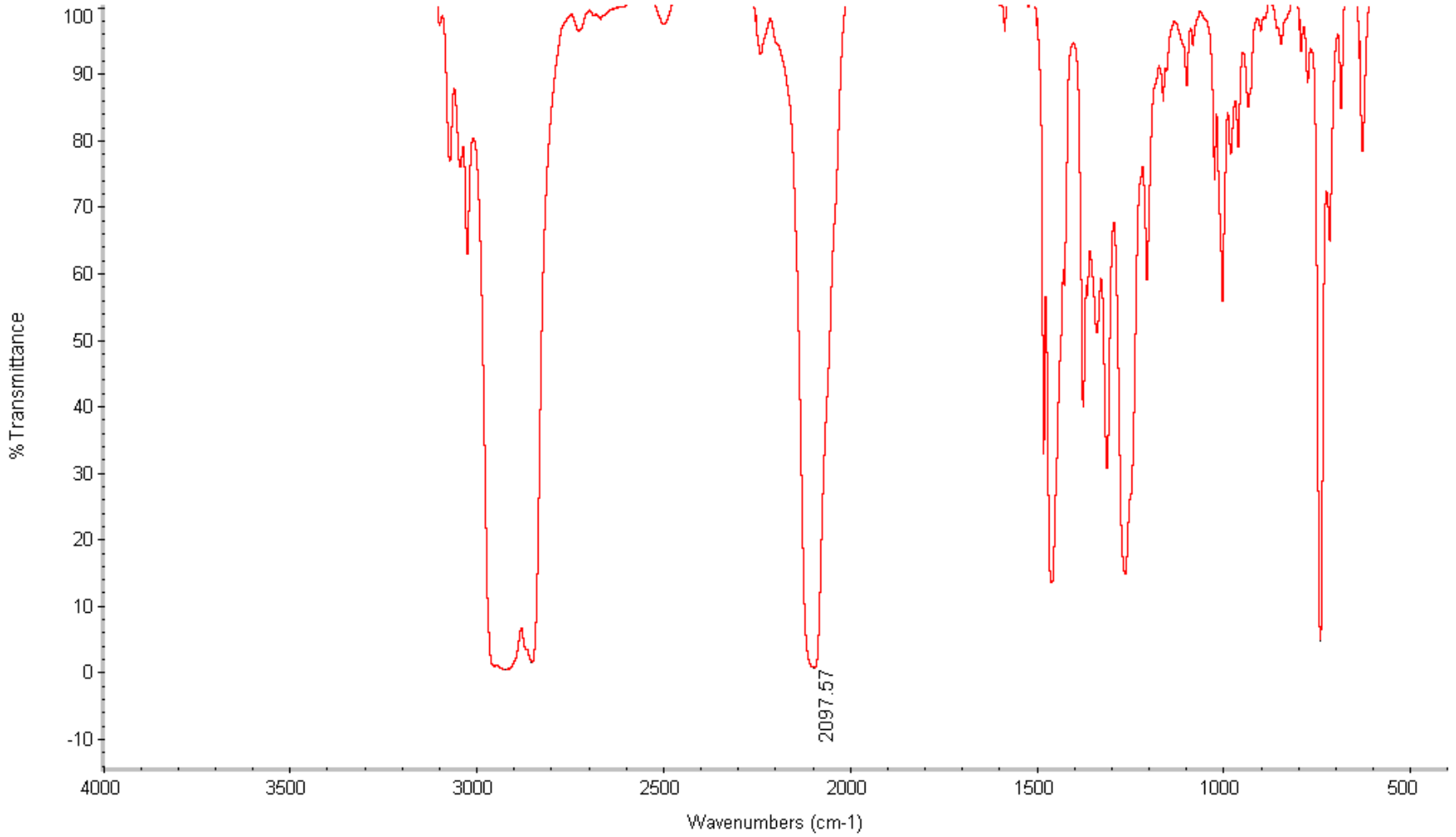

Figure 41: IR spectrum of 2-azido-2,3-dihydro-1*H*-indene (**18**).

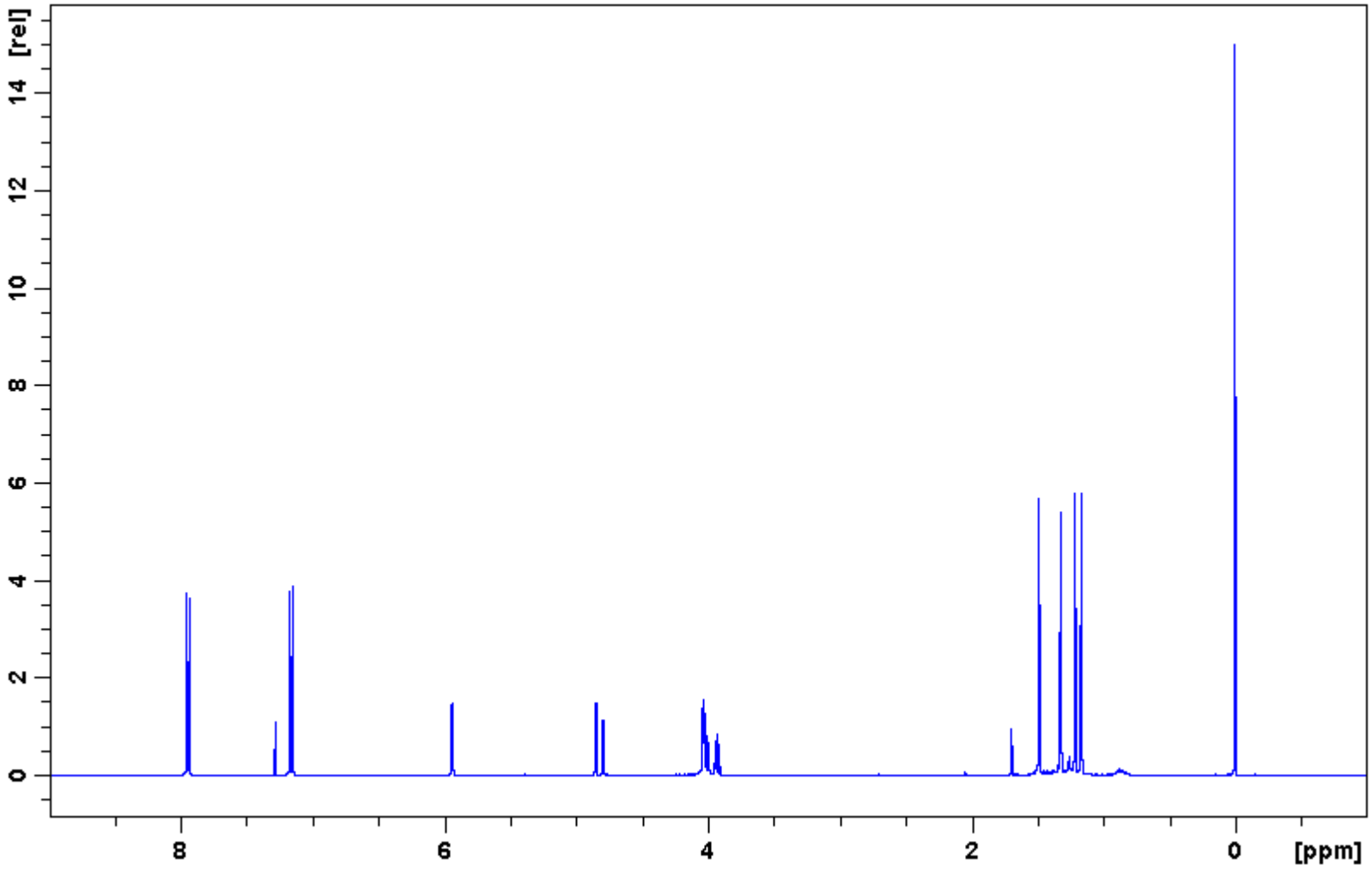

Figure 42: ^{1}H NMR spectrum of 6-*O*-(*p*-azido)benzenesulfonate ester of 1,2:5,6-di-*O*-isopropylidene-α-D-glucofuranose (**21**).

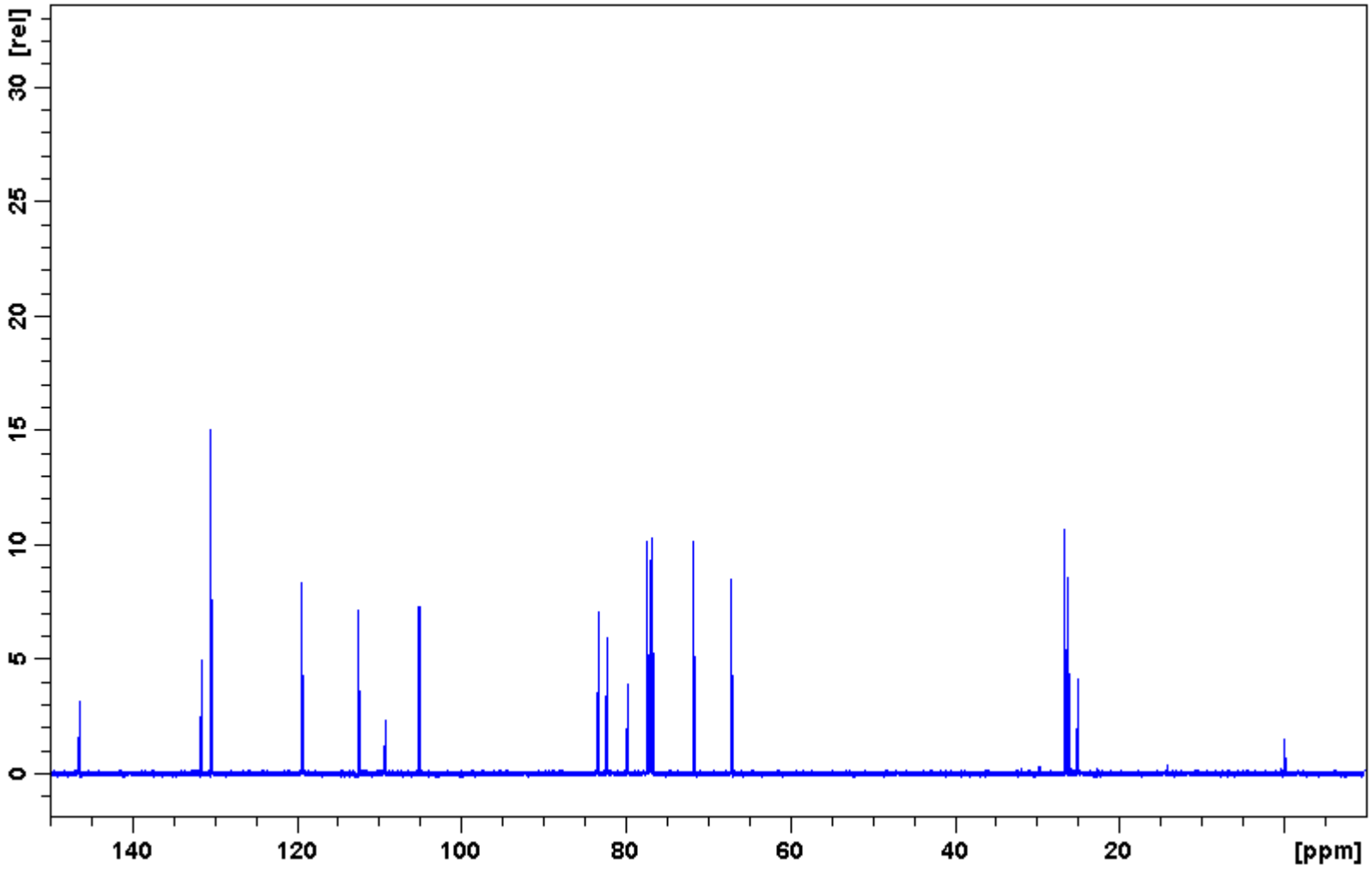

Figure 43: ^{13}C NMR spectrum of 6-*O*-(*p*-azido)benzenesulfonate ester of 1,2:5,6-di-*O*-isopropylidene-α-D-glucofuranose (**21**).

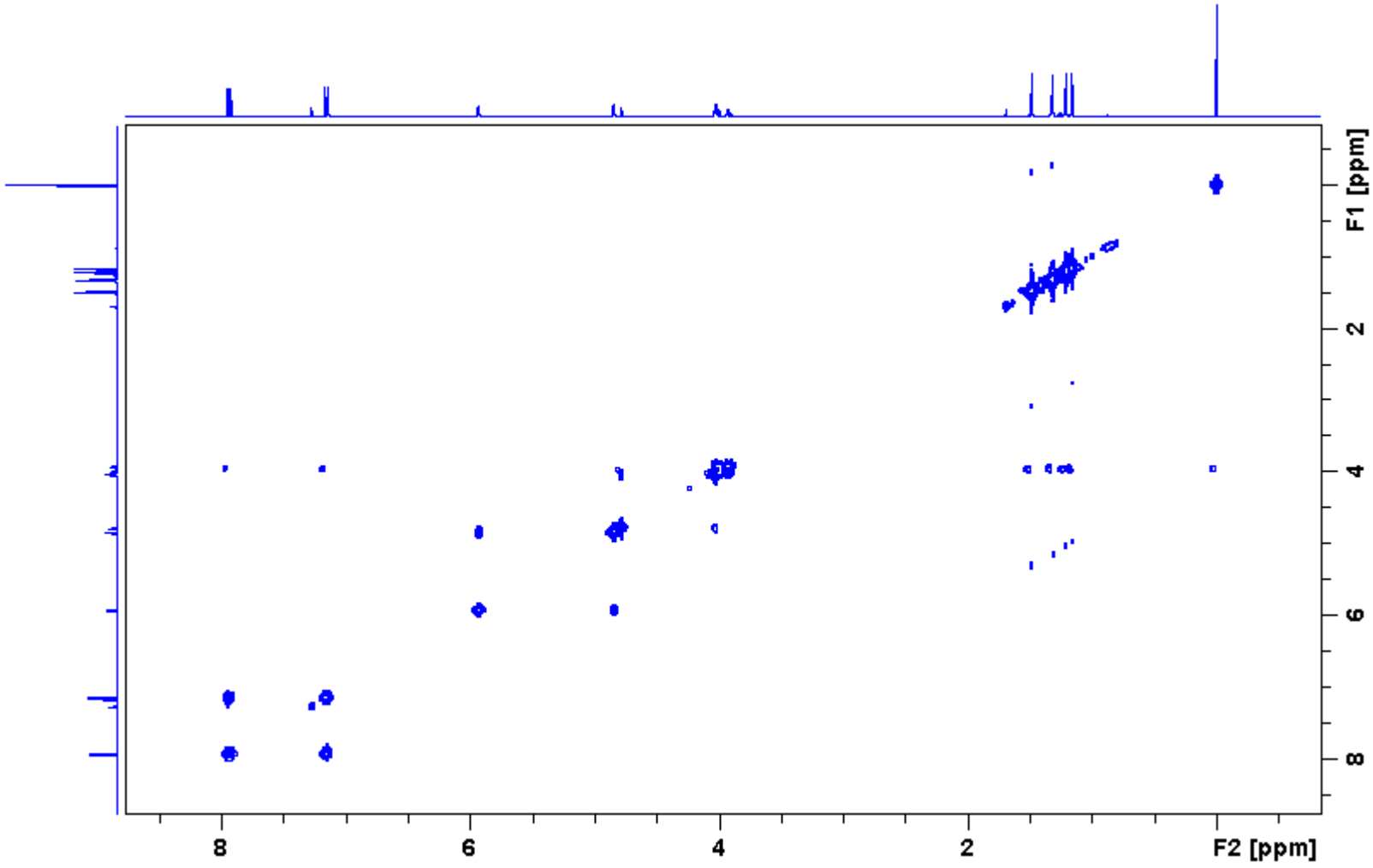

Figure 44: COSY NMR spectrum of 6-*O*-(*p*-azido)benzenesulfonate ester of 1,2:5,6-di-*O*-isopropylidene-α-D-glucofuranose (**21**).

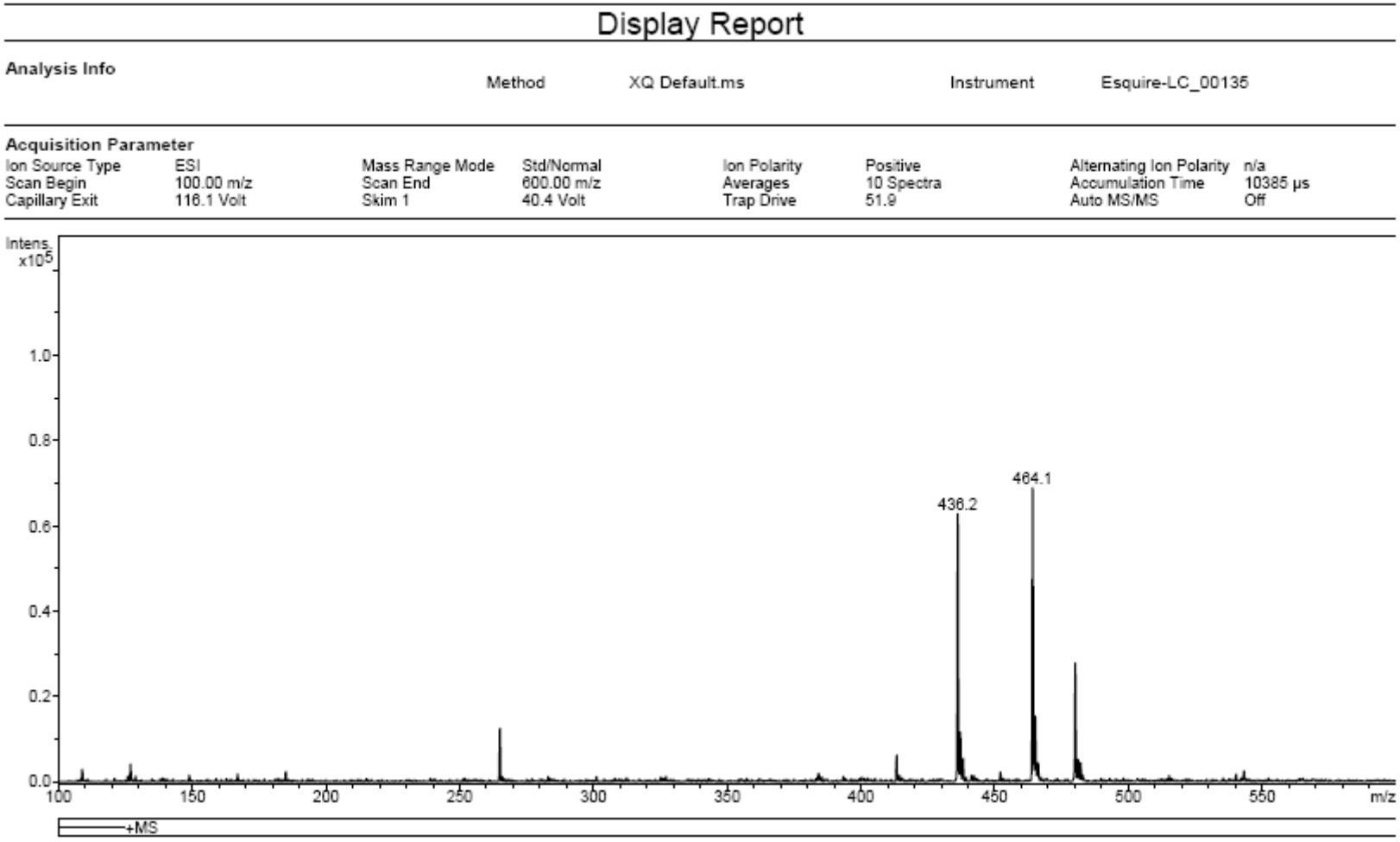

Figure 45: Mass spectrum of 6-*O*-(*p*-azido)benzenesulfonate ester of 1,2:5,6-di-*O*-isopropylidene-α-D-glucofuranose (**21**).

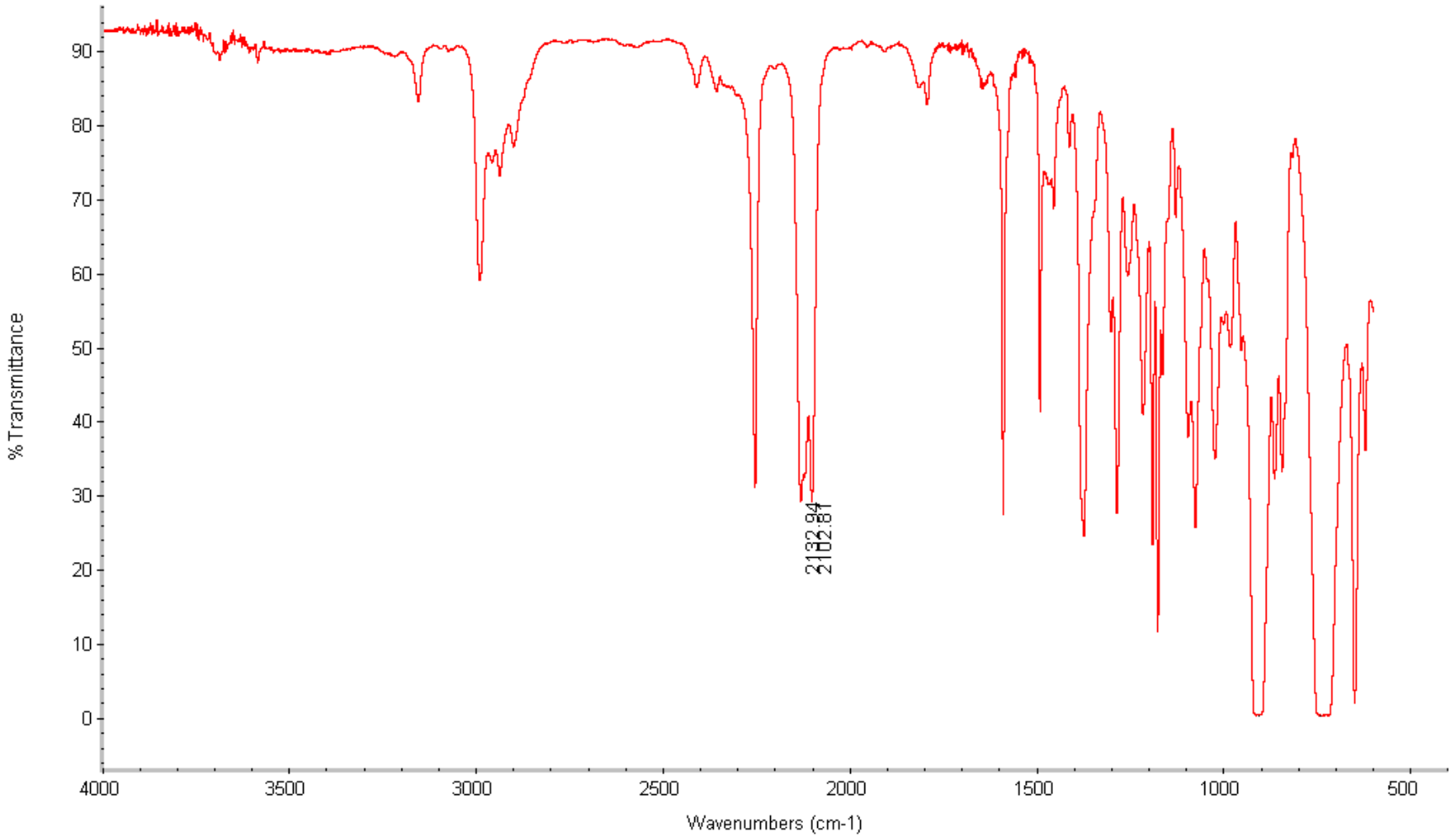

Figure 46: IR spectrum of 6-*O*-(*p*-azido)benzenesulfonate ester of 1,2:5,6-di-*O*-isopropylidene-α-D-glucofuranose (**21**).

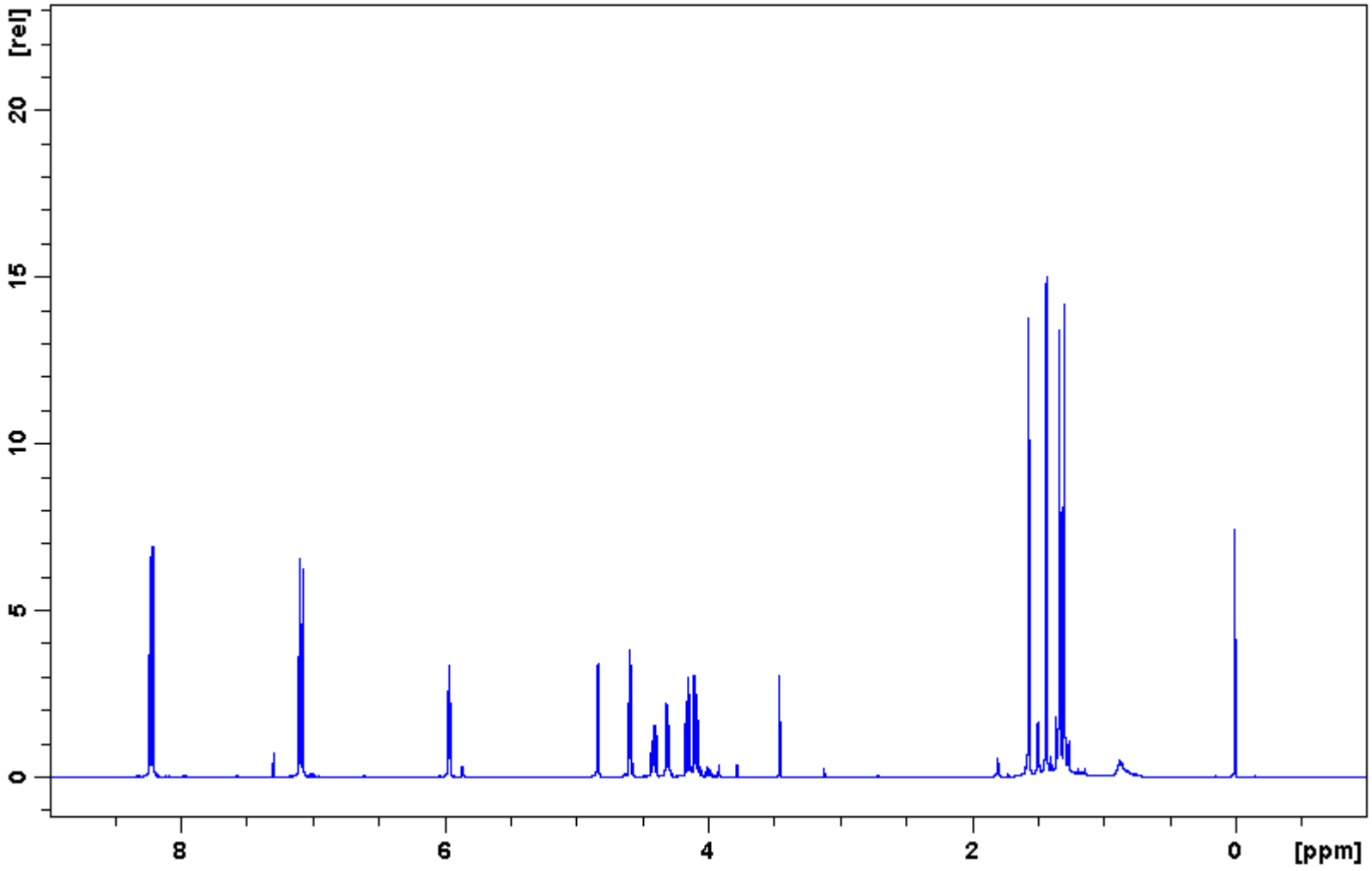

Figure 47: ^{1}H NMR spectrum of 6-*O*-(*p*-nitro)benzenesulfonate ester of 1,2:5,6-di-*O*-isopropylidene-α-D-glucofuranose (**22**).

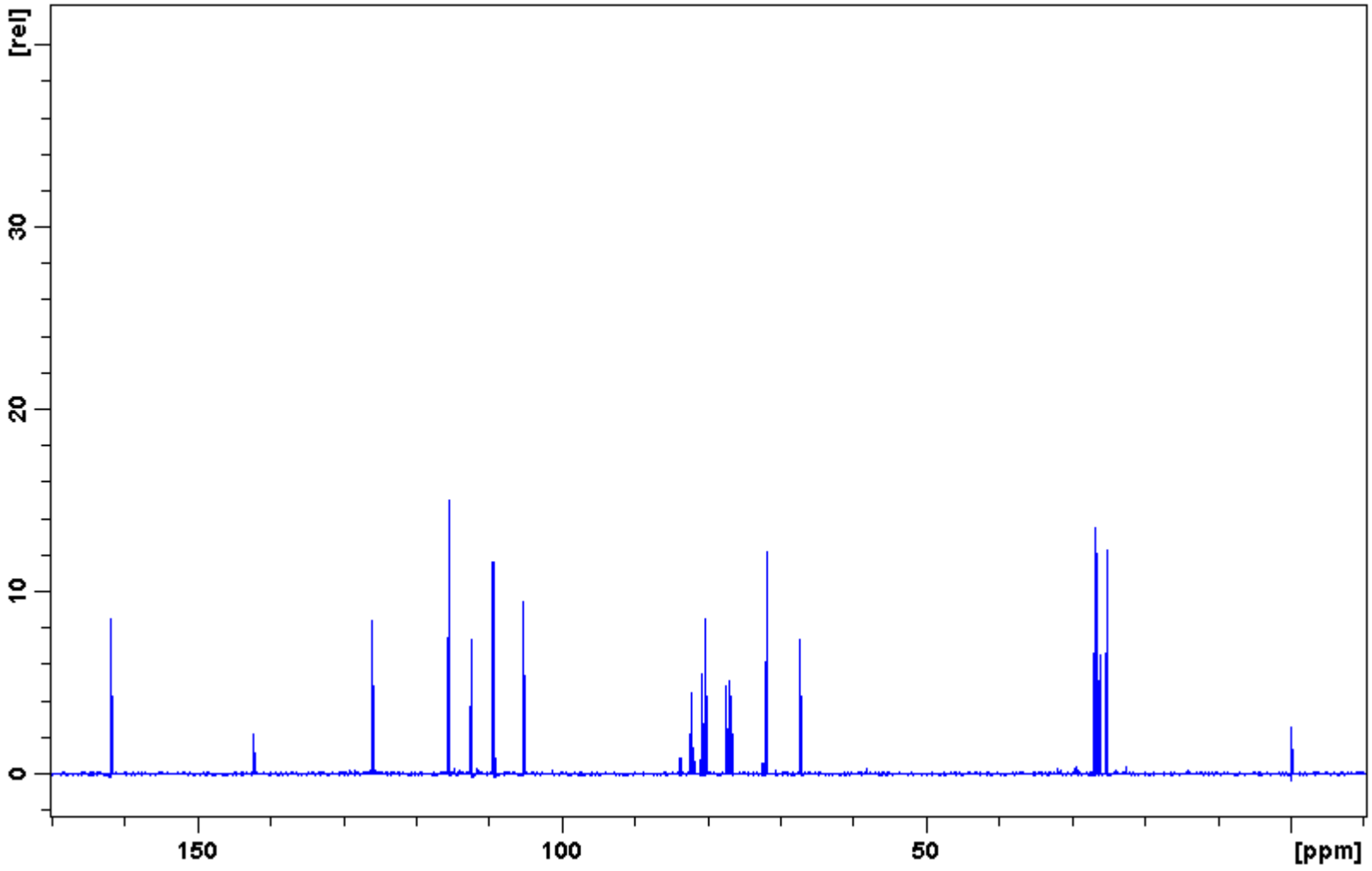

Figure 48: ^{13}C NMR spectrum of 6-*O*-(*p*-nitro)benzenesulfonate ester of 1,2:5,6-di-*O*-isopropylidene-α-D-glucofuranose (**22**).

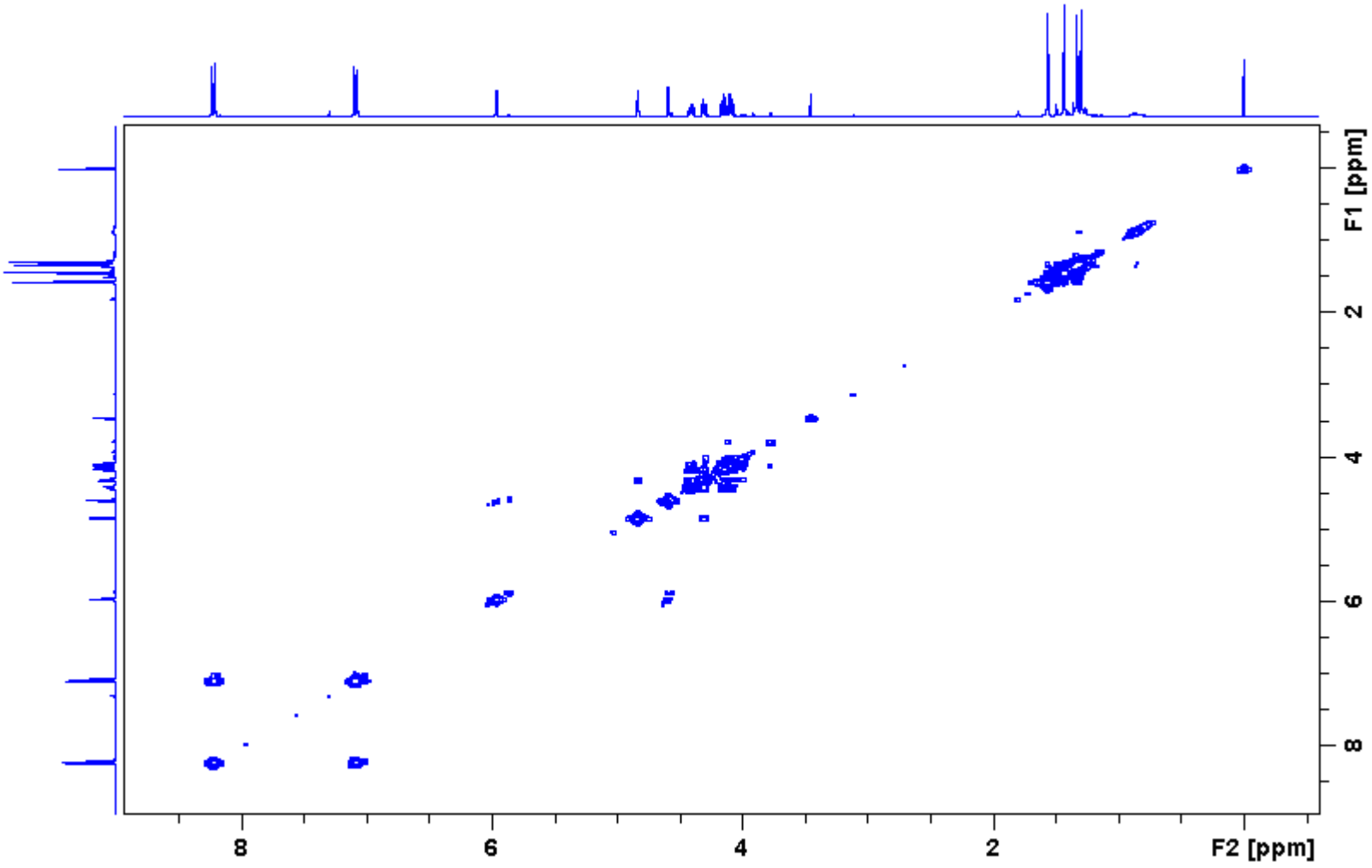

Figure 49: COSY NMR spectrum of 6-*O*-(*p*-nitro)benzenesulfonate ester of 1,2:5,6-di-*O*-isopropylidene-α-D-glucofuranose (**22**).

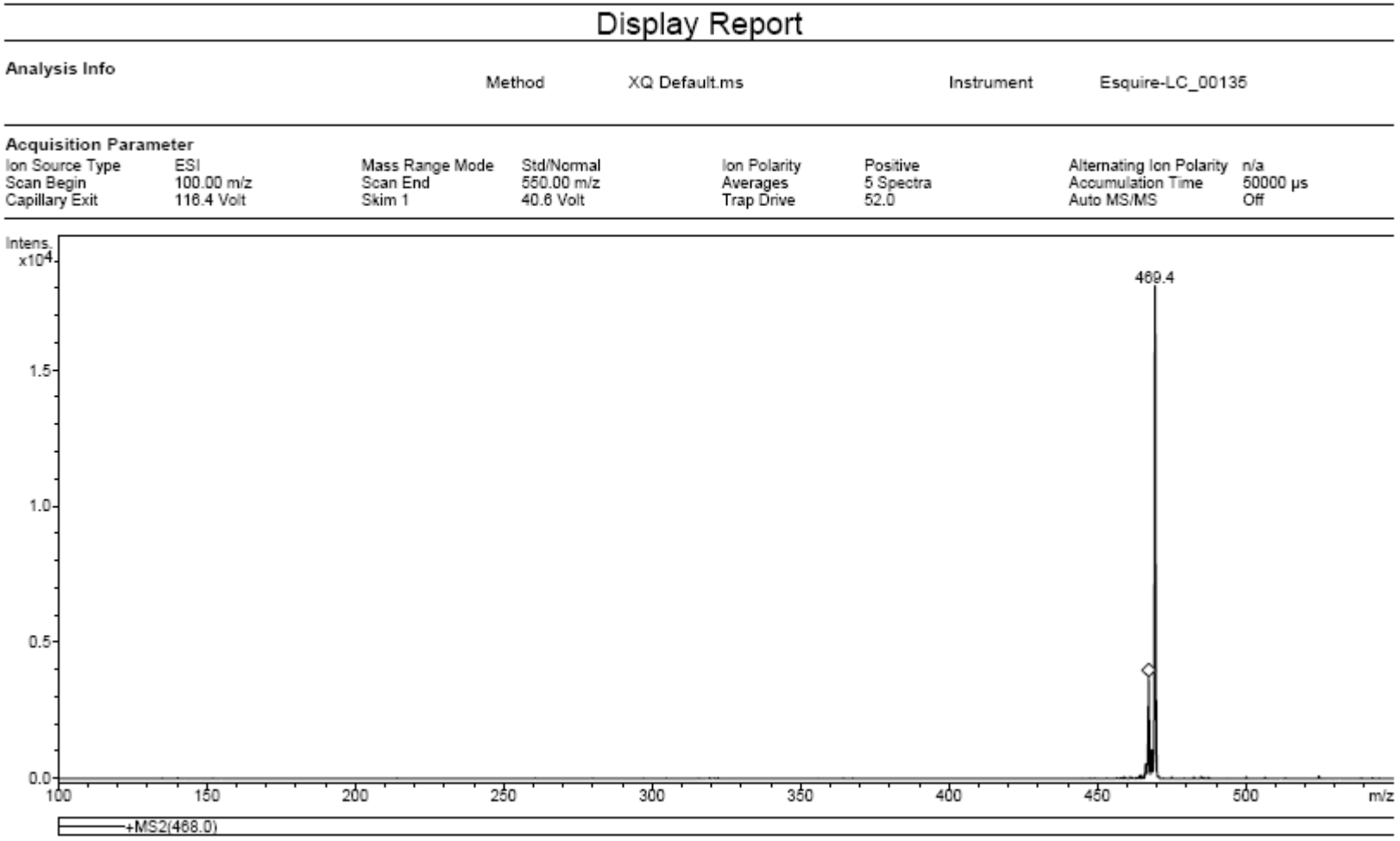

Figure 50: Mass spectrum of 6-*O*-(*p*-nitro)benzenesulfonate ester of 1,2:5,6-di-*O*-isopropylidene-α-D-glucofuranose (**22**).

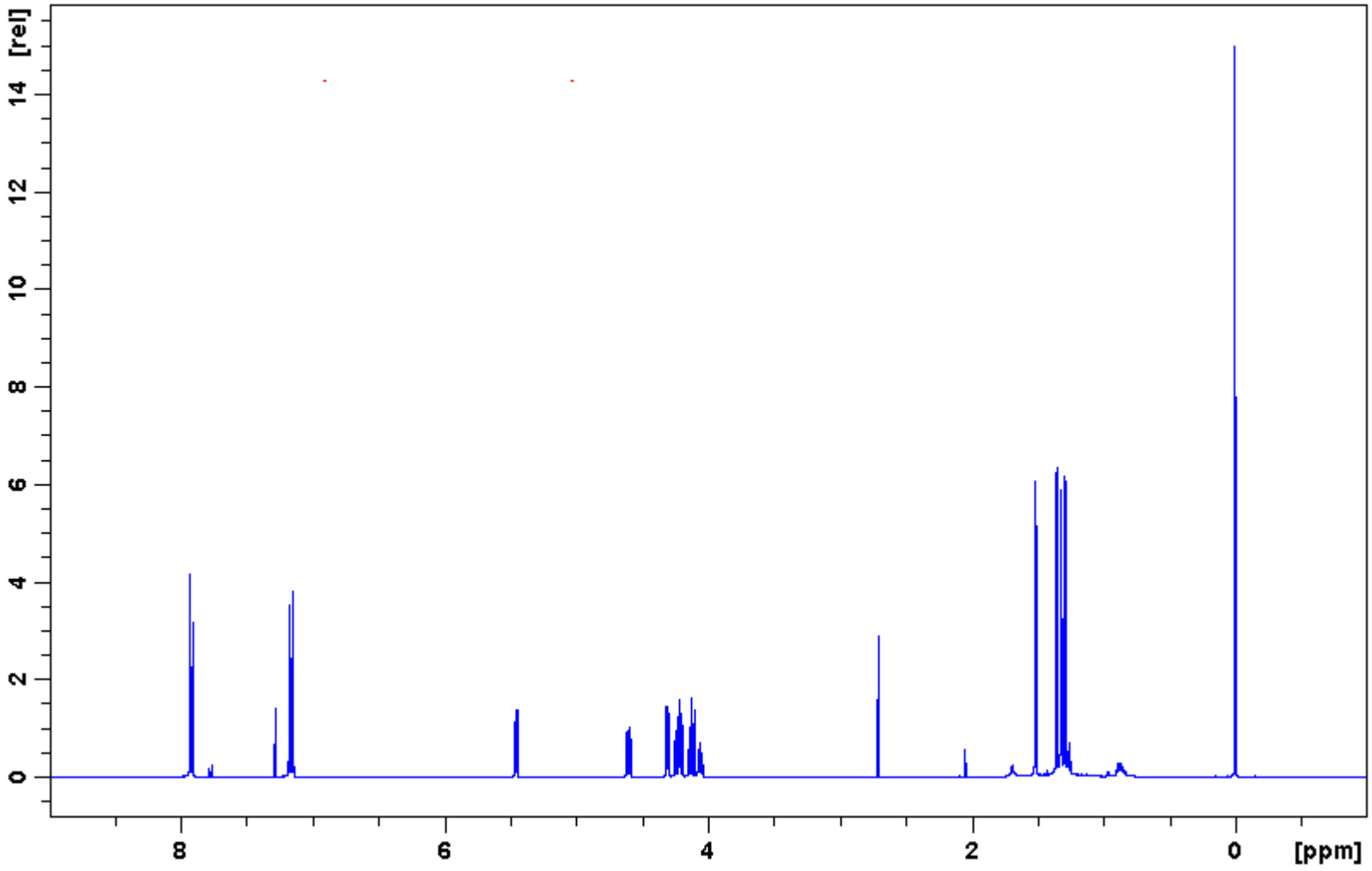

Figure 51: ^{1}H NMR spectrum of 6-*O*-(*p*-azido)benzenesulfonate ester of 1,2:3,4-di-*O*-isopropylidene-α-D-galactopyranose (**24**).

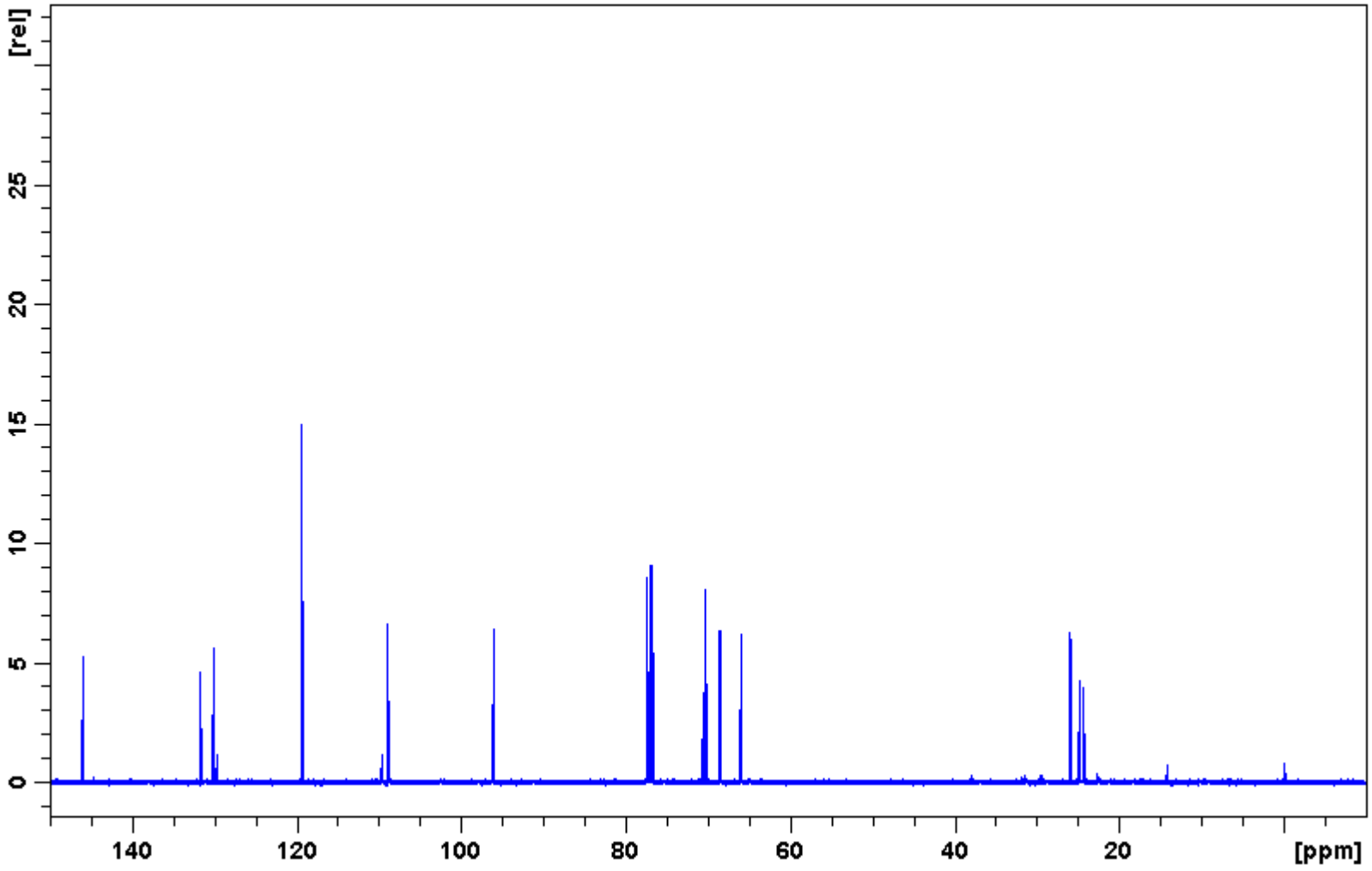

Figure 52: ^{13}C NMR spectrum of 6-*O*-(*p*-azido)benzenesulfonate ester of 1,2:3,4-di-*O*-isopropylidene-α-D-galactopyranose (**24**).

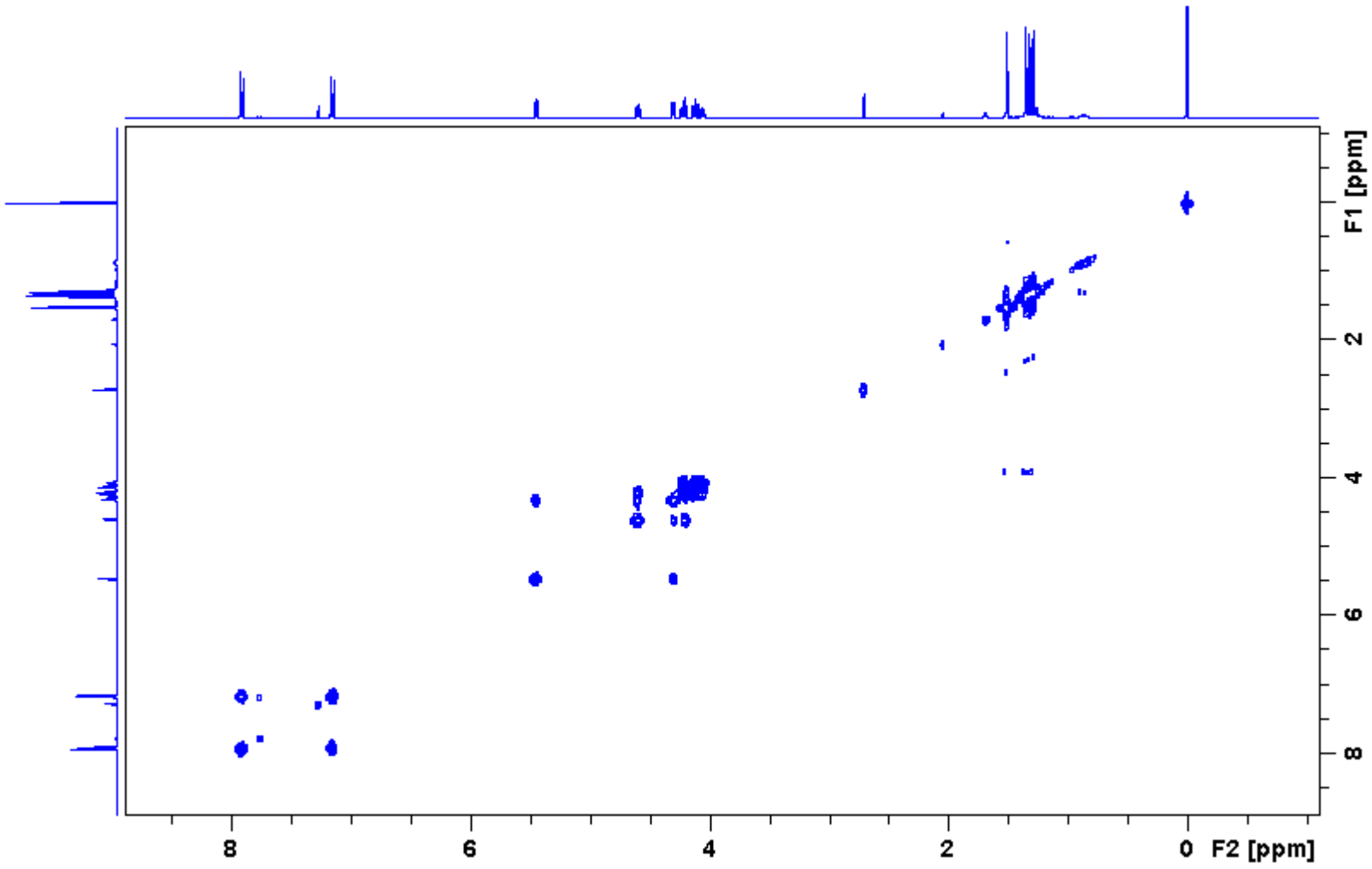

Figure 53: COSY NMR spectrum of 6-*O*-(*p*-azido)benzenesulfonate ester of 1,2:3,4-di-*O*-isopropylidene-α-D-galactopyranose (**24**).

Display Report

Analysis Info

Method XQ Default.ms Instrument Esquire-LC_00135

Acquisition Parameter

Ion Source Type	ESI	Mass Range Mode	Std/Normal	Ion Polarity	Positive	Alternating Ion Polarity	n/a
Scan Begin	100.00 m/z	Scan End	600.00 m/z	Averages	10 Spectra	Accumulation Time	1555 µs
Capillary Exit	116.1 Volt	Skim 1	40.4 Volt	Trap Drive	51.9	Auto MS/MS	Off

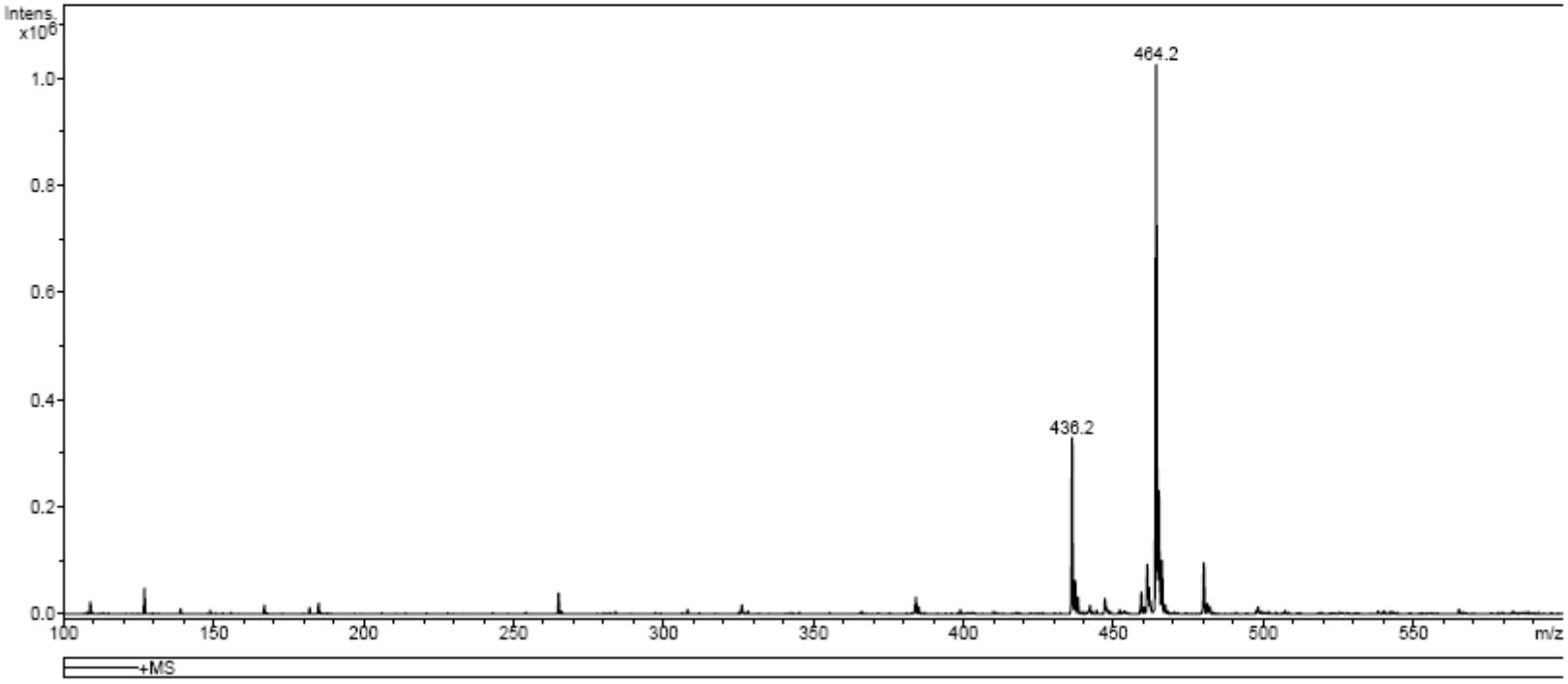

Figure 54: Mass spectrum of 6-*O*-(*p*-azido)benzenesulfonate ester of 1,2:3,4-di-*O*-isopropylidene-α-D-galactopyranose (**24**).

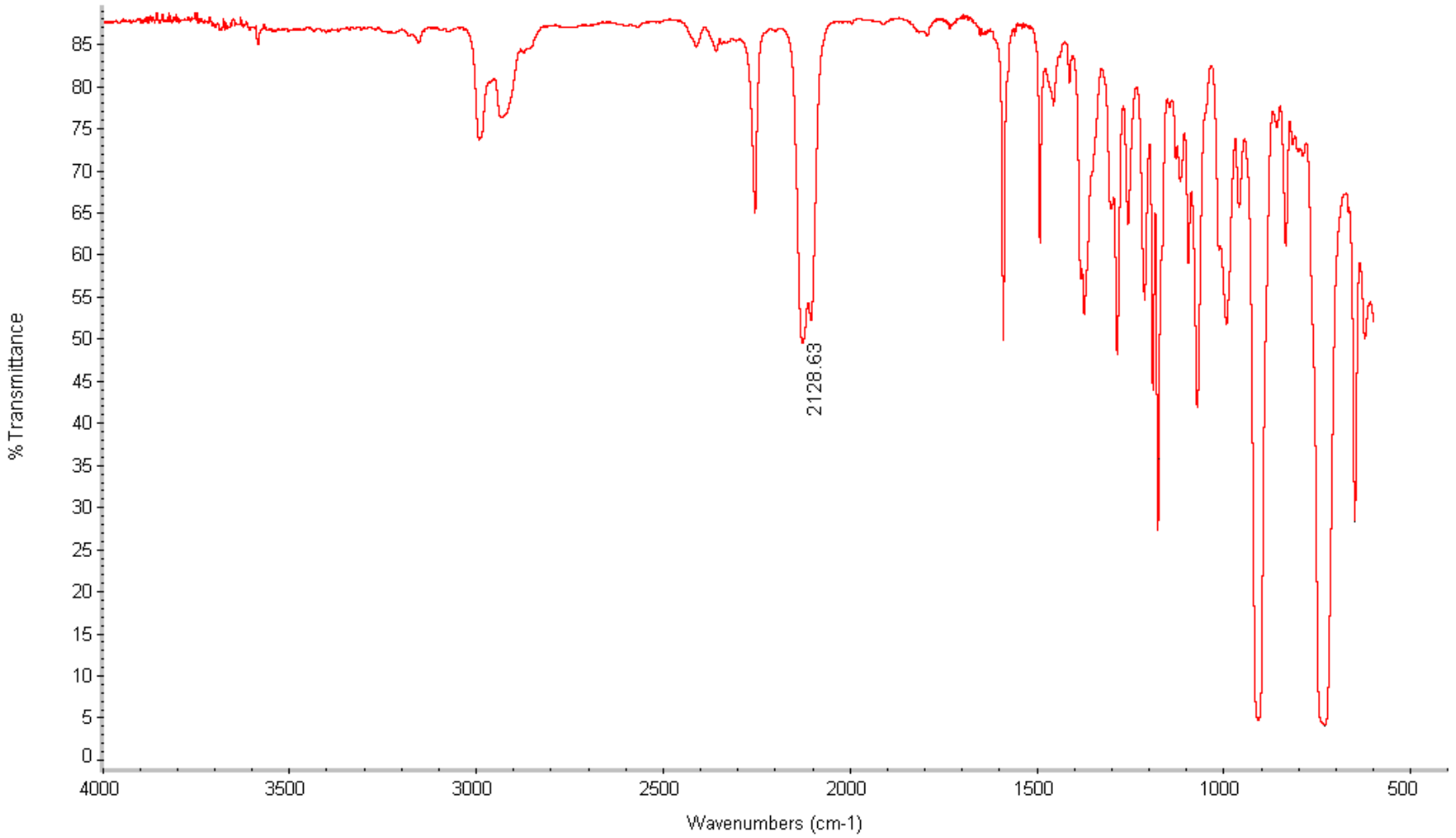

Figure 55: IR spectrum of 6-*O*-(*p*-azido)benzenesulfonate ester of 1,2:3,4-di-*O*-isopropylidene-α-D-galactopyranose (**24**).

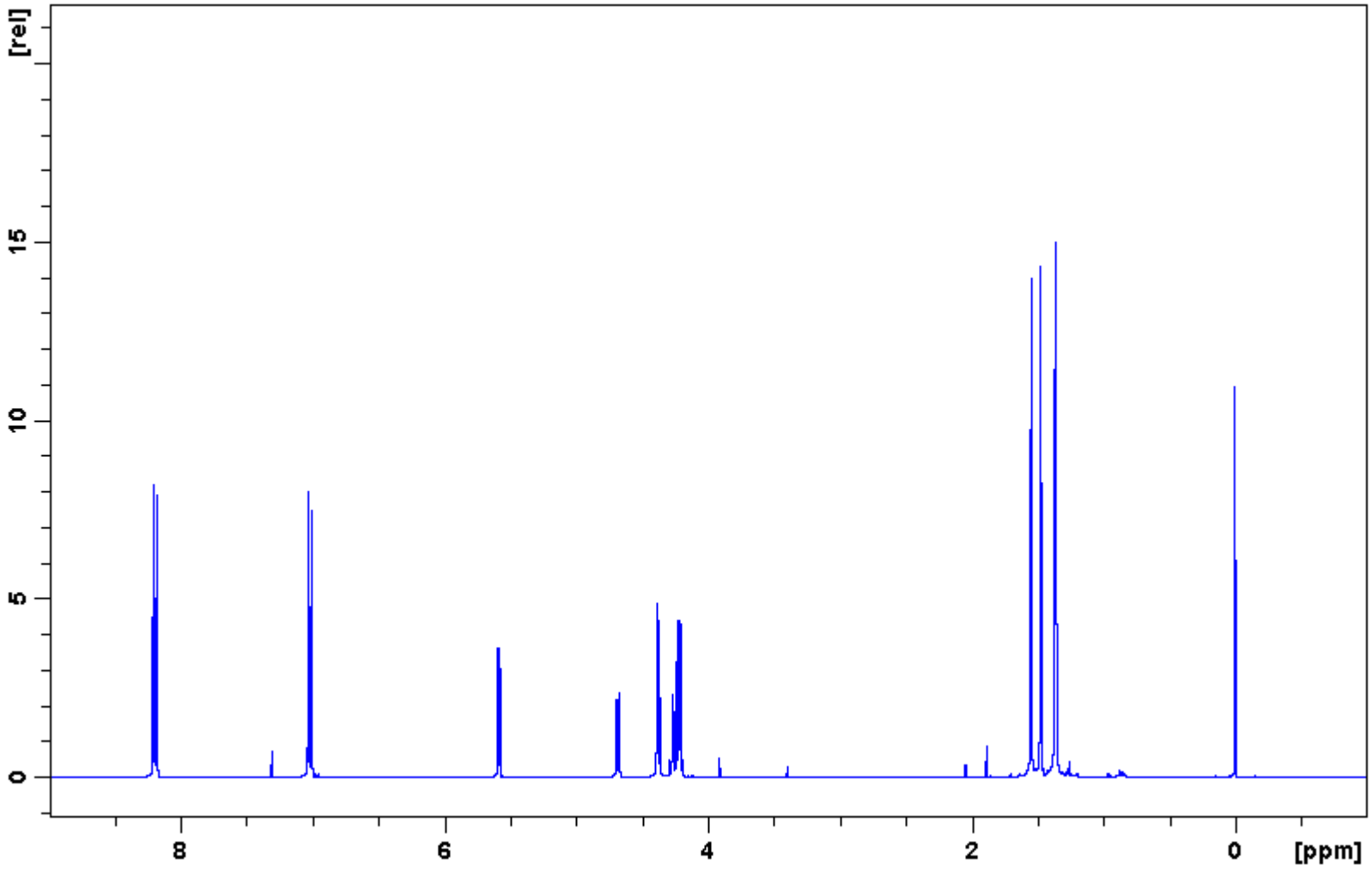

Figure 56: ^{1}H NMR spectrum of 6-*O*-(*p*-nitro)benzenesulfonate ester of 1,2:3,4-di-*O*-isopropylidene-α-D-galactopyranose (**25**).

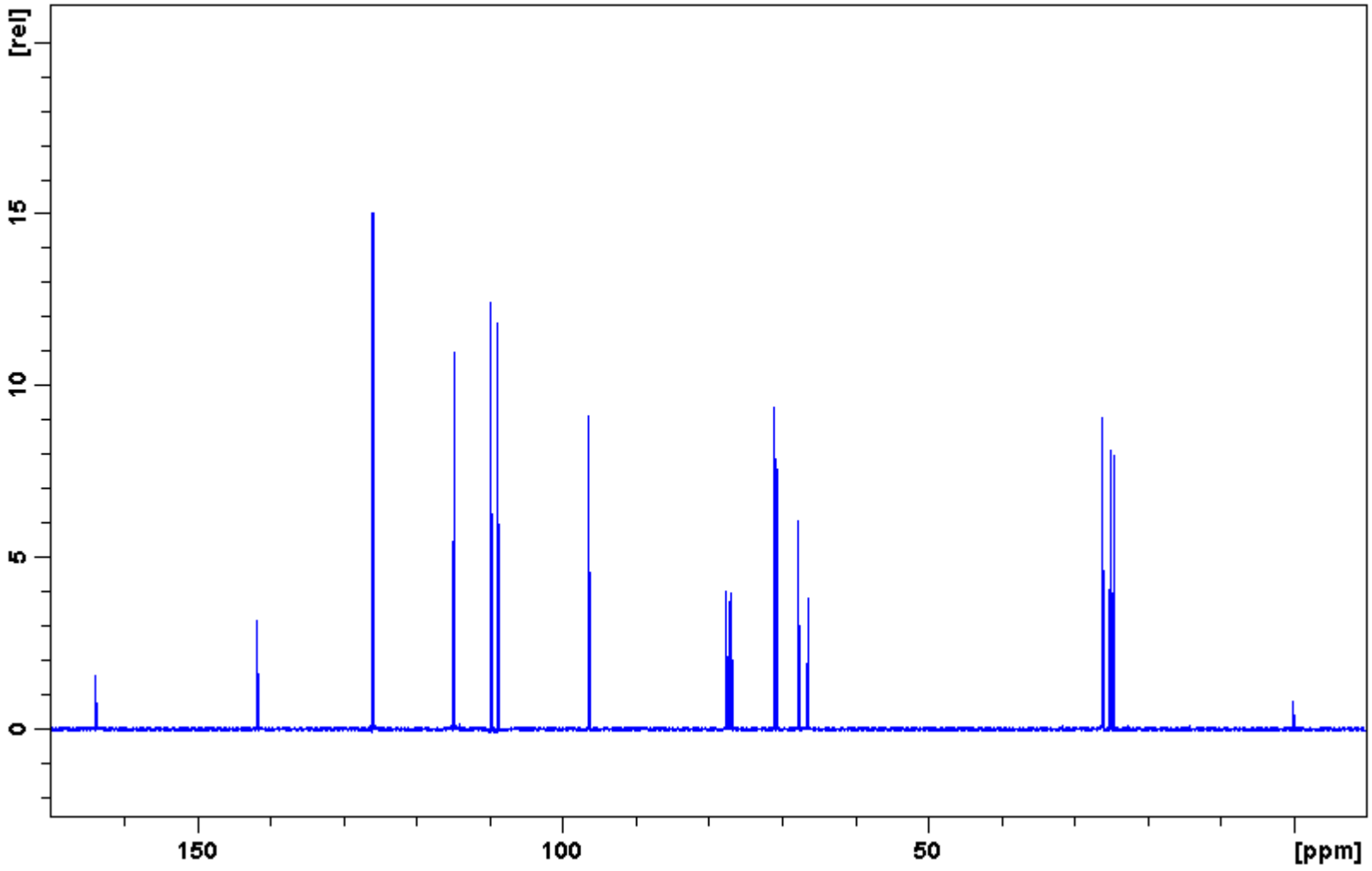

Figure 57: ^{13}C NMR spectrum of 6-*O*-(*p*-nitro)benzenesulfonate ester of 1,2:3,4-di-*O*-isopropylidene-α-D-galactopyranose (**25**).

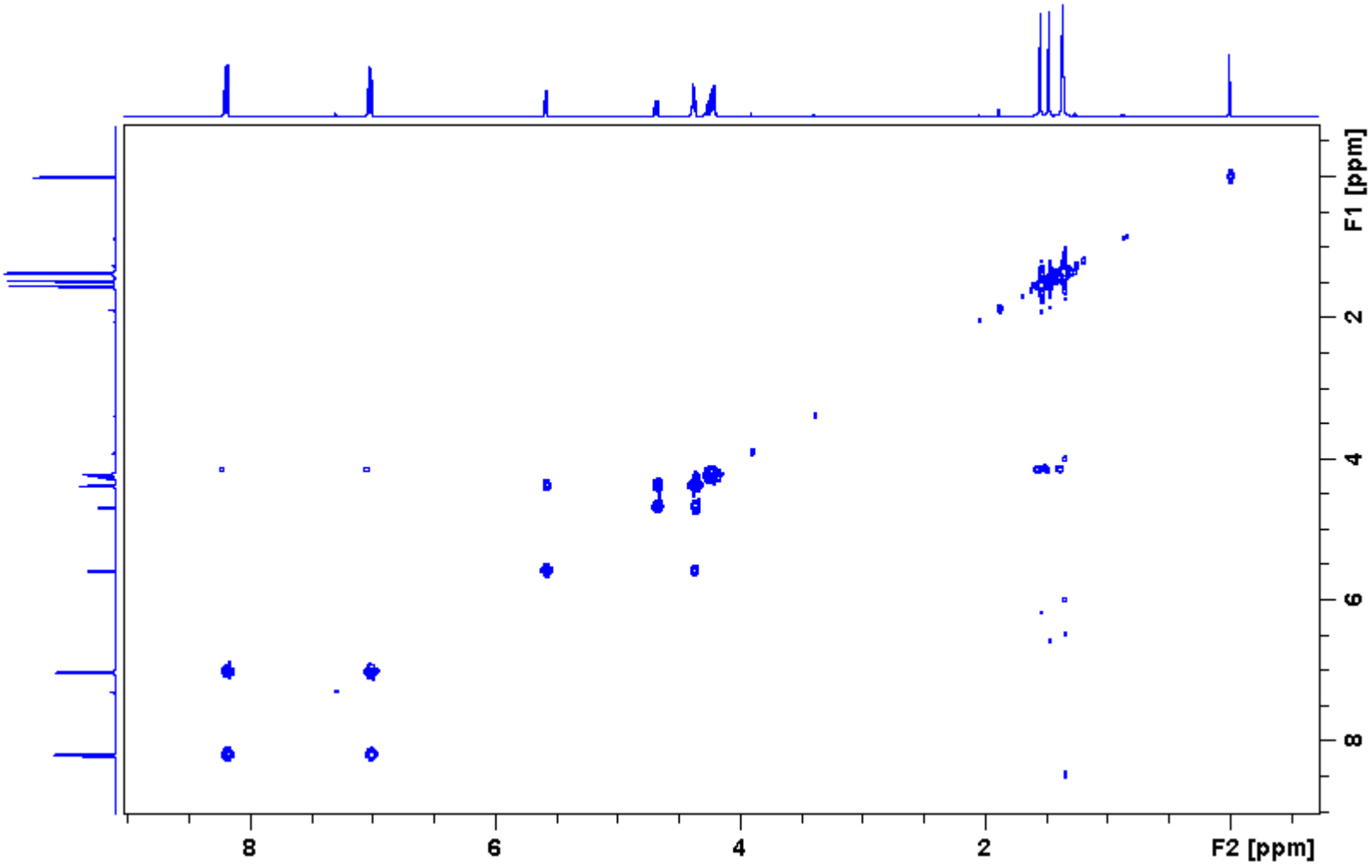

Figure 58: COSY NMR spectrum of 6-*O*-(*p*-nitro)benzenesulfonate ester of 1,2:3,4-di-*O*-isopropylidene-α-D-galactopyranose (**25**).

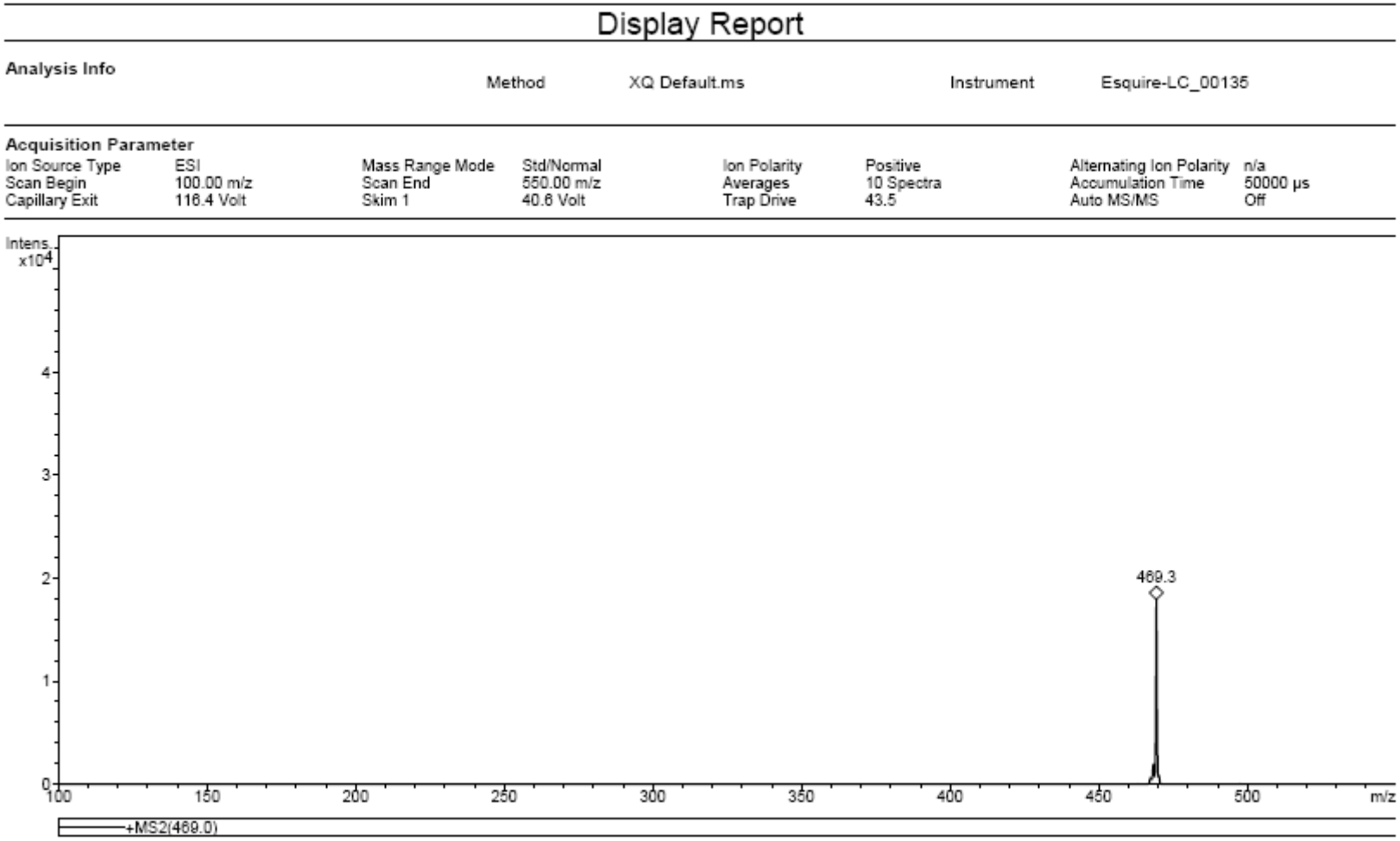

Figure 59: Mass spectrum of 6-*O*-(*p*-nitro)benzenesulfonate ester of 1,2:3,4-di-*O*-isopropylidene-α-D-galactopyranose (**25**).

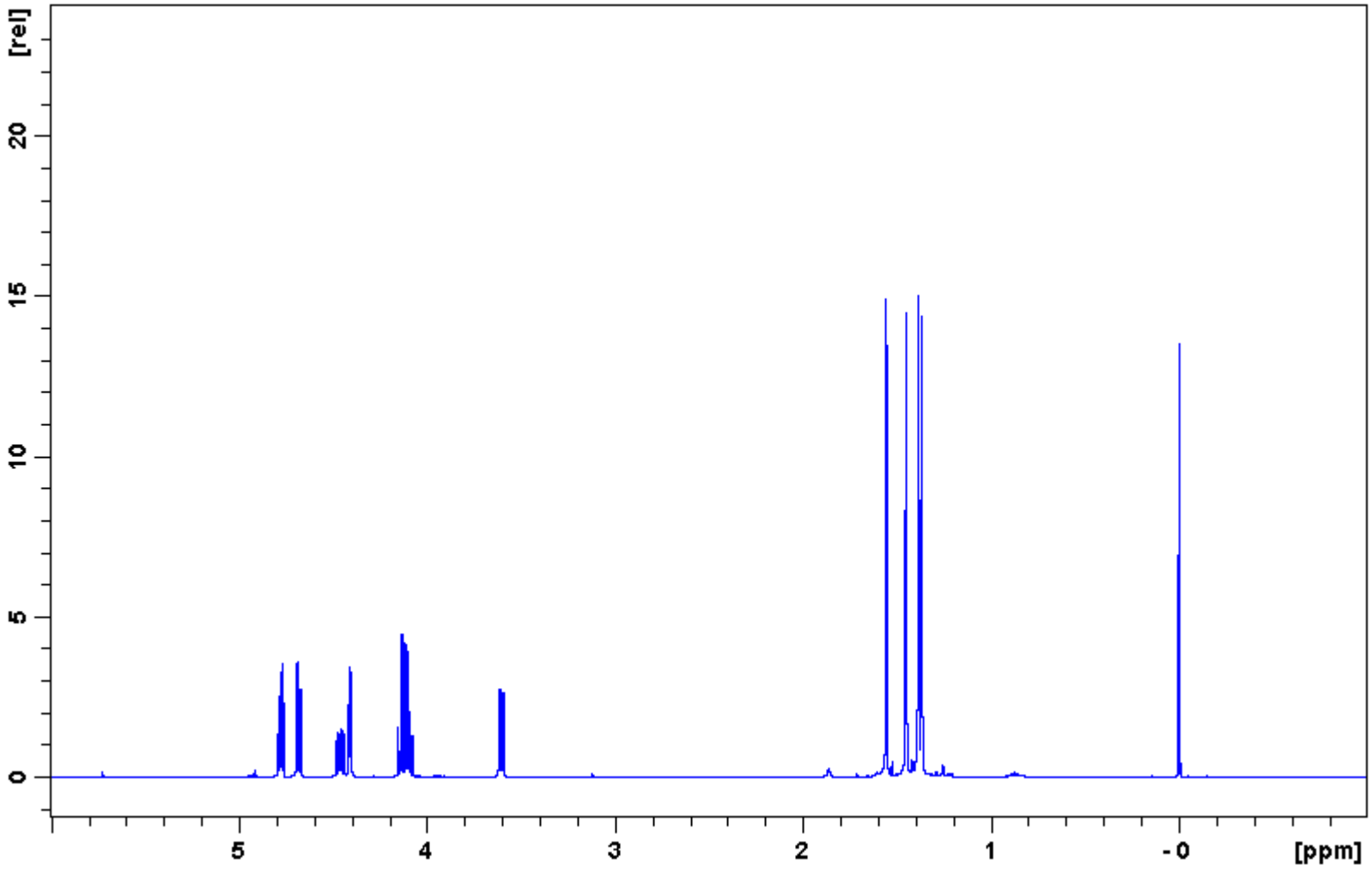

Figure 60: ^{1}H NMR spectrum of 1-Azido-1-deoxy-2,3:5,6-di-*O*-isopropylidene-β-D-mannofuranose (**27**).

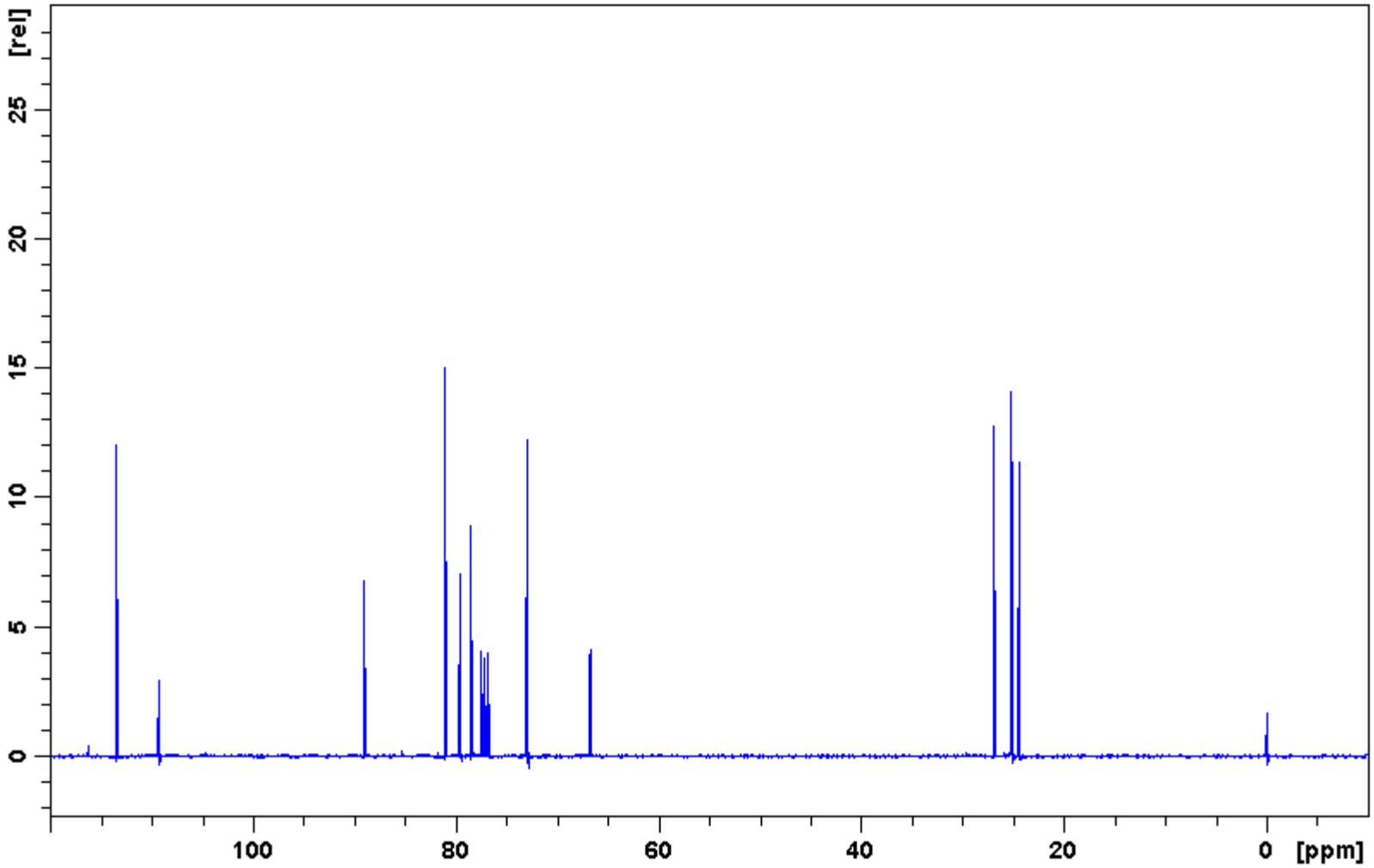

Figure 61: ^{13}C NMR spectrum of 1-Azido-1-deoxy-2,3:5,6-di-*O*-isopropylidene-β-D-mannofuranose (**27**)**.**

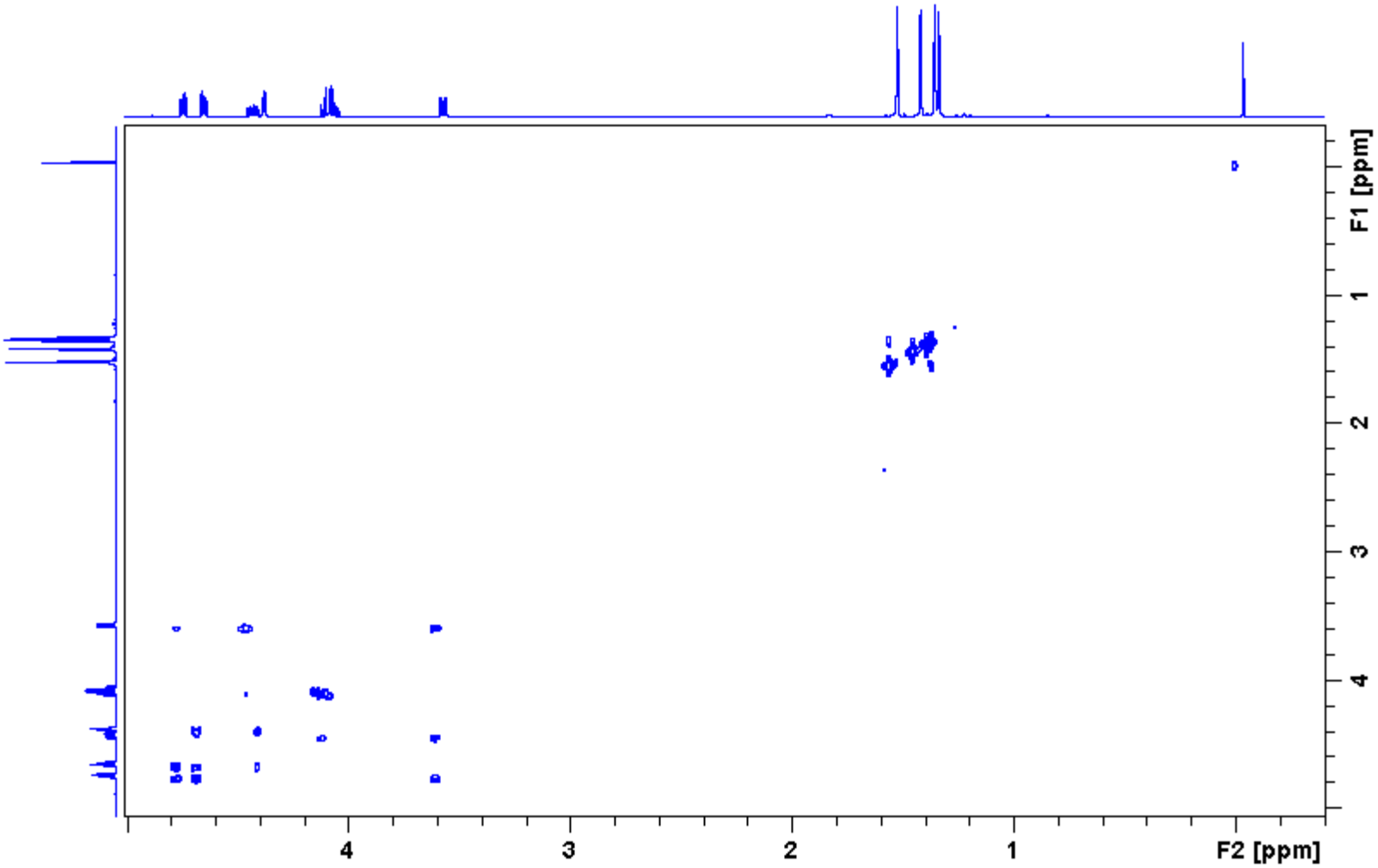

Figure 62: COSY NMR spectrum of 1-Azido-1-deoxy-2,3:5,6-di-*O*-isopropylidene-β-D-mannofuranose (**27**).

Display Report

Analysis Info Method XQ Default.ms Instrument Esquire-LC_00135

Acquisition Parameter

Ion Source Type	ESI	Mass Range Mode	Std/Normal	Ion Polarity	Positive	Alternating Ion Polarity	n/a
Scan Begin	100.00 m/z	Scan End	400.00 m/z	Averages	10 Spectra	Accumulation Time	5726 µs
Capillary Exit	90.0 Volt	Skim 1	21.4 Volt	Trap Drive	40.4	Auto MS/MS	Off

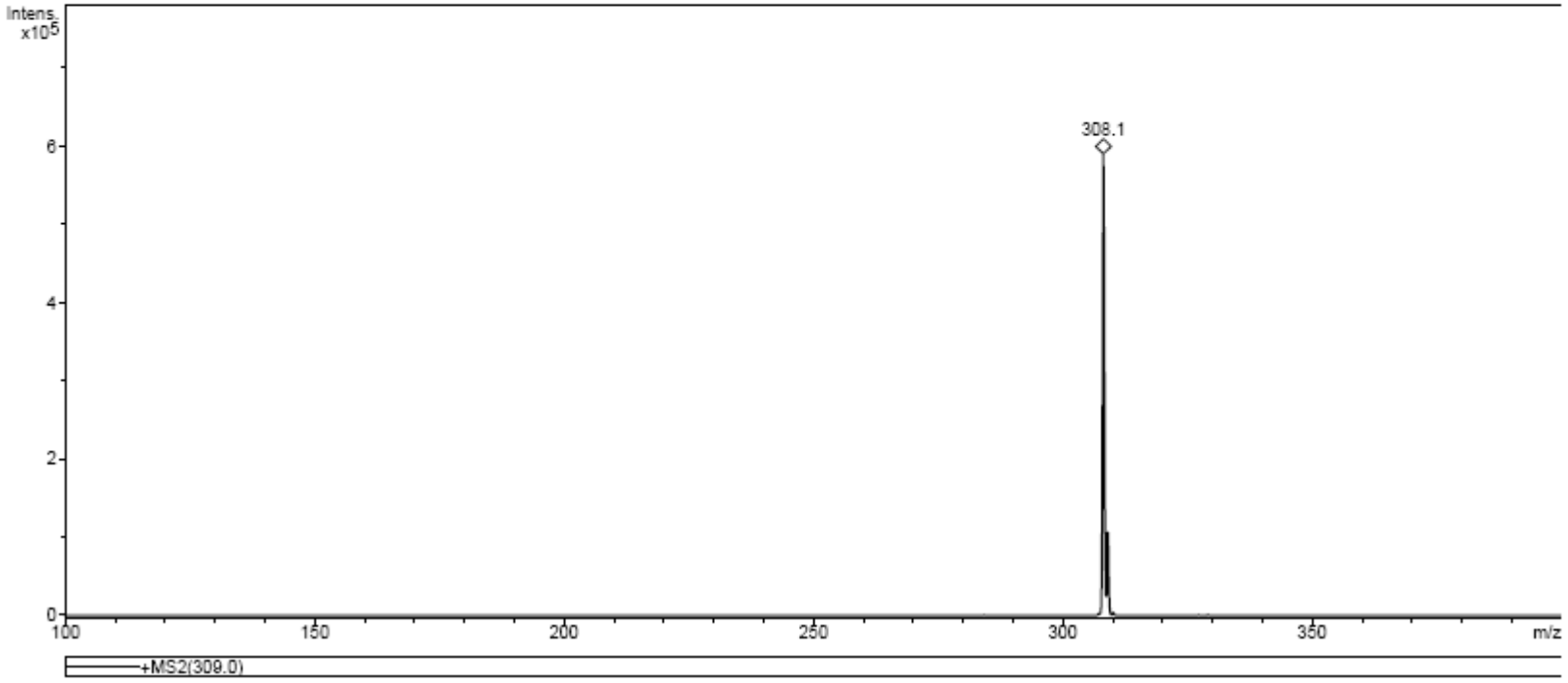

Figure 63: Mass spectrum of 1-Azido-1-deoxy-2,3:5,6-di-*O*-isopropylidene-β-D-mannofuranose (**27**).

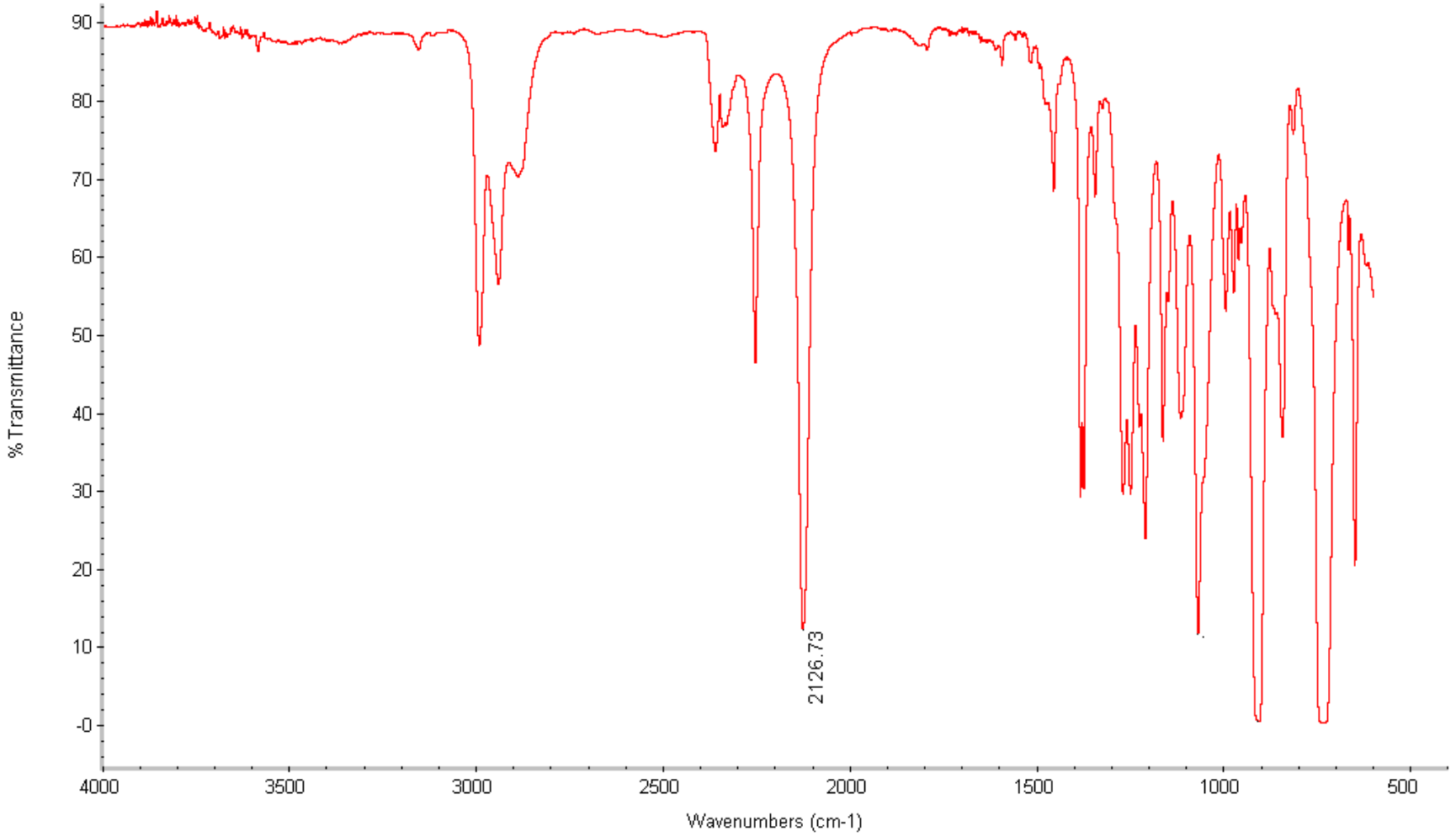

Figure 64: IR spectrum of 1-Azido-1-deoxy-2,3:5,6-di-*O*-isopropylidene-β-D-mannofuranose (**27**).

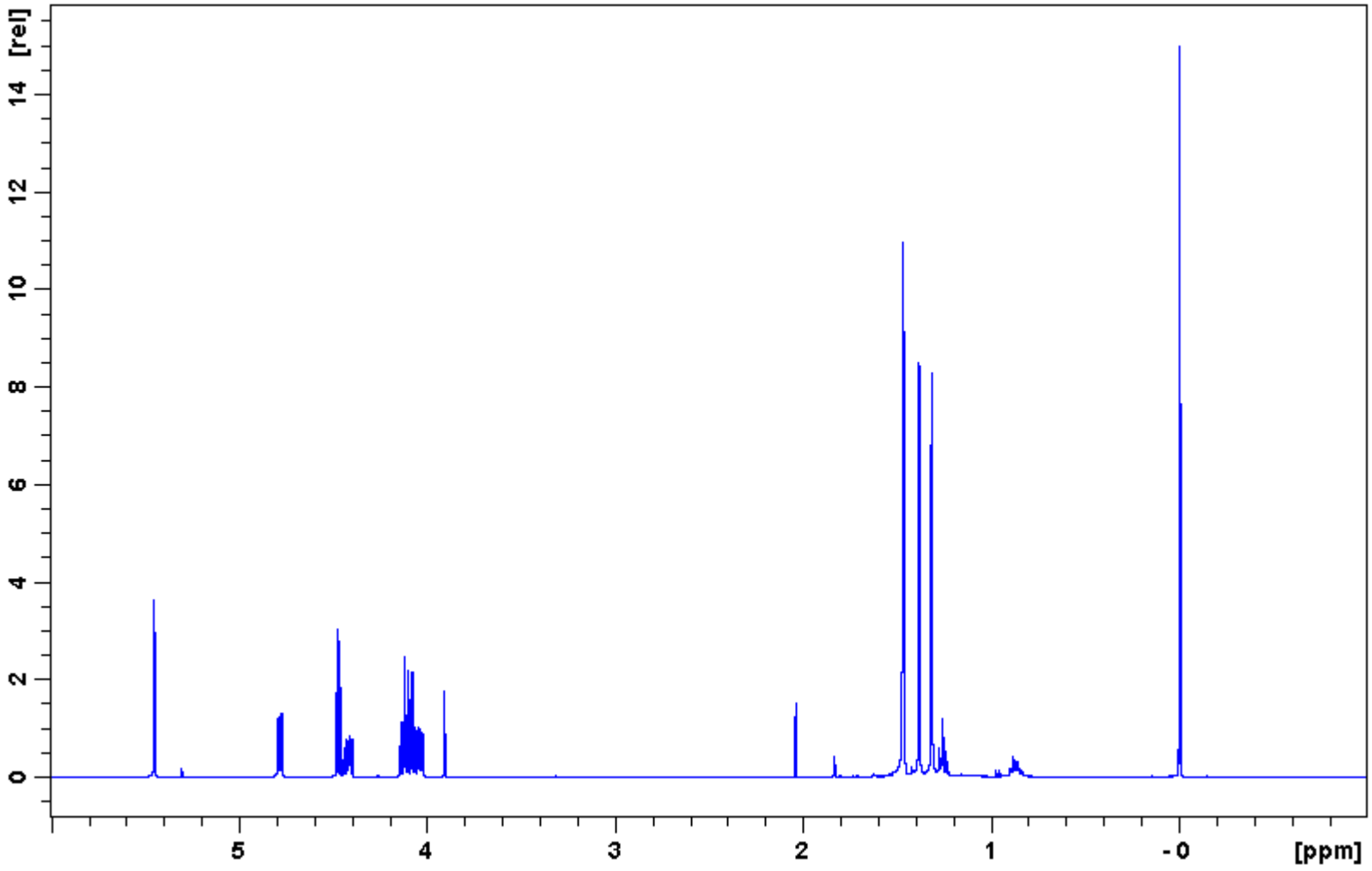

Figure 65: ^{1}H NMR spectrum of 1-Azido-1-deoxy-2,3:5,6-di-*O*-isopropylidene-α-D-mannofuranose (**28**).

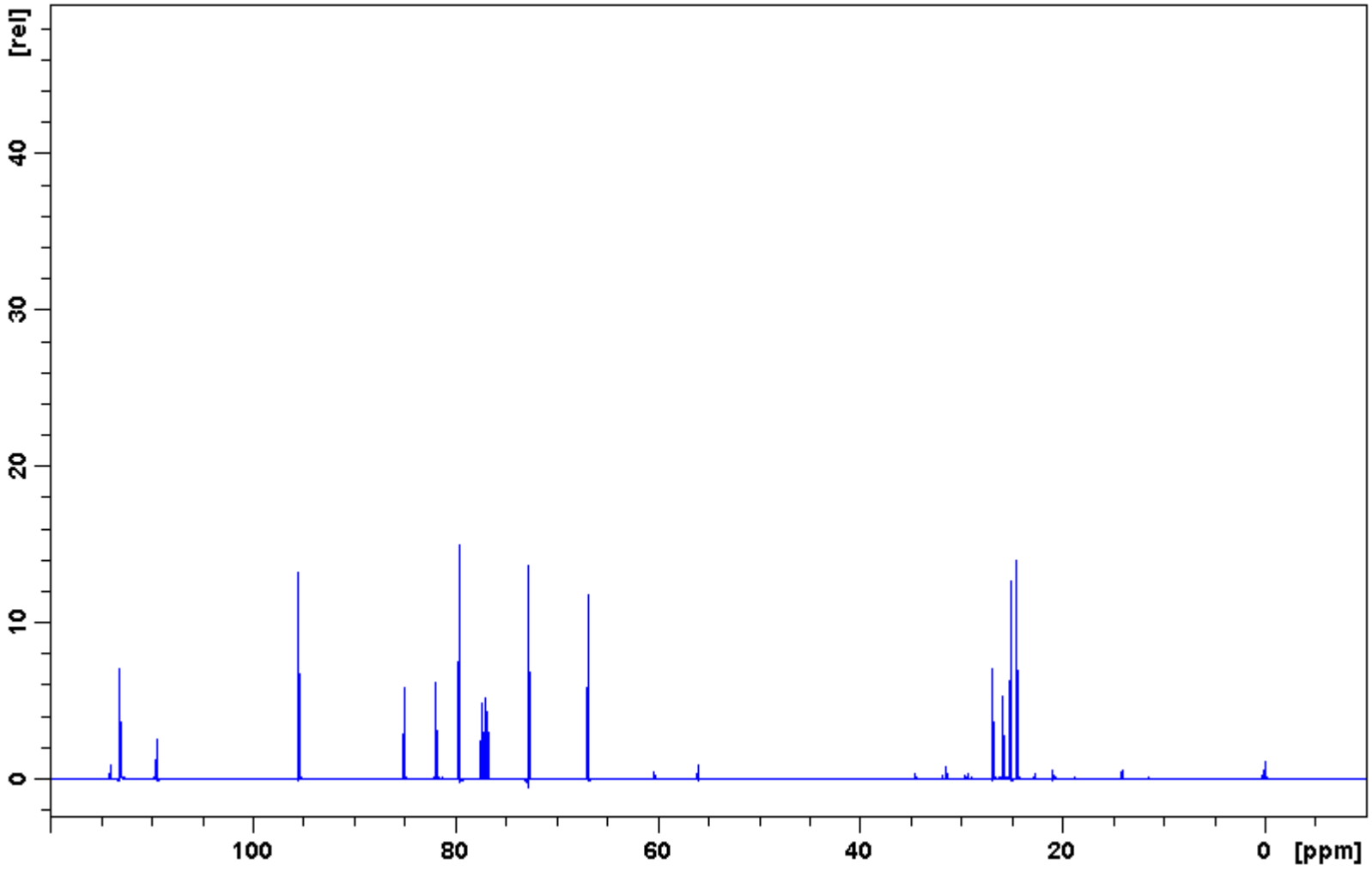

Figure 66: ^{13}C NMR spectrum of 1-Azido-1-deoxy-2,3:5,6-di-*O*-isopropylidene-α-D-mannofuranose (**28**).

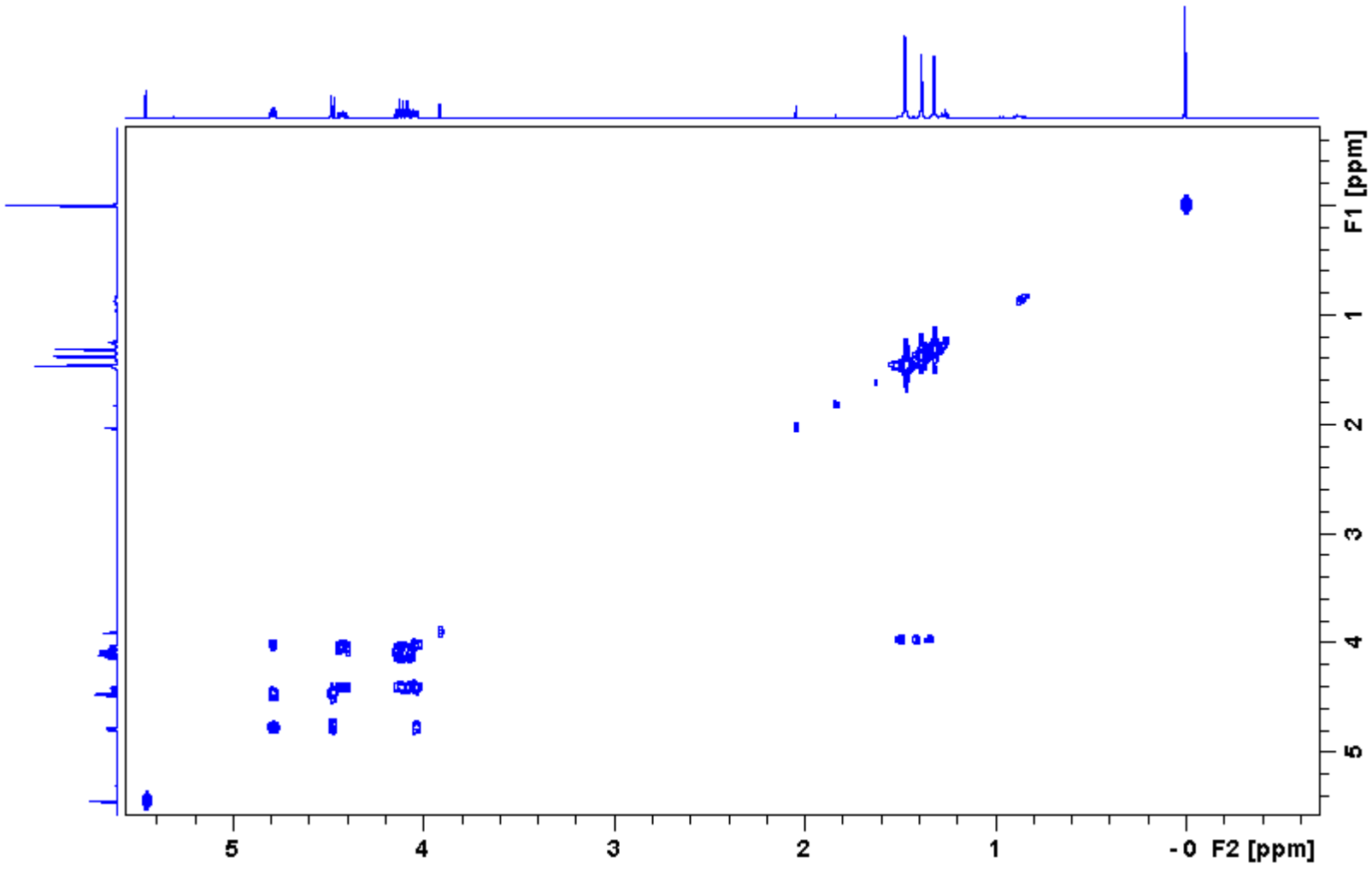

Figure 67: COSY NMR spectrum of 1-Azido-1-deoxy-2,3:5,6-di-*O*-isopropylidene-α-D-mannofuranose (**28**).

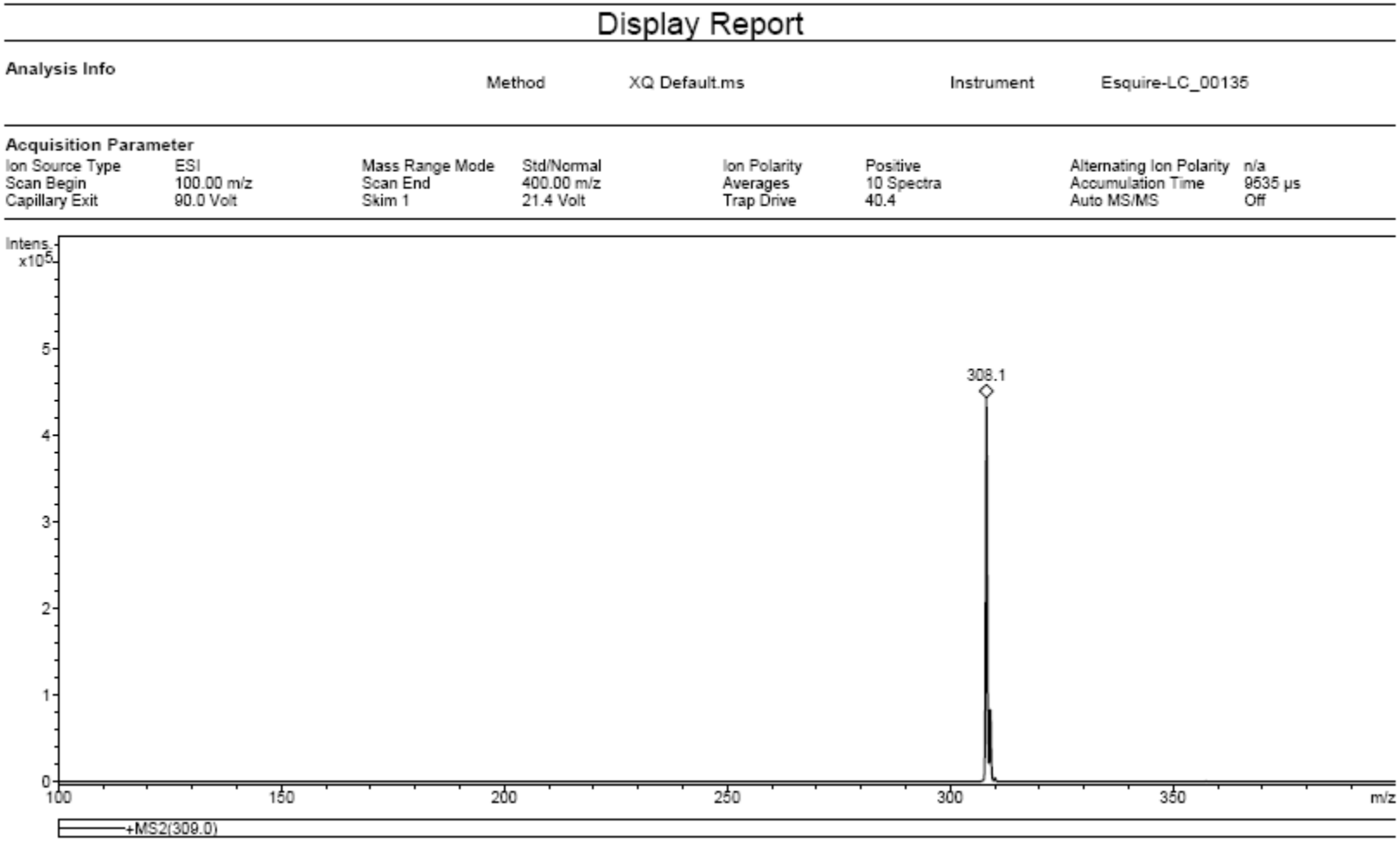

Figure 68: Mass spectrum of 1-Azido-1-deoxy-2,3:5,6-di-*O*-isopropylidene-α-D-mannofuranose (**28**).

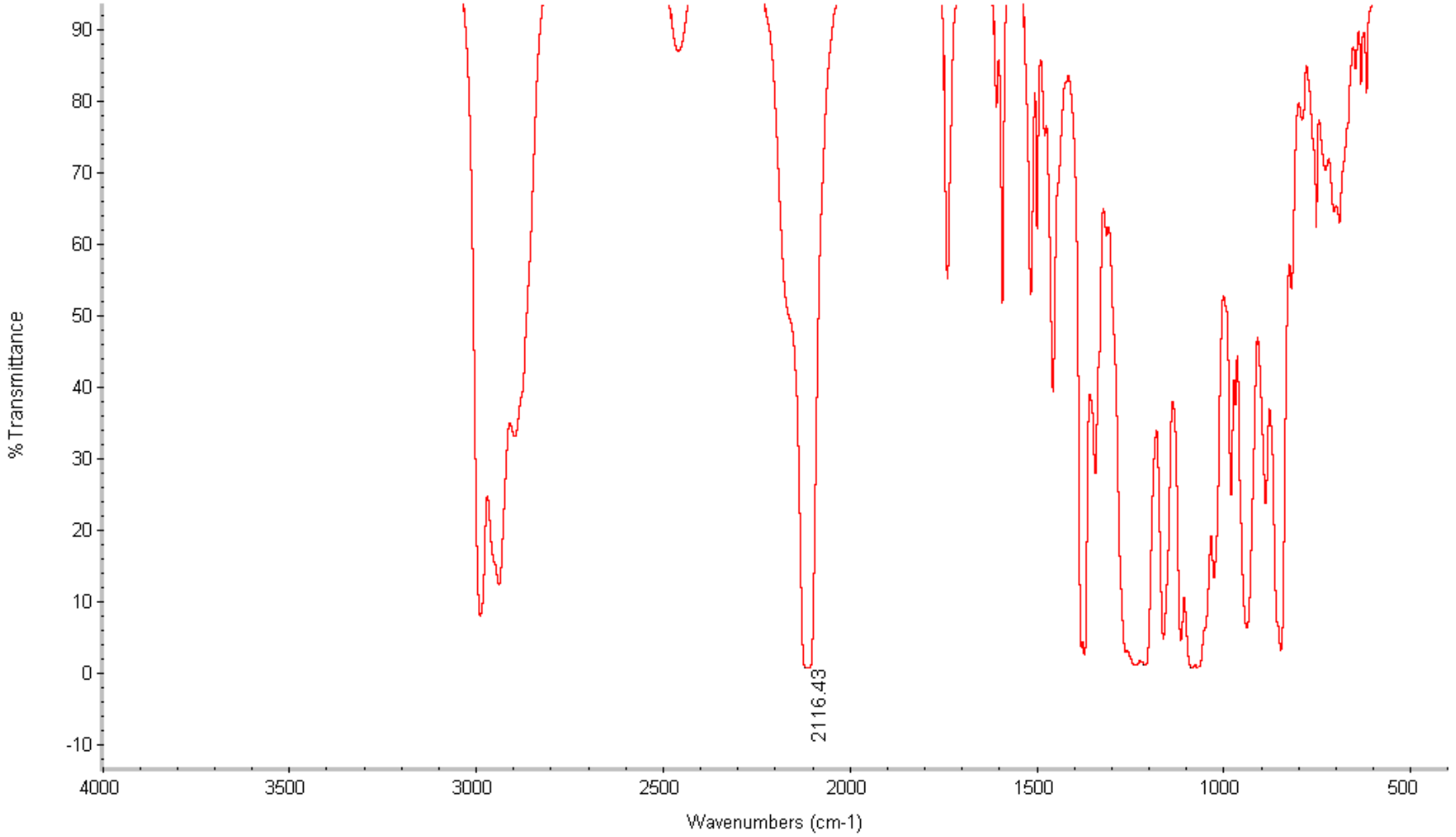

Figure 69: IR spectrum of 1-Azido-1-deoxy-2,3:5,6-di-*O*-isopropylidene-α-D-mannofuranose (**28**).

Appendix B

X-Ray Crystallography

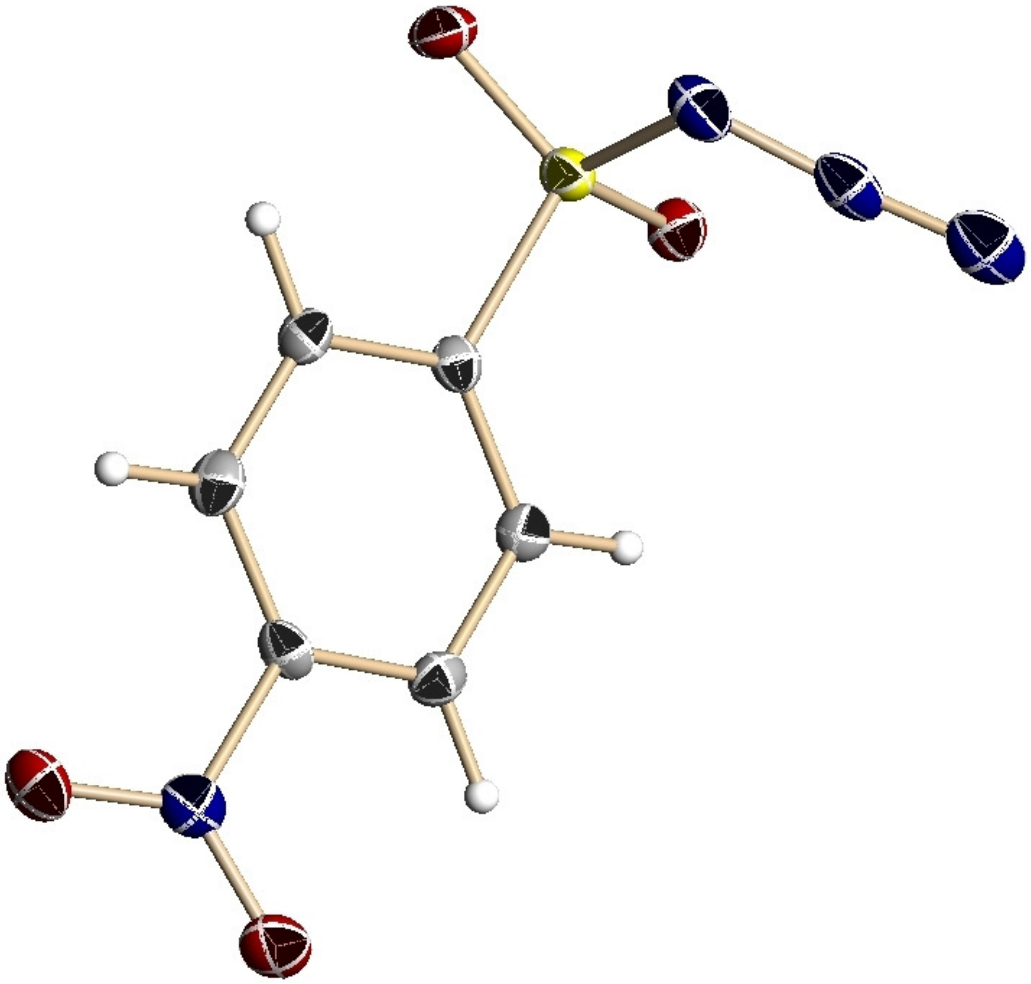

Figure 70: X-Ray crystal structure of 4-nitrobenzene sulfonyl azide (*p*-NBSA).

Table 1. Crystal data and structure refinement for 08an084_0m:

Identification code	08an084_0m
Empirical formula	C6 H4 N4 O4 S
Formula weight	228.19
Temperature	100(2) K
Wavelength	0.71073 Å
Crystal system	Orthorhombic
Space group	$Pna2_1$
Unit cell dimensions	
a	15.931(2) Å, α = 90°
b	10.7019(14) Å, β = 90°
c	10.2480(13) Å, γ = 90°
Volume, *Z*	1747.2(4) $Å^3$, 8
Density (calculated)	1.735 Mg/m^3
Absorption coefficient	0.372 mm^{-1}
F(000)	928
Crystal size	0.21 × 0.19 × 0.18 mm
Crystal shape, colour	block, colourless
θ range for data collection	2.29 to 28.28°
Limiting indices	$-21 \le h \le 21$, $-14 \le k \le 13$, $-12 \le l \le 12$
Reflections collected	9788
Independent reflections	4082 (*R*(int) = 0.0548)
Completeness to θ = 28.28°	97.2 %
Absorption correction	multi-scan
Max. and min. transmission	0.935 and 0.605
Refinement method	Full-matrix least-squares on F^2
Data / restraints / parameters	4082 / 1 / 271
Goodness-of-fit on F^2	1.051
Final *R* indices [$I>2\sigma(I)$]	R1 = 0.0390, wR2 = 0.0817
R indices (all data)	R1 = 0.0485, wR2 = 0.0893
Absolute structure parameter	0.03(7)
Largest diff. peak and hole	0.354 and −0.376 e × $Å^{-3}$

Refinement of F^2 against ALL reflections. The weighted R-factor wR and goodness of fit are based on F^2, conventional R-factors R are based on *F*, with *F* set to zero for negative F^2. The threshold expression of $F^2 > 2\sigma(F^2)$ is used only for calculating R-factors

Treatment of hydrogen atoms:
All hydrogen atoms were placed in calculated positions and were refined with an isotropic displacement parameter 1.5 (methyl) or 1.2 times (all others) that of the adjacent carbon atom.

Table 2. Atomic coordinates [× 10^4] and equivalent isotropic displacement parameters [Å^2 × 10^3] for 08an084_0m. U(eq) is defined as one third of the trace of the orthogonalized U_{ij} tensor.

	x	y	z	U(eq)
C(1)	2456(2)	3650(2)	8075(3)	17(1)
C(2)	2590(2)	4761(2)	8736(3)	20(1)
C(3)	2991(2)	4727(3)	9935(3)	22(1)
C(4)	3251(2)	3585(2)	10406(3)	18(1)
C(5)	3127(2)	2470(3)	9750(3)	19(1)
C(6)	2709(2)	2503(2)	8567(3)	18(1)
C(7)	932(2)	3119(2)	1030(2)	15(1)
C(8)	537(2)	4002(3)	267(3)	21(1)
C(9)	176(2)	3641(3)	-912(3)	24(1)
C(10)	218(2)	2387(3)	-1236(3)	19(1)
C(11)	603(2)	1497(3)	-487(3)	21(1)
C(12)	975(2)	1863(2)	668(3)	19(1)
N(1)	3687(1)	3552(2)	11677(3)	23(1)
N(2)	2735(2)	4061(2)	5496(2)	27(1)
N(3)	3101(2)	3089(3)	5095(3)	25(1)
N(4)	3454(2)	2282(3)	4668(3)	32(1)
N(5)	-192(1)	1998(2)	-2472(3)	26(1)
N(6)	588(1)	3471(2)	3598(2)	20(1)
N(7)	451(1)	2360(2)	3961(2)	20(1)
N(8)	278(2)	1420(2)	4344(3)	26(1)
O(1)	1618(1)	2510(2)	6244(2)	22(1)
O(2)	1434(1)	4806(2)	6491(2)	28(1)
O(3)	3619(1)	4466(2)	12393(2)	30(1)
O(4)	4094(1)	2615(2)	11942(2)	30(1)
O(5)	2021(1)	2693(2)	2856(2)	21(1)
O(6)	1549(1)	4885(2)	2488(2)	23(1)
O(7)	-351(1)	887(2)	-2620(2)	37(1)
O(8)	-361(1)	2814(2)	-3268(2)	36(1)
S(1)	1948(1)	3723(1)	6542(1)	19(1)
S(2)	1380(1)	3578(1)	2525(1)	17(1)

All esds (except the esd in the dihedral angle between two l.s. planes) are estimated using the full covariance matrix. The cell esds are taken into account individually in the estimation of esds in distances, angles and torsion angles; correlations between

esds in cell parameters are only used when they are defined by crystal symmetry. An approximate (isotropic) treatment of cell esds is used for estimating esds involving l.s. planes.

Table 3. Bond lengths [Å] and angles [deg] for 08an084_0m.

C(1)-C(2)	1.385(4)	C(3)-C(4)-N(1)	118.1(2)
C(1)-C(6)	1.386(4)	C(5)-C(4)-N(1)	118.4(2)
C(1)-S(1)	1.769(3)	C(6)-C(5)-C(4)	118.2(3)
C(2)-C(3)	1.386(4)	C(6)-C(5)-H(5)	120.9
C(2)-H(2)	0.9500	C(4)-C(5)-H(5)	120.9
C(3)-C(4)	1.378(4)	C(5)-C(6)-C(1)	118.8(3)
C(3)-H(3)	0.9500	C(5)-C(6)-H(6)	120.6
C(4)-C(5)	1.383(4)	C(1)-C(6)-H(6)	120.6
C(4)-N(1)	1.476(4)	C(8)-C(7)-C(12)	122.1(2)
C(5)-C(6)	1.383(4)	C(8)-C(7)-S(2)	119.2(2)
C(5)-H(5)	0.9500	C(12)-C(7)-S(2)	118.7(2)
C(6)-H(6)	0.9500	C(7)-C(8)-C(9)	119.4(3)
C(7)-C(8)	1.379(4)	C(7)-C(8)-H(8)	120.3
C(7)-C(12)	1.396(3)	C(9)-C(8)-H(8)	120.3
C(7)-S(2)	1.760(3)	C(10)-C(9)-C(8)	117.2(3)
C(8)-C(9)	1.393(4)	C(10)-C(9)-H(9)	121.4
C(8)-H(8)	0.9500	C(8)-C(9)-H(9)	121.4
C(9)-C(10)	1.384(4)	C(11)-C(10)-C(9)	124.2(3)
C(9)-H(9)	0.9500	C(11)-C(10)-N(5)	118.7(2)
C(10)-C(11)	1.368(4)	C(9)-C(10)-N(5)	117.1(3)
C(10)-N(5)	1.485(4)	C(10)-C(11)-C(12)	118.4(3)
C(11)-C(12)	1.381(4)	C(10)-C(11)-H(11)	120.8
C(11)-H(11)	0.9500	C(12)-C(11)-H(11)	120.8
C(12)-H(12)	0.9500	C(11)-C(12)-C(7)	118.7(2)
N(1)-O(4)	1.224(3)	C(11)-C(12)-H(12)	120.7
N(1)-O(3)	1.228(3)	C(7)-C(12)-H(12)	120.7
N(2)-N(3)	1.262(4)	O(4)-N(1)-O(3)	124.5(3)
N(2)-S(1)	1.688(3)	O(4)-N(1)-C(4)	117.7(2)
N(3)-N(4)	1.119(4)	O(3)-N(1)-C(4)	117.9(2)
N(5)-O(7)	1.224(3)	N(3)-N(2)-S(1)	111.9(2)
N(5)-O(8)	1.226(3)	N(4)-N(3)-N(2)	174.7(3)
N(6)-N(7)	1.264(3)	O(7)-N(5)-O(8)	124.3(3)
N(6)-S(2)	1.677(2)	O(7)-N(5)-C(10)	118.0(2)
N(7)-N(8)	1.115(3)	O(8)-N(5)-C(10)	117.7(2)
O(1)-S(1)	1.4338(19)	N(7)-N(6)-S(2)	112.82(19)
O(2)-S(1)	1.4207(19)	N(8)-N(7)-N(6)	174.3(3)
O(5)-S(2)	1.4340(19)	O(2)-S(1)-O(1)	121.33(12)
O(6)-S(2)	1.4245(18)	O(2)-S(1)-N(2)	103.28(13)
		O(1)-S(1)-N(2)	109.36(12)
C(2)-C(1)-C(6)	122.5(3)	O(2)-S(1)-C(1)	109.41(13)
C(2)-C(1)-S(1)	117.8(2)	O(1)-S(1)-C(1)	108.47(12)
C(6)-C(1)-S(1)	119.7(2)	N(2)-S(1)-C(1)	103.52(12)
C(1)-C(2)-C(3)	118.8(3)	O(6)-S(2)-O(5)	121.32(11)
C(1)-C(2)-H(2)	120.6	O(6)-S(2)-N(6)	103.11(12)
C(3)-C(2)-H(2)	120.6	O(5)-S(2)-N(6)	109.59(12)
C(4)-C(3)-C(2)	118.2(3)	O(6)-S(2)-C(7)	109.13(12)
C(4)-C(3)-H(3)	120.9	O(5)-S(2)-C(7)	108.11(12)
C(2)-C(3)-H(3)	120.9	N(6)-S(2)-C(7)	104.26(12)
C(3)-C(4)-C(5)	123.5(3)		

Table 4. Anisotropic displacement parameters [$Å^2 \times 10^3$] for 08an084_0m. The anisotropic displacement factor exponent takes the form: $-2\pi^2 [(h\ a^*)^2\ U11 + ... + 2\ h\ k\ a^*\ b^*\ U12]$

	U11	U22	U33	U23	U13	U12
C(1)	17(1)	18(1)	16(1)	-1(1)	2(1)	-2(1)
C(2)	24(1)	13(1)	22(2)	-1(1)	0(1)	0(1)
C(3)	24(1)	16(1)	25(2)	-3(1)	1(1)	-3(1)
C(4)	14(1)	26(2)	15(2)	-3(1)	-3(1)	-2(1)
C(5)	17(1)	19(1)	22(2)	1(1)	1(1)	2(1)
C(6)	16(1)	18(1)	19(2)	-2(1)	-1(1)	-2(1)
C(7)	13(1)	20(1)	12(1)	-2(1)	-1(1)	-3(1)
C(8)	22(1)	19(1)	21(2)	0(1)	-2(1)	1(1)
C(9)	23(1)	26(2)	23(2)	3(1)	-3(1)	6(1)
C(10)	14(1)	29(2)	13(1)	-5(1)	2(1)	2(1)
C(11)	21(1)	18(1)	23(2)	-4(1)	0(1)	1(1)
C(12)	18(1)	19(1)	19(2)	0(1)	-3(1)	1(1)
N(1)	16(1)	29(1)	24(1)	1(1)	0(1)	-2(1)
N(2)	35(1)	27(1)	18(1)	-1(1)	1(1)	-5(1)
N(3)	18(1)	40(2)	17(1)	-1(1)	-4(1)	-6(1)
N(4)	19(1)	52(2)	25(2)	0(1)	-3(1)	-2(1)
N(5)	18(1)	39(1)	21(1)	-5(1)	-3(1)	5(1)
N(6)	22(1)	19(1)	20(1)	-1(1)	-1(1)	-1(1)
N(7)	17(1)	24(1)	19(1)	-2(1)	-2(1)	0(1)
N(8)	25(1)	27(1)	27(2)	-2(1)	2(1)	-2(1)
O(1)	22(1)	20(1)	23(1)	-3(1)	-3(1)	-2(1)
O(2)	38(1)	19(1)	27(1)	2(1)	-9(1)	6(1)
O(3)	34(1)	33(1)	23(1)	-8(1)	-7(1)	-2(1)
O(4)	25(1)	39(1)	26(1)	1(1)	-5(1)	7(1)
O(5)	19(1)	23(1)	21(1)	0(1)	-4(1)	2(1)
O(6)	24(1)	20(1)	24(1)	-3(1)	-4(1)	-3(1)
O(7)	40(1)	39(1)	32(1)	-12(1)	-7(1)	-10(1)
O(8)	38(1)	45(1)	25(1)	-5(1)	-12(1)	14(1)
S(1)	23(1)	19(1)	17(1)	-1(1)	-3(1)	0(1)
S(2)	16(1)	18(1)	17(1)	-2(1)	-2(1)	-1(1)

Table 5. Hydrogen coordinates ($\times 10^4$) and isotropic displacement parameters ($Å^2 \times 10^3$) for 08an084_0m.

	x	y	z	U(eq)
H(2)	2410	5533	8373	23
H(3)	3085	5471	10419	26
H(5)	3323	1703	10102	23
H(6)	2599	1754	8100	21
H(8)	512	4849	542	25

H(9)	-89	4230	-1470	29
H(11)	614	648	-756	25
H(12)	1254	1272	1207	22

Table 6. Torsion angles [deg] for 08an084_0m

C(6)-C(1)-C(2)-C(3)	-0.1(4)
S(1)-C(1)-C(2)-C(3)	-179.6(2)
C(1)-C(2)-C(3)-C(4)	1.0(4)
C(2)-C(3)-C(4)-C(5)	-0.5(4)
C(2)-C(3)-C(4)-N(1)	179.3(2)
C(3)-C(4)-C(5)-C(6)	-0.9(4)
N(1)-C(4)-C(5)-C(6)	179.3(2)
C(4)-C(5)-C(6)-C(1)	1.8(4)
C(2)-C(1)-C(6)-C(5)	-1.3(4)
S(1)-C(1)-C(6)-C(5)	178.18(19)
C(12)-C(7)-C(8)-C(9)	-0.7(4)
S(2)-C(7)-C(8)-C(9)	-179.5(2)
C(7)-C(8)-C(9)-C(10)	1.6(4)
C(8)-C(9)-C(10)-C(11)	-1.2(4)
C(8)-C(9)-C(10)-N(5)	178.0(2)
C(9)-C(10)-C(11)-C(12)	0.0(4)
N(5)-C(10)-C(11)-C(12)	-179.3(2)
C(10)-C(11)-C(12)-C(7)	0.9(4)
C(8)-C(7)-C(12)-C(11)	-0.5(4)
S(2)-C(7)-C(12)-C(11)	178.2(2)
C(3)-C(4)-N(1)-O(4)	-162.3(3)
C(5)-C(4)-N(1)-O(4)	17.5(3)
C(3)-C(4)-N(1)-O(3)	17.5(4)
C(5)-C(4)-N(1)-O(3)	-162.7(2)
C(11)-C(10)-N(5)-O(7)	17.5(4)
C(9)-C(10)-N(5)-O(7)	-161.9(3)
C(11)-C(10)-N(5)-O(8)	-163.6(2)
C(9)-C(10)-N(5)-O(8)	17.1(4)
N(3)-N(2)-S(1)-O(2)	-158.8(2)
N(3)-N(2)-S(1)-O(1)	-28.4(2)
N(3)-N(2)-S(1)-C(1)	87.1(2)
C(2)-C(1)-S(1)-O(2)	-26.1(2)
C(6)-C(1)-S(1)-O(2)	154.4(2)
C(2)-C(1)-S(1)-O(1)	-160.4(2)
C(6)-C(1)-S(1)-O(1)	20.1(2)
C(2)-C(1)-S(1)-N(2)	83.5(2)
C(6)-C(1)-S(1)-N(2)	-96.0(2)
N(7)-N(6)-S(2)-O(6)	-167.1(2)
N(7)-N(6)-S(2)-O(5)	-36.6(2)
N(7)-N(6)-S(2)-C(7)	78.9(2)
C(8)-C(7)-S(2)-O(6)	-22.6(2)
C(12)-C(7)-S(2)-O(6)	158.6(2)
C(8)-C(7)-S(2)-O(5)	-156.4(2)

C(12)-C(7)-S(2)-O(5)	24.7(2)
C(8)-C(7)-S(2)-N(6)	87.0(2)
C(12)-C(7)-S(2)-N(6)	-91.8(2)

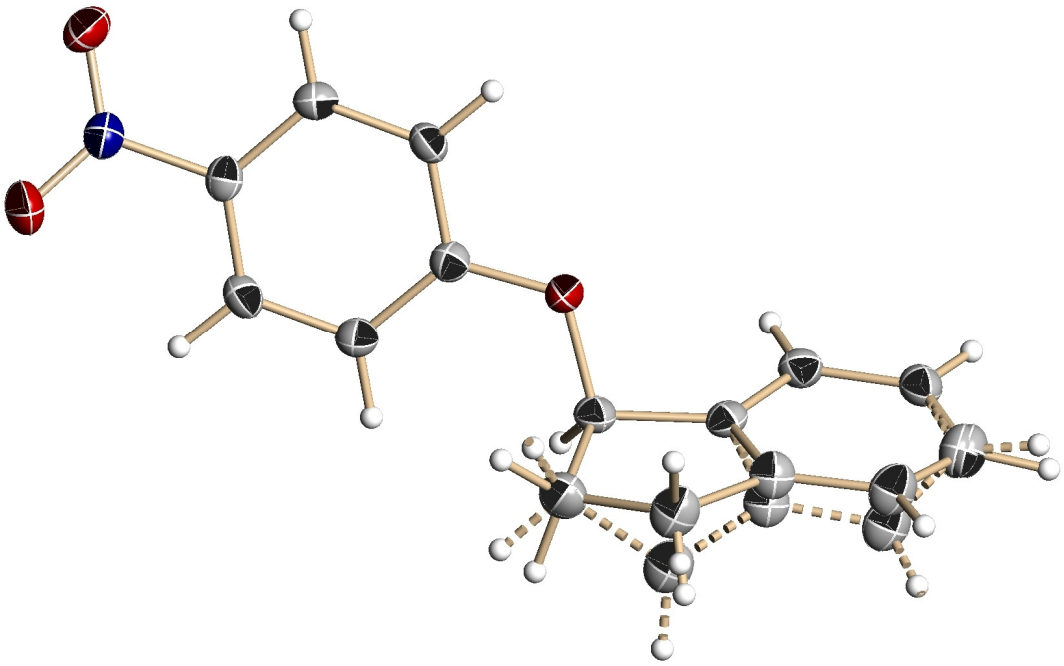

Figure 71: X-Ray crystal structure of S_NAr generated byproduct (**15**).

Table 1. Crystal data and structure refinement for 07mz223m:

Identification code: 07mz223m
Empirical formula: C15 H13 N O3
Formula weight: 255.26
Temperature: 100(2) K
Wavelength: 0.71073 Å
Crystal system: Monoclinic
Space group: $P2_1/c$
Unit cell dimensions:
a = 9.717(6) Å, α = 90°
b = 13.982(9) Å, β = 107.865(16)°
c = 9.609(6) Å, γ = 90°
Volume, *Z*: 1242.5(13) $Å^3$, 4
Density (calculated): 1.365 g/m^3
Absorption coefficient: 0.096 mm^{-1}
F(000): 536
Crystal size: 0.48 × 0.19 × 0.10
Crystal shape, colour: needle, colourless
θ range for data collection: 2.20 to 28.28°
Limiting indices: −12 ≤ h ≤ 12, 0 ≤ *k* ≤ 18, 0 ≤ *l* ≤ 12
Reflections collected: 12104
Independent reflections: 3292 (*R*(int) = not defined)
Completeness to θ = 28.28°: 97.9 %
Absorption correction: multi-scan
Max. and min. transmission: 1.000 and 0.736
Refinement method: Full-matrix least-squares on F^2
Data / restraints / parameters: 3292 / 6 / 186
Goodness-of-fit on F^2: 0.969
Final *R* indices [$I>2\sigma(I)$]: R1 = 0.0547, wR2 = 0.1219
R indices (all data): R1 = 0.0788, wR2 = 0.1356
Largest diff. peak and hole: 0.332 and −0.217 e × $Å^{-3}$

Refinement of F^2 against ALL reflections. The weighted R-factor wR and goodness of fit are based on F^2, conventional R-factors R are based on *F*, with *F* set to zero for negative F^2. The threshold

expression of $F^2 > 2\sigma(F^2)$ is used only for calculating R-factors

Comments:
The crystal under investigation was found to be non-merohedrally twinned. The orientation matrices for the two components were identified using the program Cell_Now, and the two components were integrated using Saint, resulting in a total of 12104 reflections. 4969 reflections (2706 unique ones) involved component 1 only (mean I/sigma = 4.9), 4907 reflections (2677 unique ones) involved component 2 only (mean I/sigma = 3.3), and 2228 reflections (1332 unique ones) involved both components (mean I/sigma = 7.3). The exact twin matrix identified by the integration program was found to be -1.00460 -0.00214 -0.61342, 0.00499 -0.99859 0.00119, 0.01428 -0.00014 1.00422.

The data were corrected for absorption using twinabs, and the structure was solved using direct methods with only the non-overlapping reflections of component 1. The structure was refined using the hklf 5 routine with all reflections of component 1 (including the overlapping ones) below a d-spacing threshold of 0.75, resulting in a BASF value of 0.341(2).

Part of the indene ring is disordered over two positions with an occupancy ratio of 0.712(6) to 0.288(6). Equivalent bonds within the disordered moieties were restrained to be each the same within a standard deviation of 0.02 Å, and equivalent atoms were set to have identical ADPs.

Treatment of hydrogen atoms:
All hydrogen atoms were placed in calculated positions and all H atoms were refined with an isotropic displacement parameter 1.5 (methyl) or 1.2 times (all others) that of the adjacent carbon atom.

Table 2. Atomic coordinates [$\times 10^4$] and equivalent isotropic displacement parameters [$Å^2 \times 10^3$] for 07mz223m. U(eq) is defined as one third of the trace of the orthogonalized U_{ij} tensor.

	x	y	z	U(eq)
C(1)	8399(2)	−1234(1)	8760(2)	23(1)
C(2)	8102(2)	−794(1)	9926(2)	26(1)
C(3)	7879(2)	186(1)	9883(2)	26(1)
C(4)	7934(2)	708(1)	8662(2)	23(1)
C(5)	8253(2)	245(1)	7504(2)	24(1)
C(6)	8487(2)	−726(1)	7546(2)	24(1)
C(7)	7346(2)	2202(1)	9625(2)	23(1)
C(8)	5831(2)	2007(2)	9729(2)	34(1)
C(11)	7296(2)	3238(1)	9182(2)	22(1)
C(12)	8411(2)	3802(1)	9034(2)	26(1)
C(13)	8140(2)	4757(1)	8640(2)	27(1)
C(9A)	4869(3)	2817(2)	8900(5)	33(1)
C(10A)	5903(5)	3595(4)	8790(5)	28(1)
C(15A)	5633(7)	4545(4)	8361(5)	33(1)
C(14A)	6781(9)	5153(10)	8380(30)	32(1)
C(9B)	5007(9)	2936(6)	9677(12)	33(1)
C(10B)	5970(14)	3634(10)	9189(16)	28(1)
C(15B)	5701(19)	4602(11)	8852(13)	33(1)
C(14B)	6740(20)	5080(20)	8380(60)	32(1)
N(1)	8596(2)	−2273(1)	8794(2)	26(1)
O(1)	8166(2)	−2741(1)	9667(2)	34(1)
O(2)	9182(2)	−2636(1)	7952(2)	36(1)
O(3)	7677(1)	1662(1)	8474(1)	28(1)

All esds (except the esd in the dihedral angle between two l.s. planes) are estimated using the full covariance matrix. The cell esds are taken into account individually in the estimation of esds in distances, angles and torsion angles; correlations between esds in cell parameters are only used when they are defined by crystal symmetry. An approximate (isotropic) treatment of cell esds is used for estimating esds involving l.s. planes.

Table 3. Bond lengths [Å] and angles [deg] for 07mz223m.

C(1)-C(2)	1.385(2)	C(7)-O(3)	1.455(2)
C(1)-C(6)	1.391(3)	C(7)-C(11)	1.506(2)
C(1)-N(1)	1.464(2)	C(7)-C(8)	1.530(3)
C(2)-C(3)	1.386(3)	C(7)-H(7)	1.0000
C(2)-H(2)	0.9500	C(8)-C(9B)	1.517(8)
C(3)-C(4)	1.397(2)	C(8)-C(9A)	1.527(4)
C(3)-H(3)	0.9500	C(8)-H(8A)	0.9900
C(4)-O(3)	1.359(2)	C(8)-H(8B)	0.9900
C(4)-C(5)	1.401(2)	C(8)-H(8C)	0.9924
C(5)-C(6)	1.375(2)	C(8)-H(8D)	0.9920
C(5)-H(5)	0.9500	C(11)-C(10A)	1.382(5)
C(6)-H(6)	0.9500	C(11)-C(12)	1.383(3)

C(11)-C(10B)	1.404(13)	C(9B)-C(8)-H(8C)	109.0
C(12)-C(13)	1.391(3)	C(7)-C(8)-H(8C)	109.5
C(12)-H(12)	0.9500	C(9B)-C(8)-H(8D)	110.5
C(13)-C(14B)	1.379(15)	C(7)-C(8)-H(8D)	109.1
C(13)-C(14A)	1.382(7)	H(8B)-C(8)-H(8D)	129.1
C(13)-H(13)	0.9500	H(8C)-C(8)-H(8D)	108.0
C(9A)-C(10A)	1.506(5)	C(10A)-C(11)-C(12)	119.9(3)
C(9A)-H(9A1)	0.9900	C(12)-C(11)-C(10B)	121.6(6)
C(9A)-H(9A2)	0.9900	C(10A)-C(11)-C(7)	111.6(3)
C(10A)-C(15A)	1.392(5)	C(12)-C(11)-C(7)	128.27(16)
C(15A)-C(14A)	1.399(9)	C(10B)-C(11)-C(7)	109.2(6)
C(15A)-H(15A)	0.9500	C(11)-C(12)-C(13)	119.09(17)
C(14A)-H(14A)	0.9500	C(11)-C(12)-H(12)	120.5
C(9B)-C(10B)	1.522(13)	C(13)-C(12)-H(12)	120.5
C(9B)-H(9B1)	0.9900	C(14B)-C(13)-C(12)	117.1(12)
C(9B)-H(9B2)	0.9900	C(14A)-C(13)-C(12)	121.7(5)
C(10B)-C(15B)	1.397(13)	C(14B)-C(13)-H(13)	123.7
C(15B)-C(14B)	1.397(17)	C(14A)-C(13)-H(13)	119.1
C(15B)-H(15B)	0.9500	C(12)-C(13)-H(13)	119.1
C(14B)-H(14B)	0.9500	C(10A)-C(9A)-C(8)	104.9(3)
N(1)-O(2)	1.2328(19)	C(10A)-C(9A)-H(9A1)	110.8
N(1)-O(1)	1.2341(19)	C(8)-C(9A)-H(9A1)	110.8
		C(10A)-C(9A)-H(9A2)	110.8
C(2)-C(1)-C(6)	122.22(16)	C(8)-C(9A)-H(9A2)	110.8
C(2)-C(1)-N(1)	118.79(16)	H(9A1)-C(9A)-H(9A2)	108.8
C(6)-C(1)-N(1)	118.98(16)	C(11)-C(10A)-C(15A)	120.4(5)
C(1)-C(2)-C(3)	119.05(17)	C(11)-C(10A)-C(9A)	109.8(4)
C(1)-C(2)-H(2)	120.5	C(15A)-C(10A)-C(9A)	129.9(4)
C(3)-C(2)-H(2)	120.5	C(10A)-C(15A)-C(14A)	120.0(7)
C(2)-C(3)-C(4)	119.69(17)	C(10A)-C(15A)-H(15A)	120.0
C(2)-C(3)-H(3)	120.2	C(14A)-C(15A)-H(15A)	120.0
C(4)-C(3)-H(3)	120.2	C(13)-C(14A)-C(15A)	118.2(9)
O(3)-C(4)-C(3)	124.86(16)	C(13)-C(14A)-H(14A)	120.9
O(3)-C(4)-C(5)	115.09(16)	C(15A)-C(14A)-H(14A)	120.9
C(3)-C(4)-C(5)	120.04(17)	C(8)-C(9B)-C(10B)	101.0(7)
C(6)-C(5)-C(4)	120.51(17)	C(8)-C(9B)-H(9B1)	111.6
C(6)-C(5)-H(5)	119.7	C(10B)-C(9B)-H(9B1)	111.6
C(4)-C(5)-H(5)	119.7	C(8)-C(9B)-H(9B2)	111.6
C(5)-C(6)-C(1)	118.47(17)	C(10B)-C(9B)-H(9B2)	111.6
C(5)-C(6)-H(6)	120.8	H(9B1)-C(9B)-H(9B2)	109.4
C(1)-C(6)-H(6)	120.8	C(15B)-C(10B)-C(11)	119.2(12)
O(3)-C(7)-C(11)	106.24(14)	C(15B)-C(10B)-C(9B)	127.2(12)
O(3)-C(7)-C(8)	113.51(15)	C(11)-C(10B)-C(9B)	113.5(9)
C(11)-C(7)-C(8)	103.97(15)	C(14B)-C(15B)-C(10B)	115.7(18)
O(3)-C(7)-H(7)	110.9	C(14B)-C(15B)-H(15B)	122.1
C(11)-C(7)-H(7)	110.9	C(10B)-C(15B)-H(15B)	122.1
C(8)-C(7)-H(7)	110.9	C(13)-C(14B)-C(15B)	124(2)
C(9B)-C(8)-C(7)	110.7(3)	C(13)-C(14B)-H(14B)	118.1
C(9A)-C(8)-C(7)	106.31(18)	C(15B)-C(14B)-H(14B)	118.1
C(9A)-C(8)-H(8A)	110.5	O(2)-N(1)-O(1)	123.32(16)
C(7)-C(8)-H(8A)	110.5	O(2)-N(1)-C(1)	118.50(15)
C(9A)-C(8)-H(8B)	110.5	O(1)-N(1)-C(1)	118.18(15)
C(7)-C(8)-H(8B)	110.5	C(4)-O(3)-C(7)	118.89(14)
H(8A)-C(8)-H(8B)	108.7		

Table 4. Anisotropic displacement parameters [$Å^2 \times 10^3$] for 07mz223m. The anisotropic displacement factor exponent takes the form: $-2\pi^2$ [$(h\ a^*)^2$ U11 + ... + 2 h k a* b* U12]

	U11	U22	U33	U23	U13	U12

C(1)	21(1)	20(1)	26(1)	1(1)	4(1)	-1(1)
C(2)	30(1)	26(1)	22(1)	4(1)	7(1)	-2(1)
C(3)	32(1)	26(1)	22(1)	-1(1)	9(1)	1(1)
C(4)	23(1)	23(1)	23(1)	-1(1)	6(1)	0(1)
C(5)	26(1)	24(1)	22(1)	5(1)	9(1)	0(1)
C(6)	23(1)	27(1)	23(1)	-3(1)	9(1)	0(1)
C(7)	27(1)	24(1)	20(1)	-2(1)	8(1)	-1(1)
C(8)	35(1)	33(1)	40(1)	1(1)	19(1)	-2(1)
C(11)	24(1)	22(1)	19(1)	-4(1)	6(1)	0(1)
C(12)	25(1)	29(1)	27(1)	2(1)	11(1)	4(1)
C(13)	31(1)	26(1)	23(1)	-1(1)	9(1)	-2(1)
C(9A)	22(1)	33(2)	44(2)	-2(2)	9(2)	-1(1)
C(10A)	23(1)	30(1)	30(3)	1(2)	5(2)	0(1)
C(15A)	24(1)	32(1)	40(3)	1(2)	6(2)	5(1)
C(14A)	34(1)	21(2)	37(1)	2(2)	7(1)	3(1)
C(9B)	22(1)	33(2)	44(2)	-2(2)	9(2)	-1(1)
C(10B)	23(1)	30(1)	30(3)	1(2)	5(2)	0(1)
C(15B)	24(1)	32(1)	40(3)	1(2)	6(2)	5(1)
C(14B)	34(1)	21(2)	37(1)	2(2)	7(1)	3(1)
N(1)	27(1)	23(1)	26(1)	0(1)	4(1)	0(1)
O(1)	39(1)	25(1)	40(1)	7(1)	13(1)	-3(1)
O(2)	47(1)	28(1)	34(1)	-3(1)	15(1)	8(1)
O(3)	40(1)	21(1)	26(1)	1(1)	16(1)	4(1)

Table 5. Hydrogen coordinates ($\times 10^4$) and isotropic displacement parameters ($Å^2 \times 10^3$) for 07mz223m.

	x	y	z	U(eq)
H(2)	8052	-1158	10744	31
H(3)	7690	502	10681	32
H(5)	8307	605	6684	29
H(6)	8704	-1042	6764	29
H(7)	8098	2095	10590	28
H(8A)	5469	1382	9282	41
H(8B)	5845	2000	10763	41
H(8C)	5908	1674	10662	41
H(8D)	5306	1581	8914	41
H(12)	9351	3541	9199	31
H(13)	8908	5147	8549	32
H(9A1)	4281	2602	7916	40
H(9A2)	4214	3045	9441	40
H(15A)	4670	4781	8058	39
H(14A)	6630	5820	8211	38
H(9B1)	4930	3107	10650	40
H(9B2)	4027	2902	8961	40
H(15B)	4865	4917	8939	39
H(14B)	6469	5656	7848	38

Table 6. Torsion angles [deg] for 07mz223m.

C(6)-C(1)-C(2)-C(3)	0.2(3)
N(1)-C(1)-C(2)-C(3)	-178.41(15)
C(1)-C(2)-C(3)-C(4)	1.0(3)
C(2)-C(3)-C(4)-O(3)	177.29(16)
C(2)-C(3)-C(4)-C(5)	-1.8(3)
O(3)-C(4)-C(5)-C(6)	-177.92(16)
C(3)-C(4)-C(5)-C(6)	1.2(3)
C(4)-C(5)-C(6)-C(1)	0.0(3)
C(2)-C(1)-C(6)-C(5)	-0.8(3)
N(1)-C(1)-C(6)-C(5)	177.86(16)
O(3)-C(7)-C(8)-C(9B)	-126.9(5)
C(11)-C(7)-C(8)-C(9B)	-11.9(5)
O(3)-C(7)-C(8)-C(9A)	-97.8(2)
C(11)-C(7)-C(8)-C(9A)	17.2(3)
O(3)-C(7)-C(11)-C(10A)	109.9(3)
C(8)-C(7)-C(11)-C(10A)	-10.1(3)
O(3)-C(7)-C(11)-C(12)	-65.0(2)
C(8)-C(7)-C(11)-C(12)	174.98(18)
O(3)-C(7)-C(11)-C(10B)	126.1(7)
C(8)-C(7)-C(11)-C(10B)	6.0(7)
C(10A)-C(11)-C(12)-C(13)	6.9(3)
C(10B)-C(11)-C(12)-C(13)	-10.9(8)
C(7)-C(11)-C(12)-C(13)	-178.62(17)
C(11)-C(12)-C(13)-C(14B)	-2(3)
C(11)-C(12)-C(13)-C(14A)	-0.7(13)
C(7)-C(8)-C(9A)-C(10A)	-18.1(3)
C(12)-C(11)-C(10A)-C(15A)	-5.4(5)
C(7)-C(11)-C(10A)-C(15A)	179.3(3)
C(12)-C(11)-C(10A)-C(9A)	174.0(2)
C(7)-C(11)-C(10A)-C(9A)	-1.3(4)
C(8)-C(9A)-C(10A)-C(11)	12.3(4)
C(8)-C(9A)-C(10A)-C(15A)	-168.4(4)
C(11)-C(10A)-C(15A)-C(14A)	-2.3(13)
C(9A)-C(10A)-C(15A)-C(14A)	178.4(12)
C(12)-C(13)-C(14A)-C(15A)	-7(2)
C(10A)-C(15A)-C(14A)-C(13)	8(2)
C(7)-C(8)-C(9B)-C(10B)	12.5(9)
C(12)-C(11)-C(10B)-C(15B)	8.3(16)
C(7)-C(11)-C(10B)-C(15B)	178.1(10)
C(12)-C(11)-C(10B)-C(9B)	-167.9(7)
C(7)-C(11)-C(10B)-C(9B)	1.9(12)
C(8)-C(9B)-C(10B)-C(15B)	175.2(13)
C(8)-C(9B)-C(10B)-C(11)	-8.9(12)
C(11)-C(10B)-C(15B)-C(14B)	7(3)
C(9B)-C(10B)-C(15B)-C(14B)	-178(3)
C(12)-C(13)-C(14B)-C(15B)	18(6)
C(10B)-C(15B)-C(14B)-C(13)	-20(6)
C(2)-C(1)-N(1)-O(2)	-163.31(16)
C(6)-C(1)-N(1)-O(2)	18.0(2)
C(2)-C(1)-N(1)-O(1)	16.7(2)
C(6)-C(1)-N(1)-O(1)	-162.03(16)
C(3)-C(4)-O(3)-C(7)	1.3(3)
C(5)-C(4)-O(3)-C(7)	-179.63(15)
C(11)-C(7)-O(3)-C(4)	173.38(15)

C(8)-C(7)-O(3)-C(4)	-72.98(19)

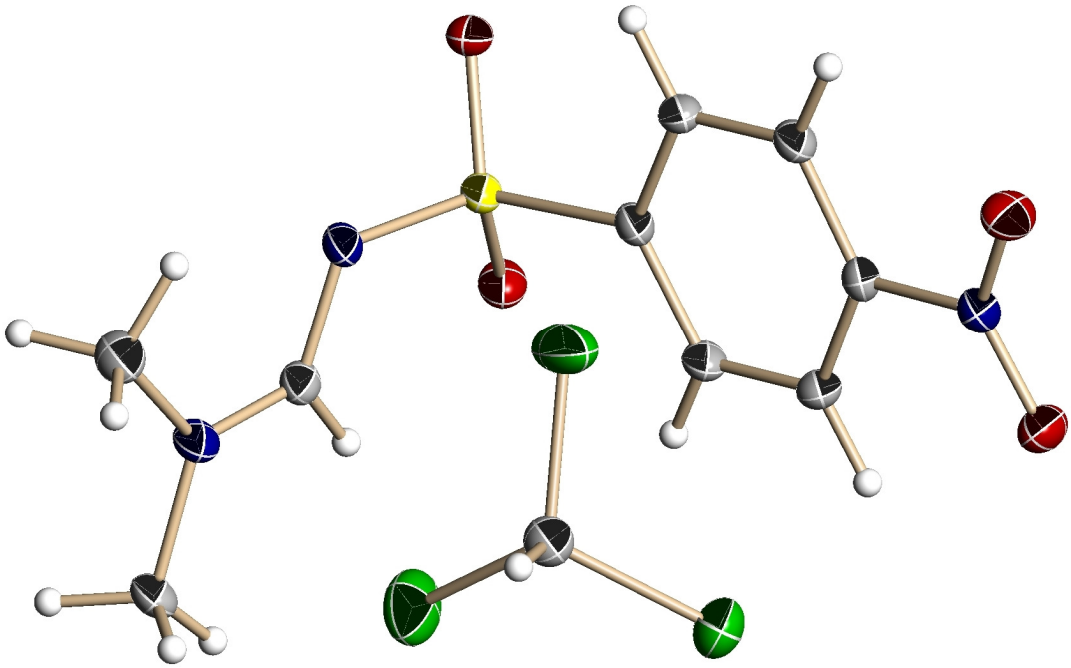

Figure 72: X-Ray crystal structure of DMF and *p*-NBSA reaction product (**16**).

Table 1. Crystal data and structure refinement for 07mz256m:

Identification code: 07mz256m
Empirical formula: C10 H12 Cl3 N3 O4 S
Moiety formula: C9 H11 N3 O4 S, C H Cl3
Formula weight: 376.64
Temperature: 100(2) K
Wavelength: 0.71073 Å
Crystal system: Monoclinic
Space group: $P2_1/c$
Unit cell dimensions:
a = 10.5008(16) Å, α = 90°
b = 5.9383(9) Å, β = 90.114(3))°
c = 24.210(4) Å, γ = 90°
Volume, *Z*: 1509.7(4) $Å^3$, 4
Density (calculated): 1.657 Mg/m^3
Absorption coefficient: 0.762 mm^{-1}
F(000): 768
Crystal size: 0.44 × 0.40 × 0.18 mm
Crystal shape, colour: plate, colourless
θ range for data collection: 1.68 to 28.28°
Limiting indices: $-14 \leq h \leq 14$, $-7 \leq k \leq 7$, $-32 \leq l \leq 32$
Reflections collected: 12512
Independent reflections: 3725 (*R*(int) = 0.0331)
Completeness to θ = 28.28°: 99.9 %
Absorption correction: multi-scan
Max. and min. transmission: 0.872 and 0.636
Refinement method: Full-matrix least-squares on F^2
Data / restraints / parameters: 3725 / 0 / 193
Goodness-of-fit on F^2: 1.053
Final *R* indices [$I>2\sigma(I)$]: R1 = 0.0503, wR2 = 0.1274
R indices (all data): R1 = 0.0538, wR2 = 0.1294
Largest diff. peak and hole: 0.742 and −0.481 e × $Å^{-3}$

Refinement of F^2 against ALL reflections. The weighted R-factor wR and goodness of fit are based on F^2, conventional R-factors R are based on *F*, with *F* set to zero for negative F^2. The threshold expression of $F^2 > 2\sigma(F^2)$ is used only for calculating R-factors

Comments:
The crystal was slightly pseudomerohedrally twinned (twin matrix 1 0 0 0 −1 0 0 0 −1), the BASF value refined to 0.030(6). The application of the twin law resulted in a drop of 2 and 4 % in R1 and wR2.

Treatment of hydrogen atoms:
All hydrogen atoms were placed in calculated positions and were refined with an isotropic displacement parameter 1.5 (methyl) or 1.2 times (all others) that of the adjacent carbon or oxygen atom.

Table 2. Atomic coordinates [× 10^4] and equivalent isotropic displacement parameters [Å^2 × 10^3] for 07mz256m. U(eq) is defined as one third of the trace of the orthogonalized U_{ij} tensor.

	x	y	z	U(eq)
C(1)	−8(2)	3798(5)	9004(1)	18(1)
C(2)	1159(2)	2843(5)	9131(1)	19(1)
C(3)	1998(2)	4068(5)	9454(1)	19(1)
C(4)	1651(2)	6209(5)	9634(1)	18(1)
C(5)	467(2)	7119(5)	9510(1)	18(1)
C(6)	−378(2)	5897(5)	9190(1)	19(1)
C(8)	4573(2)	8220(5)	9357(1)	18(1)
C(10)	4819(3)	11131(5)	8665(1)	25(1)
C(11)	6350(2)	7961(5)	8734(1)	22(1)
C(12)	2381(3)	5501(5)	7616(1)	24(1)
Cl(1)	3940(1)	5955(2)	7859(1)	42(1)
Cl(2)	1291(1)	7176(2)	7974(1)	43(1)
Cl(3)	1989(1)	2633(1)	7675(1)	32(1)
N(1)	−886(2)	2541(4)	8645(1)	20(1)
N(2)	3524(2)	9178(4)	9544(1)	19(1)
N(3)	5209(2)	9079(4)	8942(1)	20(1)
O(1)	−1880(2)	3462(4)	8500(1)	26(1)
O(2)	−589(2)	637(3)	8504(1)	25(1)
O(3)	2059(2)	9433(3)	10331(1)	21(1)
O(4)	3573(2)	6257(3)	10310(1)	21(1)

All esds (except the esd in the dihedral angle between two l.s. planes) are estimated using the full covariance matrix. The cell esds are taken into account individually in the estimation of esds in distances, angles and torsion angles; correlations between esds in cell parameters are only used when they are defined by crystal symmetry. An approximate (isotropic) treatment of cell esds

is used for estimating esds involving l.s. planes.

Table 3. Bond lengths [Å] and angles [deg] for 07mz256m.

C(1)-C(6)	1.381(4)	C(5)-C(4)-S(1)	119.7(2)
C(1)-C(2)	1.385(4)	C(3)-C(4)-S(1)	118.8(2)
C(1)-N(1)	1.470(3)	C(6)-C(5)-C(4)	119.4(3)
C(2)-C(3)	1.383(4)	C(6)-C(5)-H(5)	120.3
C(2)-H(2)	0.9500	C(4)-C(5)-H(5)	120.3
C(3)-C(4)	1.393(4)	C(1)-C(6)-C(5)	118.4(2)
C(3)-H(3)	0.9500	C(1)-C(6)-H(6)	120.8
C(4)-C(5)	1.388(3)	C(5)-C(6)-H(6)	120.8
C(4)-S(1)	1.772(3)	N(3)-C(8)-N(2)	121.5(2)
C(5)-C(6)	1.383(4)	N(3)-C(8)-H(8)	119.3
C(5)-H(5)	0.9500	N(2)-C(8)-H(8)	119.3
C(6)-H(6)	0.9500	N(3)-C(10)-H(10A)	109.5
C(8)-N(3)	1.310(3)	N(3)-C(10)-H(10B)	109.5
C(8)-N(2)	1.321(3)	H(10A)-C(10)-H(10B)	109.5
C(8)-H(8)	0.9500	N(3)-C(10)-H(10C)	109.5
C(10)-N(3)	1.450(4)	H(10A)-C(10)-H(10C)	109.5
C(10)-H(10A)	0.9800	H(10B)-C(10)-H(10C)	109.5
C(10)-H(10B)	0.9800	N(3)-C(11)-H(11A)	109.5
C(10)-H(10C)	0.9800	N(3)-C(11)-H(11B)	109.5
C(11)-N(3)	1.461(3)	H(11A)-C(11)-H(11B)	109.5
C(11)-H(11A)	0.9800	N(3)-C(11)-H(11C)	109.5
C(11)-H(11B)	0.9800	H(11A)-C(11)-H(11C)	109.5
C(11)-H(11C)	0.9800	H(11B)-C(11)-H(11C)	109.5
C(12)-Cl(2)	1.748(3)	Cl(2)-C(12)-Cl(3)	110.91(16)
C(12)-Cl(3)	1.758(3)	Cl(2)-C(12)-Cl(1)	110.83(17)
C(12)-Cl(1)	1.759(3)	Cl(3)-C(12)-Cl(1)	109.82(16)
C(12)-H(12)	1.0000	Cl(2)-C(12)-H(12)	108.4
N(1)-O(2)	1.222(3)	Cl(3)-C(12)-H(12)	108.4
N(1)-O(1)	1.228(3)	Cl(1)-C(12)-H(12)	108.4
N(2)-S(1)	1.607(2)	O(2)-N(1)-O(1)	123.3(2)
O(3)-S(1)	1.4368(19)	O(2)-N(1)-C(1)	118.4(2)
O(4)-S(1)	1.442(2)	O(1)-N(1)-C(1)	118.3(2)
		C(8)-N(2)-S(1)	116.10(19)
C(6)-C(1)-C(2)	123.1(2)	C(8)-N(3)-C(10)	122.5(2)
C(6)-C(1)-N(1)	118.3(2)	C(8)-N(3)-C(11)	120.5(2)
C(2)-C(1)-N(1)	118.5(2)	C(10)-N(3)-C(11)	117.0(2)
C(3)-C(2)-C(1)	118.2(2)	O(3)-S(1)-O(4)	117.98(12)
C(3)-C(2)-H(2)	120.9	O(3)-S(1)-N(2)	107.51(12)
C(1)-C(2)-H(2)	120.9	O(4)-S(1)-N(2)	112.71(12)
C(2)-C(3)-C(4)	119.4(2)	O(3)-S(1)-C(4)	107.01(12)
C(2)-C(3)-H(3)	120.3	O(4)-S(1)-C(4)	107.26(13)
C(4)-C(3)-H(3)	120.3	N(2)-S(1)-C(4)	103.22(12)
C(5)-C(4)-C(3)	121.5(2)		

Table 4. Anisotropic displacement parameters [$Å^2 \times 10^3$] for 07mz256m.

The anisotropic displacement factor exponent takes the form: $-2\pi^2$ [(h a*)^2 U11 + ... + 2 h k a* b* U12]

	U11	U22	U33	U23	U13	U12
C(1)	15(1)	17(1)	22(1)	0(1)	2(1)	-3(1)
C(2)	18(1)	14(1)	26(1)	0(1)	2(1)	3(1)
C(3)	14(1)	16(1)	27(1)	1(1)	2(1)	3(1)
C(4)	13(1)	17(1)	24(1)	2(1)	2(1)	-1(1)
C(5)	17(1)	14(1)	24(1)	0(1)	3(1)	2(1)
C(6)	14(1)	18(1)	26(1)	2(1)	2(1)	1(1)
C(8)	14(1)	16(1)	23(1)	1(1)	-1(1)	0(1)
C(10)	22(1)	22(1)	30(1)	7(1)	1(1)	2(1)
C(11)	13(1)	24(1)	28(1)	0(1)	3(1)	1(1)
C(12)	22(1)	22(1)	28(1)	2(1)	2(1)	1(1)
Cl(1)	29(1)	38(1)	59(1)	1(1)	-12(1)	-7(1)
Cl(2)	44(1)	26(1)	58(1)	6(1)	25(1)	9(1)
Cl(3)	34(1)	21(1)	39(1)	0(1)	2(1)	-4(1)
N(1)	16(1)	19(1)	25(1)	-1(1)	2(1)	-1(1)
N(2)	14(1)	16(1)	27(1)	2(1)	2(1)	0(1)
N(3)	14(1)	19(1)	27(1)	2(1)	1(1)	3(1)
O(1)	18(1)	25(1)	35(1)	-4(1)	-5(1)	4(1)
O(2)	23(1)	19(1)	33(1)	-4(1)	-1(1)	1(1)
O(3)	17(1)	18(1)	28(1)	-4(1)	2(1)	2(1)
O(4)	17(1)	19(1)	28(1)	3(1)	-2(1)	2(1)
S(1)	13(1)	15(1)	23(1)	0(1)	0(1)	1(1)

Table 5. Hydrogen coordinates ($\times 10^4$) and isotropic displacement parameters (Å^2 $\times 10^3$) for 07mz256m.

	x	y	z	U(eq)
H(2)	1378	1386	9000	23
H(3)	2803	3455	9552	23
H(5)	240	8569	9643	22
H(6)	-1194	6487	9100	23
H(8)	4874	6878	9526	21
H(10A)	4865	10915	8264	37
H(10B)	5385	12366	8774	37
H(10C)	3942	11500	8770	37
H(11A)	6516	6602	8952	32
H(11B)	7079	8985	8763	32
H(11C)	6221	7546	8346	32
H(12)	2349	5925	7216	29

Table 6. Torsion angles [deg] for 07mz242m.

C(6)-C(1)-C(2)-C(3)	-0.8(4)
N(1)-C(1)-C(2)-C(3)	177.9(2)
C(1)-C(2)-C(3)-C(4)	-0.7(4)
C(2)-C(3)-C(4)-C(5)	1.8(4)
C(2)-C(3)-C(4)-S(1)	-176.5(2)
C(3)-C(4)-C(5)-C(6)	-1.4(4)
S(1)-C(4)-C(5)-C(6)	176.9(2)
C(2)-C(1)-C(6)-C(5)	1.2(4)
N(1)-C(1)-C(6)-C(5)	-177.5(2)
C(4)-C(5)-C(6)-C(1)	0.0(4)
C(6)-C(1)-N(1)-O(2)	-176.3(2)
C(2)-C(1)-N(1)-O(2)	5.0(4)
C(6)-C(1)-N(1)-O(1)	4.1(4)
C(2)-C(1)-N(1)-O(1)	-174.7(2)
N(3)-C(8)-N(2)-S(1)	174.4(2)
N(2)-C(8)-N(3)-C(10)	0.6(4)
N(2)-C(8)-N(3)-C(11)	-178.5(2)
C(8)-N(2)-S(1)-O(3)	154.4(2)
C(8)-N(2)-S(1)-O(4)	22.7(2)
C(8)-N(2)-S(1)-C(4)	-92.7(2)
C(5)-C(4)-S(1)-O(3)	24.6(3)
C(3)-C(4)-S(1)-O(3)	-157.0(2)
C(5)-C(4)-S(1)-O(4)	152.1(2)
C(3)-C(4)-S(1)-O(4)	-29.5(2)
C(5)-C(4)-S(1)-N(2)	-88.6(2)
C(3)-C(4)-S(1)-N(2)	89.7(2)